AD NUMBER

AD824373

NEW LIMITATION CHANGE

TO

Approved for public release, distribution unlimited

FROM

Distribution authorized to U.S. Gov't. agencies and their contractors; Critical Technology; SEP 1967. Other requests shall be referred to Air Force Materials Laboratory, Attn: Metals and Ceramics Division, Wright-Patterson AFB, OH 45433.

AUTHORITY

afml, usaf ltr, 12 jan 1972

AFML-TR-67-293

INVESTIGATION OF MAGNITUDE AND DISTRIBUTION OF STRESSES IN WELDED STRUCTURES

Rocco Robelotto
Albert Toy
John M. Lambase

North American Aviation, Inc., Los Angeles Division

TECHNICAL REPORT AFML-TR-67-293

September 1967

Air Force Materials Laboratory
Research and Technology Division
Air Force Systems Command
Wright-Patterson Air Force Base, Ohio

NOTICES

When Government drawings, specifications, or other data are used for any purpose other than in connection with a definitely related Government procurement operation, the United States Government thereby incurs no responsibility nor any obligation whatsoever; and the fact that the Government may have formulated, furnished, or in any way supplied the said drawings, specifications, or other data, is not to be regarded by implication or otherwise as in any manner licensing the holder or any other person or corporation, or conveying any rights or permission to manufacture, use, or sell any patented invention that may in any way be related thereto.

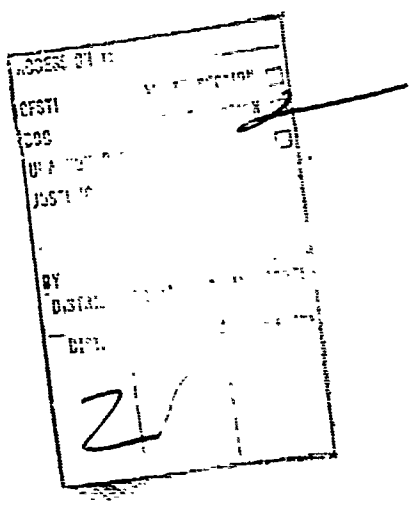

Copies of this report should not be returned unless return is required by security considerations, contractual obligations, or notice on a specific document.

AFML-TR-67-293

INVESTIGATION OF MAGNITUDE AND DISTRIBUTION OF STRESSES IN WELDED STRUCTURES

Rocco Robelotto
Albert Toy
John M. Lambase

FOREWORD

The final technical documentary report covers the work performed under Contract AF33(615)-5433, BPSN No. 66(687351-735102-62405514), from 1 July 1966 to 31 August 1967. The contract was initiated under Project 7351, "Metallic Materials", Task 735102, "Welding and Brazing". The work was performed in the Materials and Producibility Laboratory of the Los Angeles Division of North American Aviation. It was accomplished under the technical direction of Mr. Robert Bowman of the Metals Branch, Metals and Ceramics Division, Air Force Materials Laboratory, Wright-Patterson Air Force Base, Ohio.

This report was submitted by the author in September 1967.

Mr. Rocco Robelotto, Supervisor, and Mr. Albert Toy, Research Specialist, of the Welding Group at NAA/LAD Research and Engineering Division, were Program Manager and Project Engineer, respectively. Others contributing to the program were Mr. John M. Lambase, Mr. Gary Keller, Mr. Charles Moore, and Mr. Alfred Steinberg.

This program was undertaken to determine the pattern and magnitude of weld-induced residual stresses in titanium weldments and their effects on mechanical behavior. The experimental results can provide valuable information for the design and fabrication of welded titanium structures.

This report has been given the internal NAA/LAD number NA-67-716.

This technical report has been reviewed and is approved.

I. Perlmutter
Chief, Metals Branch
Metals and Ceramics Division
Air Force Materials Laboratory

ABSTRACT

An investigation on the magnitude and distribution of residual stresses in titanium sheets induced by TIG welding and their effects on mechanical properties was conducted. The study was made on three titanium alloys. Ti-6Al-4V, Ti-8Al-1Mo-1V, and Ti-5Al-2.5Sn. Residual stresses of similar patterns and magnitudes were obtained for all three alloys at two sheet thicknesses. The transition of residual stresses parallel to the weld occurs abruptly from a peak tension of about 60,000 psi in the weld to compression in the parent metal within 1/2 inch from the weld centerline. There was no apparent adverse effect attributable to residual stresses on the static tensile properties or fracture toughness behavior. Complete removal of residual stresses by thermal treatment significantly improves the fatigue life of unnotched welded specimens and of the center-notched specimens provided the crack tip is not within a compressive residual stress field. Greater notched fatigue resistance was found to occur in as-welded specimens when the notch is in the compressive residual field because the effective net fatigue stress is lowered. Ti-6Al-4V was found to be superior to Ti-8Al-1Mo-1V and Ti-5Al-2.5Sn based on the overall fracture toughness performance, particularly in sea water environment. All three alloys suffer degradation in fracture toughness when heat treated to 1000°F.

Fractographic analysis shows modes of failure of fatigue and fracture toughness tests, and results generally correlate with mechanical test data.

This abstract is subject to special export controls and each transmittal to foreign nationals may be made only with prior approval of the Air Force Materials Laboratory, MAMP, Wright-Patterson Air Force Base, Ohio 45433.

TABLE OF CONTENTS

LIST OF ILLUSTRATIONS

LIST OF ILLUSTRATIONS

LIST OF ILLUSTRATIONS

LIST OF TABLES

Section I

INTRODUCTION

The high strength-to-weight ratio of titanium alloys combined with their good elevated temperature properties makes these alloys attractive for use in high-speed advanced aircraft such as the supersonic aircraft where temperatures in the range of 500°F to 600°F are encountered. In order to minimize weight, however, it is necessary to use welding as a major joining process. One of the disadvantages in using welding for joining titanium alloys is that little information is available concerning the effects of weld-induced residual stresses on the structural capabilities of the weld joint from both metallurgical and mechanical viewpoints. In order to alleviate the potential deleterious effects of residual stresses on titanium alloy weldments, it has been the practice to stress relieve these structures prior to use. Although this practice has resulted in the fabrication of satisfactory structural components and systems, the use of stress relieving imposes severe limitations upon the design of the structure because of the potential hazard of material contamination during stress relief, the limited size of heating facilities suitable for stress relieving, and the increased cost of fabrication.

Numerous studies have been conducted concerning residual stresses in steel. These studies have indicated that the effect of residual stresses on the structural capacity of steel is dependent upon the metallurgical structure of the steel, the test conditions and the environment. If sufficient ductility is present, residual stresses will have no effect upon the failure. However, under certain conditions, such as temperatures below the ductile to brittle transition range, a ductile steel will become brittle and consequently can fail at loads well below the yield strength, particularly in the presence of a flaw. Even under conditions of low cycle cyclic loading at strain aging temperatures, premature failure can occur. This is ostensibly due to strain aging which occurs at the crack tip, thereby producing a microstructure which is brittle. Thus, it can be seen that in order to establish the effects of weld-induced residual stresses on weldments, it is necessary to study those environments under which the structure must function.

The objectives of this program were:

1. Establish the magnitude and distribution of residual stresses in tungsten inert gas (TIG) welded Ti-6Al-4V, Ti-5Al-2.5Sn, and Ti-8Al-1Mo-1V titanium alloys.

2. Determine the effect of residual stress on static tensile, fatigue, and fracture toughness properties under various environments.

3. Analyze and compare the mechanical behavior and metallurgical structure of the welded materials in the as-welded and stress-relieved conditions.

Section II

SUMMARY

A program was conducted to determine the magnitude and distribution of residual stresses in titanium sheet materials induced by TIG welding and their effects on mechanical properties. The study was made on three titanium alloys, Ti-6Al-4V, Ti-8Al-1Mo-1V and Ti-5Al-2.5Sn.

Residual stresses of similar patterns and magnitudes were obtained for all three alloys at two sheet thicknesses. The transition of residual stresses longitudinal to the weld occurs sharply from a peak tensile stress of about 60,000 psi in the weld to a compressive stress within 1/2 inch from the weld edge. The longitudinal compressive stress maximized at less than 10,000 psi at a distance about 1 inch from the edge of the weld. There was scatter in the results of the stresses transverse to the weld although these stresses are small when compared to the longitudinal tensile stress and nearly all compressive. Complete removal of residual stresses was accomplished by a stress-relieving heat treatment of 1450°F for 15 minutes.

The effect of residual stresses on fatigue properties was investigated using unnotched and center notched welded Ti-6Al-4V specimens. Results of unnotched specimens indicate that it took about twice as many cycles to fail the stress-relieved specimens than the as-welded specimens. Data also show that the fatigue resistance of the parent Ti-6Al-4V metal can be fully recovered by the stress-relieving treatment of 1450°F for 15 minutes. Results of notched specimens indicate that the fatigue life in the as-welded condition is two times greater than in the stress-relieved condition using single weld specimens, whereas the direct opposite is true if twin weld specimens were used. It is concluded that if the crack propagation front lies in the compressive residual stress field of the specimen, greater fatigue resistance can be expected from the as-welded condition. This beneficial effect is attributable to the compressive stresses counteracting the tensile fatigue load and consequently reducing the effective maximum fatigue stress.

Fracture toughness studies encompassed three types of testing: (1) center-cracked, (2) edge-cracked, and (3) slow bend fracture toughness. Center-cracked fracture toughness was determined for TIG welded Ti-6Al-4V, Ti-8Al-1Mo-1V, and Ti-5Al-2.5Sn at room temperature in air and in a synthetic sea water environment; additional tests were performed in liquid nitrogen at -100°F for TIG welded Ti-8Al-1Mo-1V and Ti-5Al-2.5SN. The fatigue crack growth rate is considerably higher in the stress-relieved condition than in the as-welded condition concurring with results obtained in fatigue testing. However, there is no distinguishable difference between the as-welded and stress-relieved specimens in each alloy on the basis of net area fracture stress regardless of the test condition. In terms of the overall fracture toughness performance, particularly in sea water environment, Ti-6Al-4V was found to be superior to Ti-8Al-1Mo-1V and Ti-5Al-2.5Sn. In sea water, Ti-6Al-4V retains 90 percent of its room temperature air atmosphere fracture strength as compared to 62 percent for Ti-8Al-1Mo-1V and 52 percent for Ti-5Al-2.5Sn. Fractographic analysis indicated distinct differences in fractured surface appearance between air or LN_2

tested specimens and sea water tested specimens. All air and LN_2 specimens exhibit generally a shear mode of fracture whereas the sea water specimens of Ti-8Al-1Mo-1V and Ti-5Al-2.5Sn fractured initially by corrosion-induced cracking at a slow rate followed by the air-type rapid fracture. The corrosion fractured zone is characterized by its rough and lamellar surface and lateral and transverse cracks. Similar results were obtained with edge-cracked specimens using parent metal samples of Ti-8Al-1Mo-1V and Ti-6Al-4V. The "2B2" processed Ti-8Al-1Mo-1V was significantly better than the duplex annealed material in respect to sea water crack resistance. All three alloys with a prior thermal treatment of 1000°F suffered degradation in fracture toughness in sea water environment. The effect of thermal treatment on toughness was further indicated by results of the slow bend tests on welded specimens. A gross drop in fracture energy per unit area, W/A, resulted from the 1000°F postweld heat treatment. Results of slow bend tests also show that Ti-5Al-2.5Sn has significantly higher fracture toughness than both Ti-8Al-1Mo-1V and Ti-6Al-4V.

Section III

EXPERIMENTAL MATERIALS

EVALUATION OF MATERIAL PROPERTIES

The titanium alloys selected for study in this program were Ti-6Al-4V, Ti-8Al-1Mo-1V, and Ti-5Al-2.5Sn. To provide material for program specimens, each alloy was purchased in two thicknesses, 0.200 and 0.050 inch, in the mill annealed condition, except Ti-8Al-1Mo-1V, which was duplex annealed. In addition, a limited quantity of Ti-8Al-1Mo-1V alloy in the "2B2" condition was evaluated. Condition "2B2" is a mill designation for a heat treatment performed at the mill and consists of 1850°F for 5 minutes, air cooling followed by heating at 1375°F for 15 minutes, and air cooling. The chemical compositions of the three different alloy sheet and plate materials and filler wires are listed in Table I. All materials were within NAA/LAD titanium specification requirements (Ref. 1 through 4).

Table I

PARENT METAL AND FILLER WIRE CHEMICAL COMPOSITION

Material and Condition	Wire Dia. Thick	Sheet Thick Inch	Chemical Composition Percent									
			Al	Sn	V	Mo	Fe	Mn	C	N_2	O_2	H_2
Ti-5Al-2.5Sn	.060	--	5.56	2.72	--	--	.031	.000	.007	.009	.070	.006
Annealed Condition	--	.050	4.90	2.40	--	--	.300	.005	.022	.012	.190	.007
Annealed Condition	--	.200	5.40	2.50	--	--	.420	.010	.020	.008	.140	.006
Ti-6Al-4V	.045	--	6.10	--	3.95	--	.190	--	.025	.013	.095	.010
Condition "A"	--	.050	6.00	--	4.10	--	.150	--	.023	.016	.120	.006
Condition "A"	--	.200	5.90	--	4.10	--	.140	--	.025	.012	.090	.008
Ti-8Al-1Mo-1V	.060	--	7.80	--	1.00	1.00	.080	--	.023	.009	.126	.016
Duplex Anneal	--	.050	7.91	--	0.90	1.16	.120	--	.003	.010	.066	.007
Duplex Anneal	--	.200	7.80	--	1.00	1.00	.040	--	.024	.011	.090	.007
2B2 Treatment	--	.050	7.80	--	1.00	1.00	.030	--	.024	.008	.100	.012

Following receipt of the materials, tests were conducted to determine the tensile properties of the titanium plate and sheet material in the as-received, as-welded, and stress-relieved welded conditions. Specimen configurations used for the tests were as follows:

A - Unnotched Specimen

B - Notched Specimen

Tensile data for the three alloys are shown in Tables II, III, and IV. Stress-relieving after welding was accomplished by heating at 1450°F for 15 minutes followed by air cooling. Transverse weld joint tensile specimens were made in accordance with specimen configuration B to obtain failure in the weld; parent metal tests were also made to compare the results with the unnotched specimens, and to determine the effect of the notch on the ultimate tensile strength. The K_t factor of the notched specimens is approximately 1.1, used mainly for the purpose of effecting failure in the weld rather than in the base metal. All welded specimens were TIG welded.

For the 0.200-inch thick Ti-6Al-4V specimens, the 15 percent difference between the parent metal tensile ultimate values of the two specimen configurations is due to a biaxial-type loading condition at the configuration B notch. The ultimate tensile strength of the as-welded Ti-6Al-4V specimens is 10 percent higher than the notched base metal specimens and remains the same after 1450°F stress relief treatment.

In the duplex anneal condition, the strength of the as-welded Ti-8Al-1Mo-1V specimens is 13 percent higher than the base metal. Neither the Ti-8Al-1Mo-1V nor Ti-5Al-2.5Sn specimens evidenced any difference in tensile properties due to grain orientations where longitudinal and transverse specimens were evaluated. The ultimate tensile strength of the as-welded Ti-5Al-2.5Sn specimens is 35 and 25 percent higher than the base metal for the 0.050- and 0.200-inch thick specimens, respectively. The stress relief treatment showed no noticeable effect on strength of the specimens tested. These data correlate with the differences found between the notched weld specimens and unnotched parent metal for the Ti-6Al-4V alloy.

TEST PANEL WELDING

The titanium sheet and plate stock was cut into strips measuring approximately 5 by 24 inches to provide stock to be welded into test panels measuring about 10 by 24 inches. To keep warpage at a minimum during the welding process, the weld tooling shown in figure 1 was used to position and clamp the titanium panels. The welding equipment consisted of a 400-ampere (dc, single phase) Vickers power supply and an Airco "D" automatic arc voltage head mounted on a Berkley Davis side beam travel carriage.

Initial weld tests were performed using two different weld joint configurations, a square butt and a modified U-joint. Preweld preparation of the square butt joint edges was accomplished by draw filing the edge, followed by brushing with a wire brush wheel, and then wiping with an acetone soaked cloth. The U-joint was made by milling the edges of the stock to be welded, wire brushing the milled edge, and cleaning with acetone. These cleaning procedures produced acceptable weld quality which met NAA/LAD process specification requirements (Ref. 5). The welding parameters used for this area of investigation are listed in Table V.

During the welding process, two techniques were used to shield the weld from atmospheric contamination, one being the standard technique of using a trailing shield with blanket flooding of the back side of the weld with argon. The other technique involved enclosing the weld panels in a plastic bag to provide a total inert atmospheric environment during the welding operation (figure 2). The welding torch enters the bag through a boat which opens and closes a

TABLE II

TENSILE PROPERTIES OF Ti-6Al-4V

Material Thickness (in.)	Test Specimen		Tensile Specimen Data			
			Unnotched			Notched
	Specimen Material and Condition (1)	Grain Dir. (2)	Ultimate Strength (ksi)	Yield Strength (ksi)	Elongation In 2-In. (percent)	Ultimate Strength (ksi)
0.050	PM-Mill Annealed	Trans.	146.3	140.2	12.5	---
		Trans.	146.5	143.2	12.0	---
	Average		146.4	141.7	12.2	---
	WJ- As welded	Trans.	---	---	---	173.9
		Trans.	---	---	---	173.9
		Trans.	---	---	---	174.2
		Trans.	---	---	---	187.2
	Average		---	---	---	177.3
0.200	PM-Mill Annealed	Trans.	135.1	130.9	14.5	149.8
		Trans.	136.1	131.9	12.5	165.5
	Average		135.6	131.4	13.5	157.6
	PM-Mill (3) Annealed	Trans.	134.4	125.4	14.8	158.5
		Trans.	134.3	126.0	13.8	158.5
	Average		134.3	125.7	14.3	158.5
0.200	WJ- As welded	Trans.	---	---	---	174.4
		Trans.	---	---	---	174.8
	Average		---	---	---	174.6
	WJ- As welded (3)	Trans.	---	---	---	171.4
		Trans.	---	---	---	173.1
	Average		---	---	---	172.2

(1) PM = parent metal; WJ = weld joint

(2) Grain direction of parent metal, transverse or longitudinal

(3) Heat treatment: +1450°F or stress relieved for 15 minutes, then air cooled

TABLE III

TENSILE PROPERTIES OF Ti-8Al-4V

Material Thickness (in.)	Test Specimen		Tensile Specimen Data			
			Unnotched			Notched
	Specimen Material and Condition (1)	Grain Dir. (2)	Ultimate Strength (ksi)	Yield Strength (ksi)	Elongation In 2-In. (percent)	Ultimate Strength (ksi)
0.050	PM-2B2 (mill designation)	Trans.	151.1	137.8	14.0	---
		Trans.	147.2	135.2	13.0	---
		Trans.	146.7	131.7	13.5	---
		Long.	144.4	127.6	11.5	---
	Average		147.4	133.1	13.0	---
	PM-2B2 (3)	Trans.	150.6	136.8	13.5	---
		Trans.	148.5	135.5	13.5	---
	Average		149.6	136.2	13.5	
	PM-Duplex Annealed	Trans.	145.9	132.0	11.0	
		Trans.	148.6	127.6	12.0	
	Average		147.3	129.8	11.5	---
	WJ-As welded	Trans.	---	---	---	181.9
		Trans.	---	---	---	185.0
		Trans.	---	---	---	181.4
		Trans.	---	---	---	185.8
	Average		---	---	---	183.5
0.200	PM-Duplex Annealed	Long.	149.4	132.7	18.3	---
		Long.	149.1	130.0	17.5	---
		Long.	152.2	138.5	19.1	---
		Long. (4)	142.6	131.9	17.0	---
		Long. (4)	143.9	134.3	16.5	---
		Trans (4)	150.7	138.1	15.5	---
		Trans (4)	149.4	136.5	15.0	---
		Trans.	142.9	131.2	14.5	---
		Trans.	143.2	131.9	13.5	---
	Average		147.0	133.9	16.3	---
0.200	PM-Duplex (3) Annealed	Trans.	143.0	131.3	15.0	---
		Trans.	142.2(5)	---	15.0	---
	Average		143.6	131.3	15.0	---
	WJ- As welded	Trans.	---	---	---	166.9
		Trans.	---	---	---	166.0
	Average		---	---	---	166.5
	WJ- As welded (3)	Trans.	---	---	---	181.3
		Trans.	---	---	---	165.5
	Average		---	---	---	173.4

(1) PM = parent metal; WJ = weld joint
(2) Grain Direction of parent metal, transverse or longitudinal
(3) Heat treatment: + 1450 F for 15 minutes, then air cooled
(4) Vendor data
(5) Extensometer malfunction, yield not obtainable

TABLE IV

TENSILE PROPERTIES OF Ti-5Al-2.5Sn

Material Thickness (in.)	Test Specimen		Tensile Specimen Data			
			Unnotched			Notched
	Specimen Material and Condition (1)	Grain Dir. (2)	Ultimate Strength (ksi)	Yield Strength (ksi)	Elongation In 2-In. (percent)	Ultimate Strength (ksi)
0.050	PM-Mill Annealed	Long.	136.6	128.8	15.5	---
		Trans.	138.9	129.4	15.0	---
	Average		137.7	129.1	15.2	---
	WJ- As welded	Long.	---	---	---	185.4
		Long.	---	---	---	184.3
	Average		---	---	---	184.8
0.200	PM-Mill Annealed	Long. (4)	124.5	113.0	16.0	---
		Long. (4)	122.0	115.6	16.0	---
		Long.	121.0	113.0	16.3	---
		Long.	121.7	111.3	16.0	---
		Long.	121.0	113.0	16.5	---
		Trans.	122.3	111.1	15.5	---
		Trans.	121.6	110.5	16.0	---
	Average		122.0	112.5	16.0	---
	PM-Mill Annealed (3)	Trans.	123.8	111.5	12.5 (5)	---
		Trans.	124.0	110.7	11.5 (5)	---
	Average		123.9	111.2	12.0	---
	WJ- As welded	Trans.	---	---	---	155.0
		Trans.	---	---	---	150.6
	Average		---	---	---	152.8
	WJ- As welded (3)	Trans.	---	---	---	154.1
		Trans.	---	---	---	155.4
	Average		---	---	---	154.7

(1) PM = parent metal; WJ = weld joint

(2) Grain direction of parent metal, transverse or longitudinal

(3) Heat treatment: + 1450 F for 15 minutes, then air cooled

(4) Vendor data

(5) Failed off center of gage length. Elongations in 1 inch are 27 and 24 percent in the as-received condition and 22 and 23 percent after 1450 F treatment

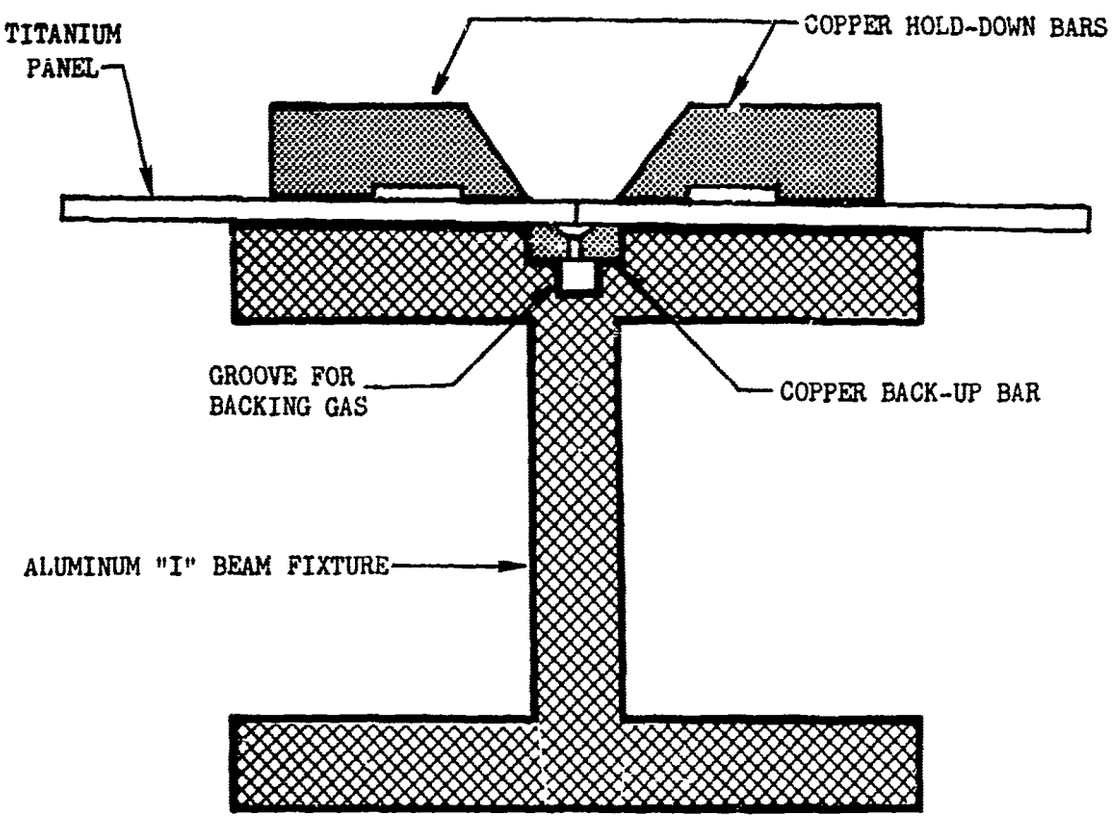

Figure 1. Sketch of Weld Tooling

TABLE V

WELDING PARAMETERS AND RESULTS FOR Ti-6Al-4V 0.200-INCH WELD PANELS

Welding Parameters	Panels						
	"A"		"6P2"		"B"		
Joint Design	Square Butt		Double "U"		Square Butt		
Weld Passes	1	2	1	2	1	2	3
Current	200	170	205	205	140	125	120
Voltage	12.5	12.5	12.5	12.5	12	12	12
Torch Travel Speed(in./min.)	4	4	6	6	6	6	6
Wire Travel Speed(in./min.)	---	30	7	7	13	46	55
Ti-6Al-4V Wire Diameter (in.)	---	0.045	0.045	0.045	0.045	0.045	0.045
Holddown Material	Cu	Cu	Cu	Cu	Cu	Cu	Cu
Holddown Spacing (in.)	3/8	3/8	13/32	13/32	13/32	13/32	13/32
Backup Material	Cu	Cu	Cu	Cu	Cu	Cu	Cu
Backup Groove Width (in.)	3/8	3/8	3/8	3/8	11/32	11/32	11/32
Tungsten Diameter (in.) *	3/32	3/32	3/32	3/32	3/32	3/32	3/32
Gas Cup Size (Airco Number)	8	8	8	8	8	8	8
Torch Helium Gas Flow (ft^3/hr)	60	60	60	60	60	60	60
Trailer Shield Argon Flow (ft^3/hr)	20	20	20	20	---	---	---
Backup Argon Gas Flow (ft^3/hr)	10	10	---	---	---	---	---
Backup Helium Gas Flow (ft^3/hr)	---	---	20	20	---	---	---

Weld Procedure and Results

Shielding	Trailing	Trailing	Plastic Bag
Welding Procedure	2 passes, one side	1 pass, each side	1 pass, one side; 2 passes opposite side
Interstitial Percent:			
Hydrogen	0.003	0.003	0.004
Oxygen	0.095	0.179	0.117
Nitrogen	0.035	0.020	0.021

* Tungsten configuration: blunt

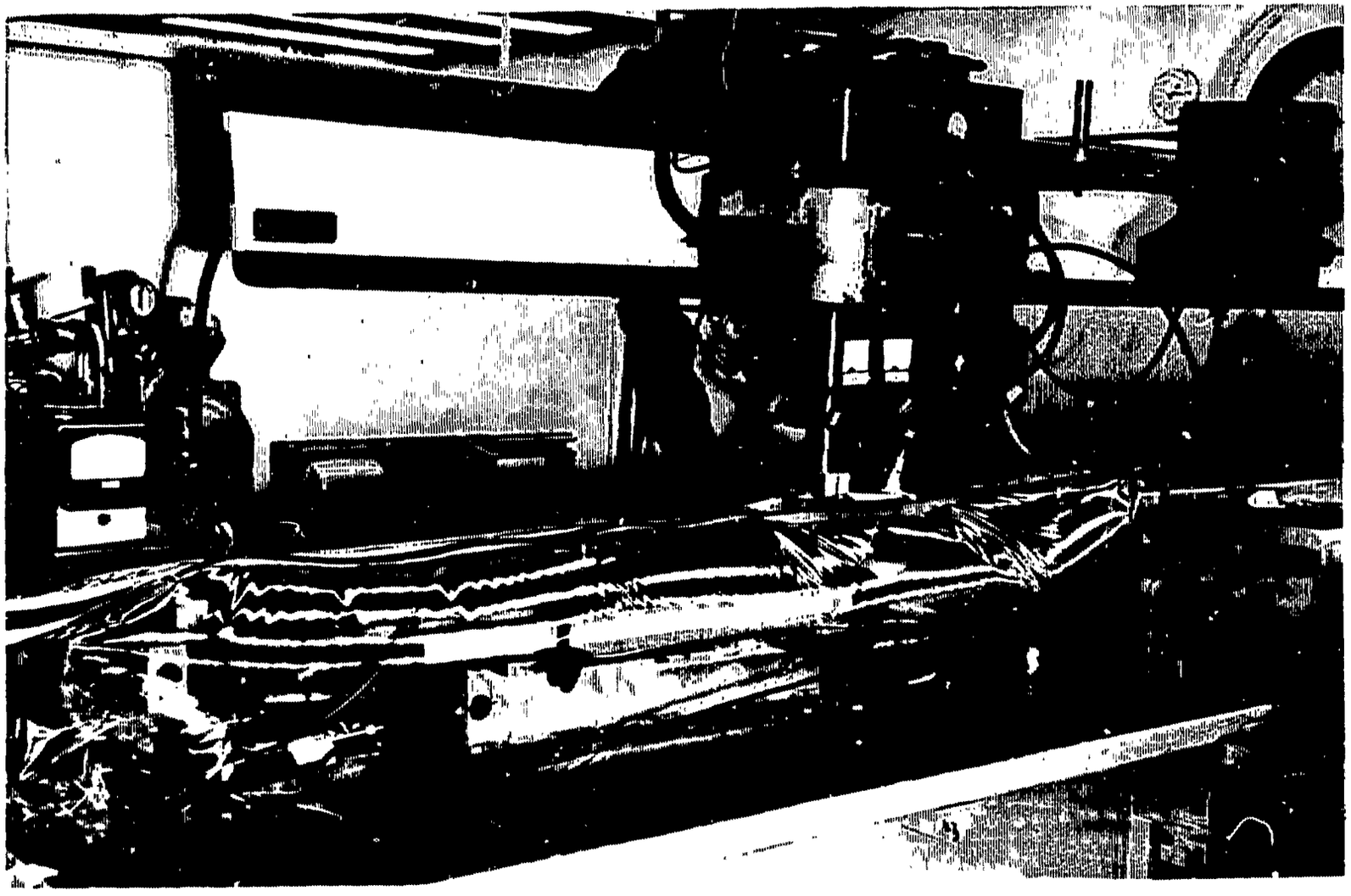

Figure 2. Weld Fixture With Plastic Bag Enclosure

zipper as the torch moves along the weld joint. The boat and zipper provide a seal for the bag, ensuring retention of the inert atmosphere. This system was developed to weld titanium corrugated sandwich where accessibility to the core for prevention of atmospheric contamination was not available. The system was used in this program for comparative purposes.

Weldments made by both techniques were free of discoloration, although those made in the plastic bag were slightly brighter. Both techniques were considered satisfactory. This conclusion was verified by chemical analysis of the welds, the results of which are included in Table V. The weld joint interstitial values were below the Ti-6Al-4V values specified in the NAA/LAD specifications (Ref. 5) which establish purchasing specifications for Ti-6Al-4V alloys at NAA/LAD; the maximum allowable concentration of interstitial contaminants in percent permitted by the specification is as follows: Hydrogen - 0.012, oxygen - 0.20, and nitrogen - 0.070.

The three-pass welds were made using the following sequence:

1. Make root pass.

2. Turn plate over and make a fill pass in opposite direction of the root pass.

3. Turn plate over and make the final pass in the same direction as the first pass.

Satisfactory welds were obtained as a result of this procedure; however, a slight rotation in the plates occurred. To alleviate this problem, larger clamps were used to increase the clamping force holding the plates onto the welding fixture. Subsequent weldments were kept relatively flat using this procedure. To obtain a comparison of the effects of weld passes on peak longitudinal stresses a two-pass weldment was also made. In this case, a burn-through fusion pass was made and a second one was made in a direction opposite to the first pass, but from the same side of the weld joint. Filler wire was added during the second pass to compensate for the loss of metal due to drop through. This weld was approximately 3/16-inch wider than the three-pass weld (3/8 versus 9/16 inch) on the torch side of the weld and 3/16-inch narrower on the root side of the weld (3/8 versus 3/16).

A second two-pass weldment was made with one weld pass from each side of the panel using a square butt joint. This technique was selected to obtain maximum panel flatness. When both weld passes were made from one side, a slight curvature of the test panel occurred, which would subject the weld joint to a bending load during subsequent testing. This would introduce another variable in the mechanical tests and could affect test results. Since welding on both sides of the joint produced the flattest panel, this procedure was chosen for joining the test panels in this program.

A photomacrograph of the weld made with a pass on each of the joints (figure 3) indicates that excellent sidewall fusion, 100 percent penetration, and no undercut were obtained. A nick break at the center of the 5/8-inch wide weld specimen also indicated no lack of fusion at the joint. Radiographic examination revealed scattered and negligible amounts of porosity in a 12-inch long weld sample which met NAA/LAD specification weld quality requirements.

Figure 3. Photomacrograph (5X) of Ti-6Al-4V Welded Joint Using Ti-6Al-4V Filler Wire and With Weld Passes Made on Both Sides of Panel

Section IV

RESIDUAL STRESS STUDIES

Studies were made to establish the residual stress distribution and magnitude resulting from automatic tungsten inert gas welding of titanium alloys. Two techniques were investigated for measuring residual stress, one of which was the strain gage method. The second method involved the measurement of elastic relaxation occurring between scribed lines, the measurements being taken before and after removal of a plug specimen from the test panel. The strain gage method appeared to be the more desirable technique based on results of the initial evaluation. As a consequence, the strain gage method was employed to obtain residual stress data from the welded titanium panels. The data obtained were plotted to provide graphic display of residual stress in the panels. The test methods and results are described in detail in subsequent paragraphs.

RESIDUAL STRESS MEASURING TECHNIQUES

In the scribed line method, which will be described first, longitudinal and transverse scribed lines are applied to a given length of material. The intersections of the scribed lines are then used as points of measurements before and after removal of the plug section from the welded specimen. This method is advantageous in that it allows multiple readings in a narrow plug, thereby allowing measurement of stress gradients. The disadvantage of this technique is that the distance being measured must be of the order of 1 inch to obtain sufficient relaxation and of the order of 0.001 inch, for valid measuring. This leads to the necessity of using a 1-inch square plug if one is to measure stress distribution in both directions or in areas where the transverse stress is substantial (greater than 10 percent of the longitudinal) and would affect the stress relaxation in the longitudinal direction. Also, the dimensions of the plug would necessarily have to be increased in areas of low stress where relaxation due to residual stress would be of a low order.

Stress plugs for the scribed line technique were prepared by scribing lines parallel and perpendicular to the weld. Three sets of lines were drawn in each direction. The intersection of the centerline of each set with the outer two lines of the opposite set formed locations of measurement approximately 1 inch apart. These distances were then measured on an optical comparator capable of reading to 0.0001 inch. All measurements were made in an air-conditioned room having constant temperature to within ±3°F. Afterwards, the plug was removed by cutting with a band saw. Care was taken to ensure that overheating of the specimen did not occur during the cutting operation. The specimens were then remeasured and the residual stresses calculated.

Strain measurements were made using Micromeasurements, Inc, SA-06-250-RA-120 three-element gage rosettes and SA-06-250-BB-120 single-element gages. Surface preparation consisted of machining the weld flush with the parent metal and followed by cleaning with metal conditioner and neutralizer. The gages were then bonded to the weld panels with Eastman 910 cement. The electrical leads were soldered to the gages and the gage area waterproofed with Gagekote No. 1. A dummy gage was prepared in a similar manner. All gages

were measured before and after plug removal and the stresses were calculated by feeding the strain gage readings, the elastic modulus, and Poisson's ratio into a computer program. The principal stresses based on Mohr circle analysis and the "Cartesian stresses" defined by the rosette leg directions were obtained from the IBM 7090 printouts.

EVALUATION OF STRESS MEASURING TECHNIQUES

The residual stress data obtained from the initial tests are listed in Table VI. The results of the scribed line technique were completely unexpected, since they indicate compressive stresses in both the longitudinal and the transverse directions. Originally only weld specimen 1 was to be studied; however, after a careful check of the data and procedures revealed no clue concerning this anomalous result, it was decided to conduct a similar measurement on another weldment. In the latter case, measurements were made on both sides of the weld to ensure that the last weld pass did not cause the first pass of the weld to go into compression, since it was known that the residual stress measurements were made on the first-pass side. The results on the second weldment again indicated longitudinal and transverse compressive stresses. Further, there was excellent correlation between the longitudinal stress values obtained for the last-pass and first-pass side of weld specimen 2 (49.7 ksi versus 55 ksi) and the longitudinal stress value obtained for weld specimen 1 (53.5 ksi). The correlation between the last-pass and the first-pass transverse residual stress was poor (7.1 ksi versus 21.3 ksi) in weld specimen 2; however, the first-pass value of transverse residual stress for weld specimen 1 was in excellent agreement with the first-pass value of transverse residual stress for weld specimen 2 (23.5 ksi versus 21.3 ksi).

It is well established by experimental evidence and theoretical considerations that the longitudinal residual stress must be tensile in the weld; it therefore must be concluded that either there was some error in the experiment or an unexpected phenomenon is occurring. In view of the fact that the results are similar for three sets of data [that all weld metal tests using the same procedure indicated tensile stress and that extreme care was taken, particularly in the case of weld specimen 2 (Table VI)], it does not seem likely that the experimental technique is in error. It would therefore appear that the area of longitudinal compression stress on either side of the weld, added together, exceeds the longitudinal tensile stress which, on averaging, would indicate a longitudinal compression stress in the weld metal. This would also mean that at some distance from the longitudinal compression area, longitudinal tension must again occur in order to obtain a balance of stresses; however, further tests using the scribed line technique and strain gages disproved this assumption as discussed later.

RESIDUAL STRESS MEASUREMENTS

Residual stresses in both thicknesses of each type of titanium alloy welded panel were measured, using the strain gaging technique described for the preliminary tests. Budd Instrument Division Type C5-121B-R35 three-element stacked rosette strain gages were used for the measurements. The overall dimensions of the gages are 0.270 by 0.220 inch. In those cases where single-element strain gages are indicated, Micromeasurements Division SA-06-062-AP-120 gages having

TABLE VI

RESIDUAL STRESS IN WELDED 0.200-INCH Ti-6Al-4V TITANIUM PANELS

Weld Specimen	Plug Dimension Inches	Plug Location Along Weld	Longitudinal Stress	Transverse Stress	No. Weld Passes
Measurement of Scribed Lines					
1	1-1/4 x 1-1/4	Center	-53,600	-23,500	3
	1-1/4 x 1-1/4	2 inches from start of weld	-24,900	-19,600	
2	1-1/4 x 1-1/4	Center, last pass side	-49,700	- 7,100	3
	1-1/4 x 1-1/4	Center, root pass side	-55,000	-21,300	
Strain Gage					
3	2-1/4 x 2	3-7/8 inches from start of weld	20,700	-13,200	3
	1-5/8 x 7/16	Center	63,400	-	
4	1-5/8 x 11/16	Center	64,600	-	2

Note: The minus sign indicates a compressive stress.

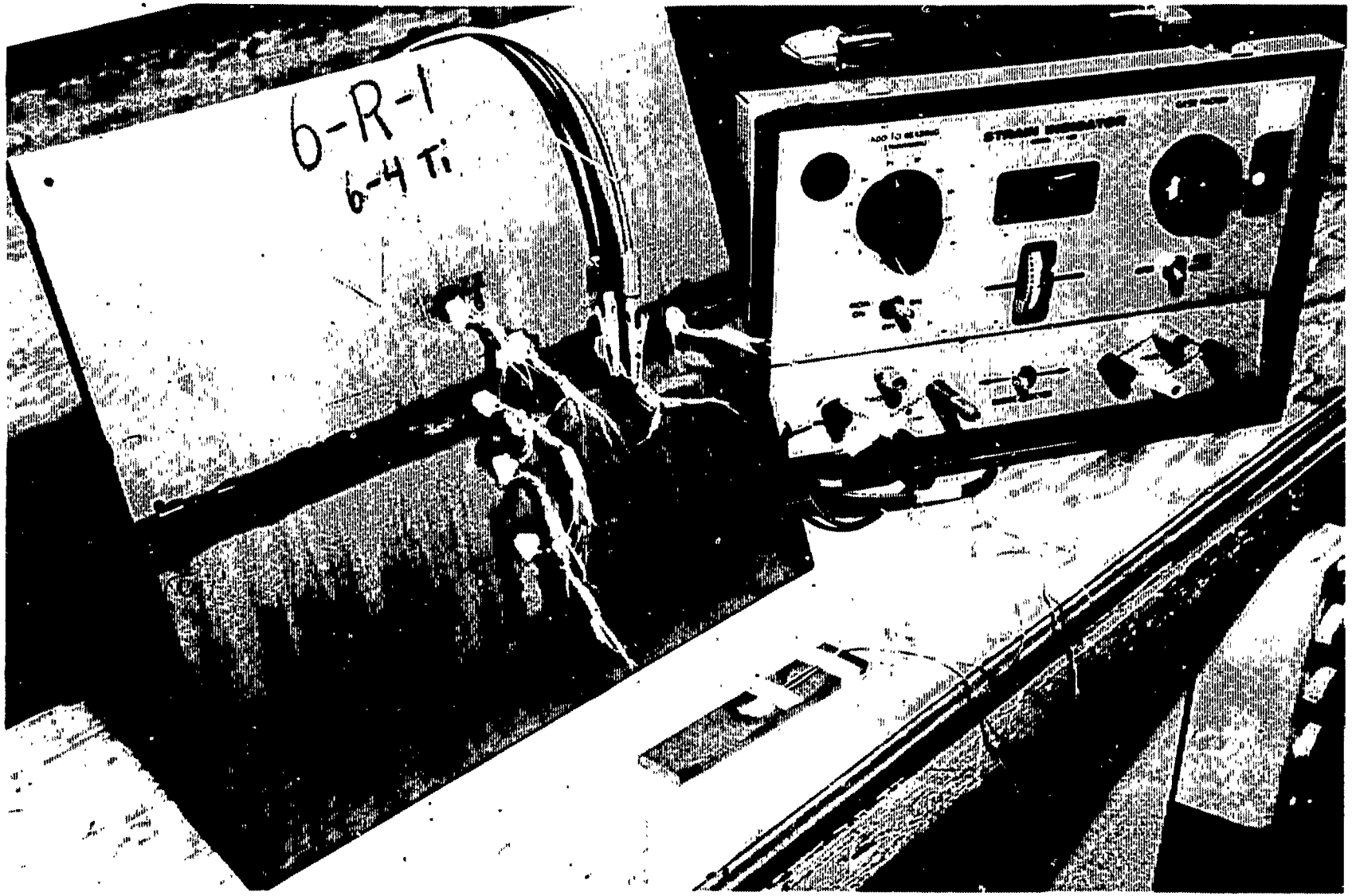

Figure 4. Strain Gage Instrumentation on 0.200-Inch Ti-6Al-4V Panel

overall dimensions of 0.114 by 0.062 inch were used. Figure 4 shows a Ti-6Al-4V alloy plate with the mounted strain gages, the dummy gage used for reference, and the Baldwin-Lima-Hamilton Model 120 Digital Strain Indicator.

STRESS RELIEVING

One 0.200-inch thick panel for each material was stress relieved at 1450°F for 15 minutes and air-cooled. Stress measurements were then made in the center of the plate on the weld using strain gages. Negligible strain was measured in each of the plates, indicating that this temperature was adequate to entirely relieve the residual stresses.

Ti-6Al-4V SPECIMENS

The longitudinal and transverse stresses along the length of the weld in 0.200-inch thick material are shown graphically in figure 5A. The longitudinal stresses in the 0.200-inch plate along the length of the weld are all tensile with a maximum value of approximately 67 ksi about 3-1/2 inches from the end of the plate, leveling off to about 57 ksi towards the center of the plate. The transverse stresses along the length of the weld are compressive towards the ends of the plate, go into tension at about 1-1/2 inches from the ends of the plate, and level out at approximately 4 ksi tension.

The longitudinal and transverse stresses in the direction perpendicular to the weld are shown in figure 5B. The longitudinal stresses in 0.200-inch material along this direction are maximum tension in the weld (57 ksi) and become compressive within 0.25 inch of the weld edge. A maximum compressive stress of approximately 8.5 ksi is attained at about 0.75 inch from the weld centerline and decreases to zero at about 3 inches from the weld centerline. The transverse stresses are tensile at about 4 ksi for approximately 1-1/2 inches from the weld centerline and then decrease to zero at 3 inches from the weld.

In the 0.050-inch thickness, figure 5C, the longitudinal stresses along the length of the weld are tensile with a maximum stress of approximately 58,000 psi occurring approximately 0.75 inches from the end of the plate and leveling off to approximately 50,000 psi 3 inches from the ends of the plate. Note that the point obtained at 7 inches from the end of the plate (55,000 psi tension) using a single-element gage is in fairly good agreement with the data obtained using three-element strain gages. The transverse stresses were found to be compressive along the length of the weld at approximately 12,000 psi.

Ti-8Al-1Mo-1V SPECIMENS

The longitudinal stresses, figure 6A, in the 0.200-inch material along the length of the weld are all tensile with a maximum value of 70 ksi approximately 3-1/2 inches from the ends of the plate, leveling off at about 66 ksi towards the center of the plate. The general shape of the curve is in agreement with that obtained for the Ti-6Al-4V alloy; however, the magnitude of the stresses is slightly higher for the Ti-8Al-1Mo-1V. The transverse

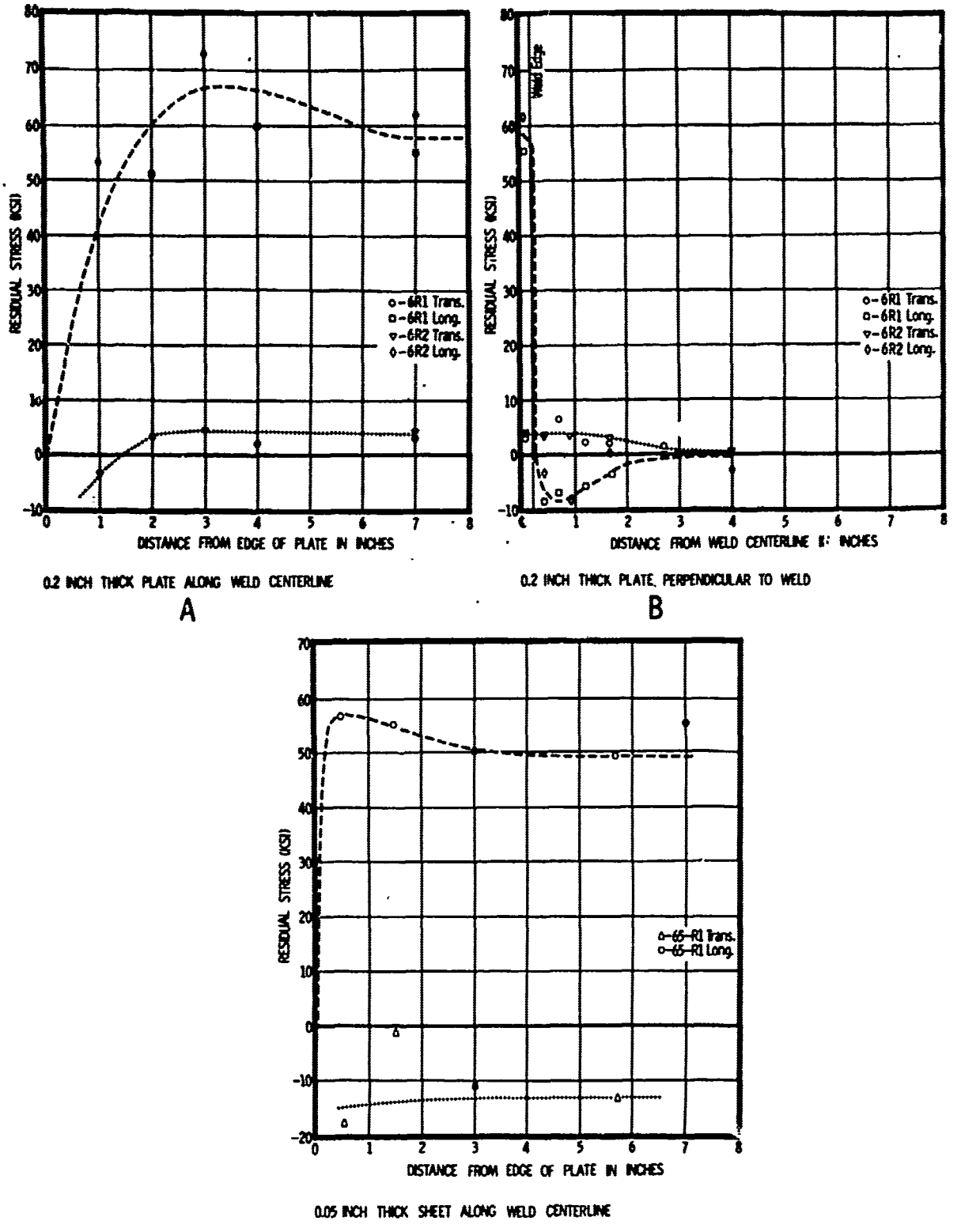

Figure 5. Longitudinal and Transverse Residual Stresses in As-Welded Ti-6Al-4V Panels

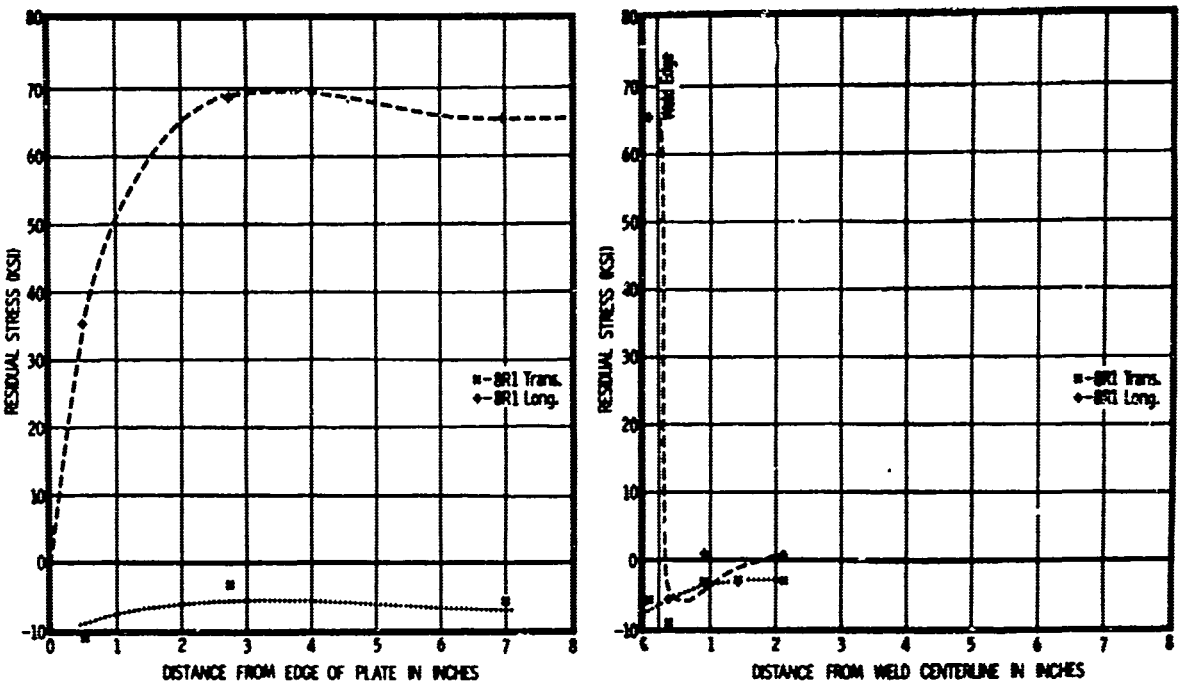

0.2 INCH THICK PLATE ALONG WELD CENTERLINE

A

0.2 INCH THICK PLATE PERPENDICULAR TO WELD

B

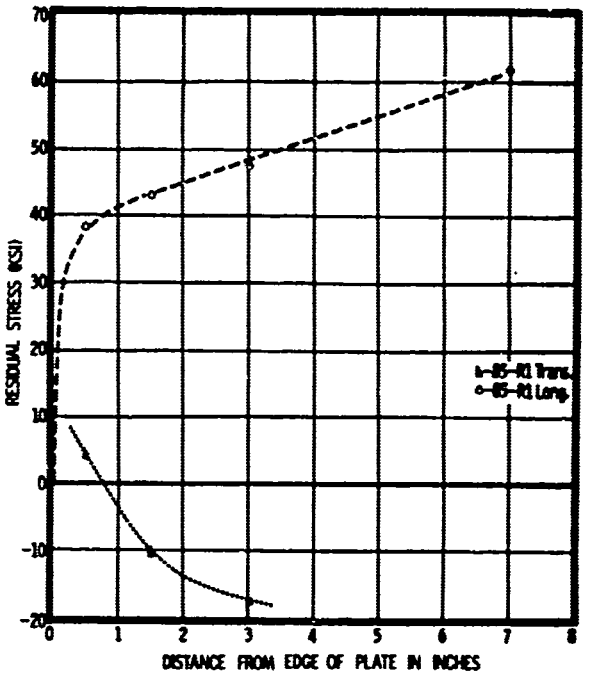

0.05 INCH THICK SHEET ALONG WELD CENTERLINE

C

Figure 6. Longitudinal and Transverse Residual Stresses in As-Welded Ti-8Al-1Mo-1V Panels

stresses are compressive along the entire length of the weld. Towards the ends of the plate the compressive stress increases, but the major length of the weld is in compression at approximately 7 ksi. This is in contrast to the transverse tensile stresses found in the Ti-6Al-4V alloy.

The longitudinal stresses, figure 6B, in a direction perpendicular to the weld direction in the center region of the plate are at a maximum of approximately 66 ksi along the weld, go into compression within 0.25 inch of the weld edge, reach a maximum compressive stress of approximately 6 ksi, and approach zero at 2 inches from the weld centerline. The transverse stresses in this direction are all compressive with a maximum compressive stress of approximately 7 ksi in the weld, decreasing to about 3 ksi at 2 inches from the weld centerline.

A single-element strain gage 7 inches from the end of the 0.050 inch sheet on the weld centerline was used to minimize the amount of base material removed with the strain gage for comparison with the larger plugs obtained using three-element gages. All three-element gages were also along the weld centerline for the 0.050-inch sheet except one, which was 3/8 inch from the weld edge and 7 inches from the end of the plate. The longitudinal stresses, figure 6C, in the 0.050-inch material along the length of the weld are all tensile. No peak value was found towards the ends of the panel as in the 0.050- and 0.200-inch Ti-6Al-4V alloy or the 0.200-inch Ti-8Al-1Mo-1V alloy. The data point obtained at a point 7 inches from the end of the sheet (62 ksi) was obtained using the single-element strain gage. The transverse stresses along the length of the weld were tension at the ends of the sheet, go into compression within 1 inch of the ends of the sheet, and level out at approxmiately 20 ksi compression towards the center of the sheet.

Ti-5Al-2.5Sn SPECIMENS

The longitudinal stresses in the 0.200-inch material along the length of the weld, figure 7A, are all tensile with a maximum value of 72 ksi in the center region of the plate. This is approximately 15 percent higher than the stresses obtained in the Ti-6Al-4V alloy (57 ksi) and approximately 10 percent higher than the stresses obtained in the Ti-8Al-1Mo-1V alloy (66 ksi) of the same thickness. Ti-5Al-2.5Sn alloy did not have a peak value of longitudinal stress towards the ends of the plate as indicated with the other two alloys. The transverse stresses along the length of the weld exhibited tension at the start of the weld and shifted into compression about 1-1/2 inches from the ends of the plate, leveling out at a compressive stress of approximately 2 ksi. The Ti-8Al-1Mo-1V alloy also contains compressive transverse stresses throughout the length of the weld, with a magnitude (7 ksi) thrice that in the Ti-5Al-2.5Sn alloy. The reverse of this was indicated by the Ti-6Al-4V alloy, which exhibited a compressive stress at the start of the weld and changed to a tensile stress after 1-1/2 inches, leveling off at about 3 ksi.

The longitudinal stresses, figure 7B, in the 0.200-inch thick Ti-5Al-2.5Sn plate dropped sharply from a 72 ksi maximum tension at the weld center to compression within 1-1/2 inches of the weld centerline.

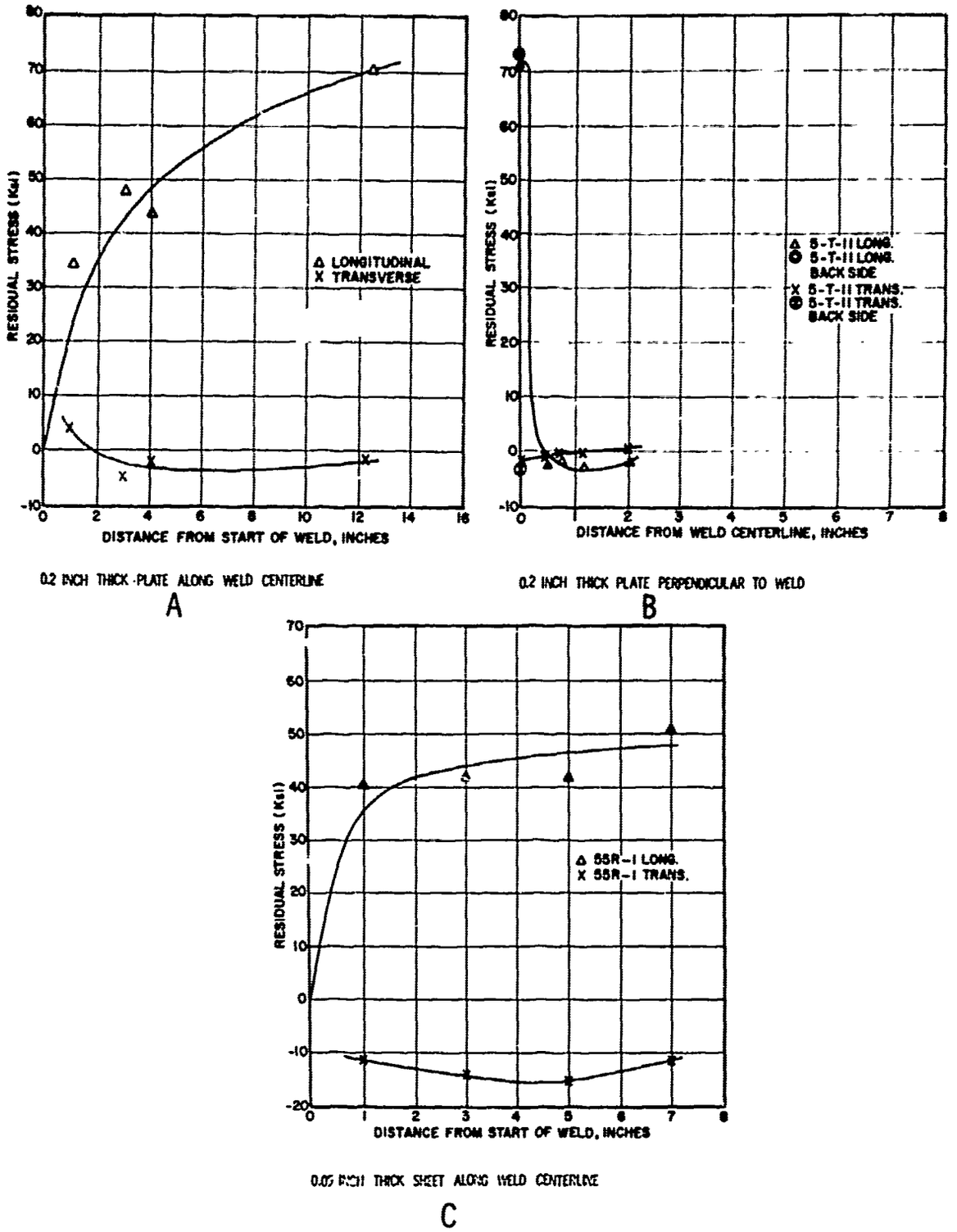

Figure 7. Longitudinal and Transverse Residual Stresses in As-Welded Ti-5Al-2.5Sn Panels

The longitudinal compressive stress reaches a maximum of about 3 ksi at a point 1-1/4 inches from the weld centerline and presumably diminishes with distance from the weld. Measurements stopped at 2 inches from the weld centerline. The transverse stress perpendicular to the weld is 2 ksi compression in the weld, becomes zero at approximately 1-1/4 inches from the weld centerline, and finally slightly tensile at 1-1/2 inches from the weld centerline.

In the 0.050-inch material, figure 7C, the longitudinal stresses along the length of the weld are tensile with a maximum stress of approximately 50 ksi occurring in the center of the weld length. The transverse stresses are compressive stresses of approximately 12 ksi. These longitudinal and transverse stresses are approximately the same as those obtained for the 0.050-inch thick Ti-6Al-4V alloy, but somewhat lower than those obtained for the Ti-8Al-1Mo-1V alloy (60 ksi longitudinal tension and 20 ksi transverse compression). As in the case of the Ti-8Al-1Mo-1V alloy, no peak longitudinal tensile stress was observed towards the ends of the sheet in contrast to the peaks obtained in the sheet and plate Ti-6Al-4V alloy and the plate Ti-8Al-1Mo-1V alloy. A three-element strain gage 7 inches from the end of the plate and 3/8 inch from the weld centerline indicated that at this point the longitudinal stress drops to approximately 25 ksi tension and the transverse stress is approximately 3 ksi tension in the 0.050-inch sheet.

RESIDUAL STRESSES BETWEEN TWO PARALLEL WELDS

Tests were conducted to measure the residual stresses in the region between two parallel welds 2 inches apart because of the unexpected phenomenon observed during the fatigue precracking of the fracture toughness specimens. It was observed that the twin-weld specimens in the as-welded condition took about five times as many cycles to grow the same crack length as the stress-relieved twin-weld specimens or the as-welded single-weld specimens. Very high compressive residual stresses were suspected to exist in the as-welded twin-weld specimens. In this experiment the strain gage locations and the corresponding residual stress results are as follows:

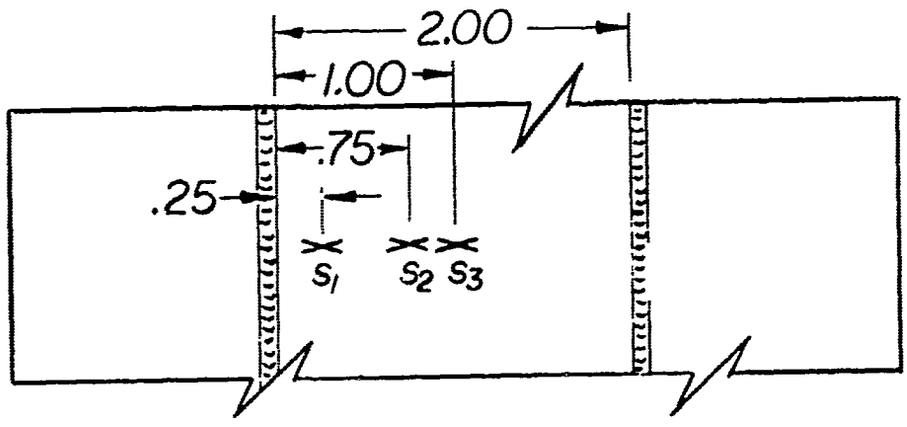

Location of Strain Gage	Longitudinal Residual Stress (psi)	Transverse Residual Stress (psi)
S_1 - 1/4 in. from weld edge	-18,200	-9,800
S_2 - 3/4 in. from weld edge	-17,000	-10,700
S_3 - 1 in. from weld edge (midway between two welds)	-21,500	-16,800

Both the longitudinal and transverse residual stresses are compressive, maximizing toward the center between the two welds, and appreciably higher than the single-weld specimens at the same locations relative to the weld edge. Therefore, the experiment confirmed that very high compressive residual stresses are present in the region between two parallel welds. The results also serve to explain the extremely high fatigue crack resistance as shown in the fracture toughness specimens. On the other hand, if the initial slot crack front is in a tensile stress field rather than in the compressive stress field, as in the case of the center-notched Ti-6Al-4V fatigue specimens with welds 1/2 inch apart, then cracking will initiate prematurely and grow more rapidly in fatigue compared to the stress-relieved condition (see figure 14).

EFFECT OF SLOT AND PRECRACKING ON RESIDUAL STRESSES

An experiment was designed to determine the effect of EDM slot and fatigue precracking on residual stresses. Since all other residual stress measurements in this program were performed on undamaged welded specimens, the influence of the crack on the magnitude and direction of the residual stresses is not known. In order to evaluate realistically the effects of residual stresses on precracked fatigue and fracture toughness behavior, it is highly desirable to perform this experiment. In this investigation, two gages were used, one located at the weld centerline and the other 1/2 inch from the weld edge and 5/8 inch from the line of precracking as shown in the following sketch.

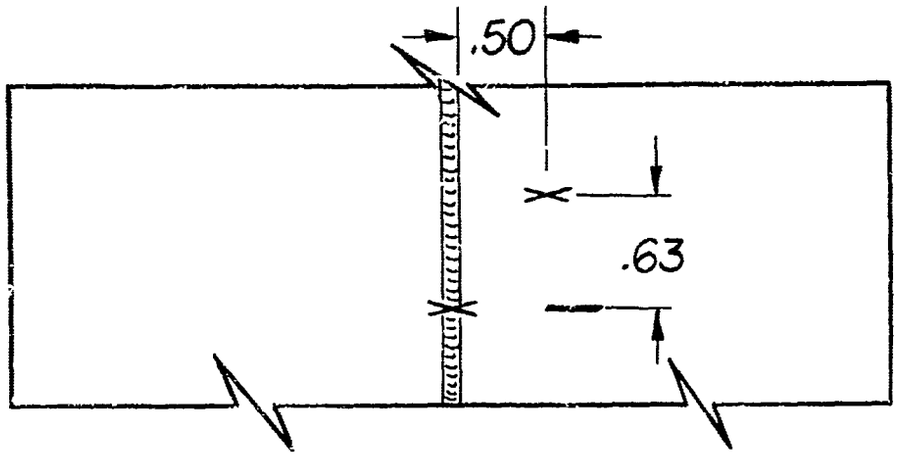

Strain readings were taken prior to EDM machining of the slot, after machining the slot and after fatigue precracking. The following tabulation shows the changes in residual stresses resulting from each processing step:

Process	Change in Residual Stress (psi)			
	Weld Center		1/2 In. From Weld Edge	
	Long.	Trans	Long.	Trans
As-Welded	None*	None	None	None
After EDM Slot	-410	-280	+5100	+230
After Fatigue Precracking	-375	+980	+3100	-1700

* Longitudinal stress in the weld center was 72,900 for this test panel.

There is practically no change in the longitudinal residual stress in the weld. The appreciable change occurring in the area 1/2 inch from the weld edge could be due to the relieving effect of the precrack experienced by the strain gage immediately adjacent to it. After fatigue cracking, a plug containing the weld center gage was removed and the strain was measured. The result shows a longitudinal tensile stress of 72,900 psi, which agrees with previous data. It is therefore concluded that the EDM slot and fatigue cracking have little effect on the residual stresses at the weld. One probable explanation for this is that the size of the test panel is very large compared to the size of the crack area.

VERIFICATION OF STRESS DISTRIBUTION BY THE SCRIBED LINE TECHNIQUE

A limited series of tests was performed employing the scribed line technique previously described. This series of tests was conducted to verify the strain gage data curve in areas where steep stress gradients were known to exist and in an attempt to clarify the changes in stress measurements with changes in stress plug size. It was believed that the multiple readings obtained by the scribed line technique would show any unexpected variations in stress. In the 0.200-inch Ti-6Al-4V welded panel, the tensile stress gradient obtained in this manner (Table VII) closely follows the strain gage data curve verifying the strain gage data.

A series of tests was also conducted on the Ti-8Al-1Mo-1V weld panels to verify that there were no high compression stresses lost due to the size of the strain gage test plugs. Using a 1-1/4 by 1-1/4 inch square strain-gaged plug, the longitudinal stress was 50 ksi tension and 18.5 ksi compression. This is a variance of approximately 14 ksi in the tension data (52.2 versus 66.0 ksi) and of 11 ksi in the compression data (18.5 versus 7.0 ksi) obtained when using the smaller strain-gaged stress plugs for the data plotted in figure 6B. Attempts to clarify the reasons for this difference using the scribed line technique were fruitless. Scribed lines on the same plug indicated a longitudinal tensile stress of approximately 70 ksi (Table VII) which is in fairly good agreement with the strain gage data obtained on the smaller stress plugs. These results also are not in agreement with the scribed line results obtained in the measuring techniques evaluation tests. Scribed line studies in the compresssive stress field area, 0.3 to 0.8 inch, as listed in Table VII, did not show any marked new information. All values indicated low tensile stresses. This is due to disregarding the transverse stresses. Based upon these results, it is believed that no narrow region of high compression stresses exists in the vicinity of the weld.

TABLE VII

SCRIBED LINE STRESS DATA ON 0.200-INCH THICK TITANIUM ALLOY PANELS

Distance From Weld Centerline (inches)	Original Length (inches)	Length After Removal (inches)	Change in Length (inches)	Tensile Stress (ksi)
Ti-6Al-4V				
0.185 (weld edge)	0.9992	0.9963	0.0029	47.3
0.200	0.9993	0.9965	0.0028	45.6
0.235	0.9992	0.9966	0.0026	42.4
0.260	0.9992	0.9970	0.0022	35.9
0.285	0.9996	0.9977	0.0019	31.0
0.310	0.9992	0.9975	0.0019	27.7
0.335	0.9993	0.0077	0.0016	26.1
0.360	0.9995	0.9990	0.0005	8.15
0.385	0.9996	0.9986	0.0010	16.3
0.410	0.9996	0.9988	0.0008	13.1
0.435	0.9995	0.9991	0.0004	6.5
Ti-8Al-1Mo-1V				
0	1.0005	0.9964	0.0041	71.0
0.367	0.9998	0.9995	0.0003	---
0.417	0.9999	0.9996	0.0003	---
0.467	1.0000	0.9995	0.0005	---
0.517	0.9999	0.9995	0.0004	---
0.567	1.0000	0.9996	0.0004	---
0.577	0.9996	0.9991	0.0005	---
0.617	0.9999	0.9994	0.0005	---
0.627	0.9995	0.9993	0.0002	---
0.677	0.9995	0.9994	0.0001	---
0.727	0.9996	0.9995	0.0001	---
0.777	0.9997	0.9995	0.0002	---
0.827	0.9997	0.9997	0.0000	---

Section V

FATIGUE STUDIES

Fatigue studies were conducted on specimens prepared from each of the three types of titanium alloy weld panels. Two basic types of fatigue specimens were used for fatigue testing, unnotched and center-notched. The studies encompassed testing of as-welded and stress-relieved specimens to obtain comparative data. Testing procedures and results are presented in subsequent paragraphs.

CENTER-NOTCHED Ti-6Al-4V FATIGUE TESTS

All precracked fatigue specimens were of the configuration shown in figure 8. The crack starter was made by drilling a hole 1 inch from the edge of the weld and making a saw cut as shown. Stress relieving and pickling of the stress-relieved specimens were performed before machining to prevent contamination of the crack starter. After machining, the crack starter was washed with acetone to ensure cleanliness.

The specimens were mounted with load plates into a Baldwin-Lima-Hamilton IV-12 fatigue machine with a load multiplier. Fatiguing was performed at 1200 cpm at a stress ratio (R factor) of 0.1 with a maximum stress of 25,000 psi.

Crack length measurements were made during cyclic loading with 20-power telescopes and a surveyor's transit (figure 9). A machinist's scale with 0.01-inch graduations was attached to the specimen directly above the fatigue crack. Crack growth was recorded by simultaneously observing the scale and each side of the crack tip through each telescope. With the panels cycled at 1200 cpm, a synchronized stroboscopic light was used to provide clear observation of the crack and the readings which were taken during cycling.

The fatigue data for the stress-relieved and as-welded specimens are presented graphically in figure 10. Failure of the stress-relieved specimens occurred at 21,900 and 24,000 cycles, while failure of the as-welded specimens occurred at 54,800 and 38,100 cycles. For comparison purposes, the crack length versus cycles to grow the total crack for these specimens is also plotted in figure 11. In order to eliminate the variable of dwell time to initiate the crack and to obtain data using the same initial length, all graphs start with the origin at the 0-0 axis with a total fatigue crack length equal to 1/2 inch and with the cycles of fatigue at this point being considered as zero. Using these starting points, the cycles to failure for stress-relieved specimens are 18,800 and 14,900, and the cycles to failure for the as-welded specimens are 29,700 and 39,200.

The difference in fatigue life of the as-welded specimens compared to the stress-relieved specimens is attributed to the location of fatigue crack. The original crack starter notch was located within the residual stress compressive field for the as-welded specimens and was still within the original compressive field well after the crack length had increased beyond the 1/2 inch fatigue crack length. Thus, it can be assumed that the effective fatigue stress is the

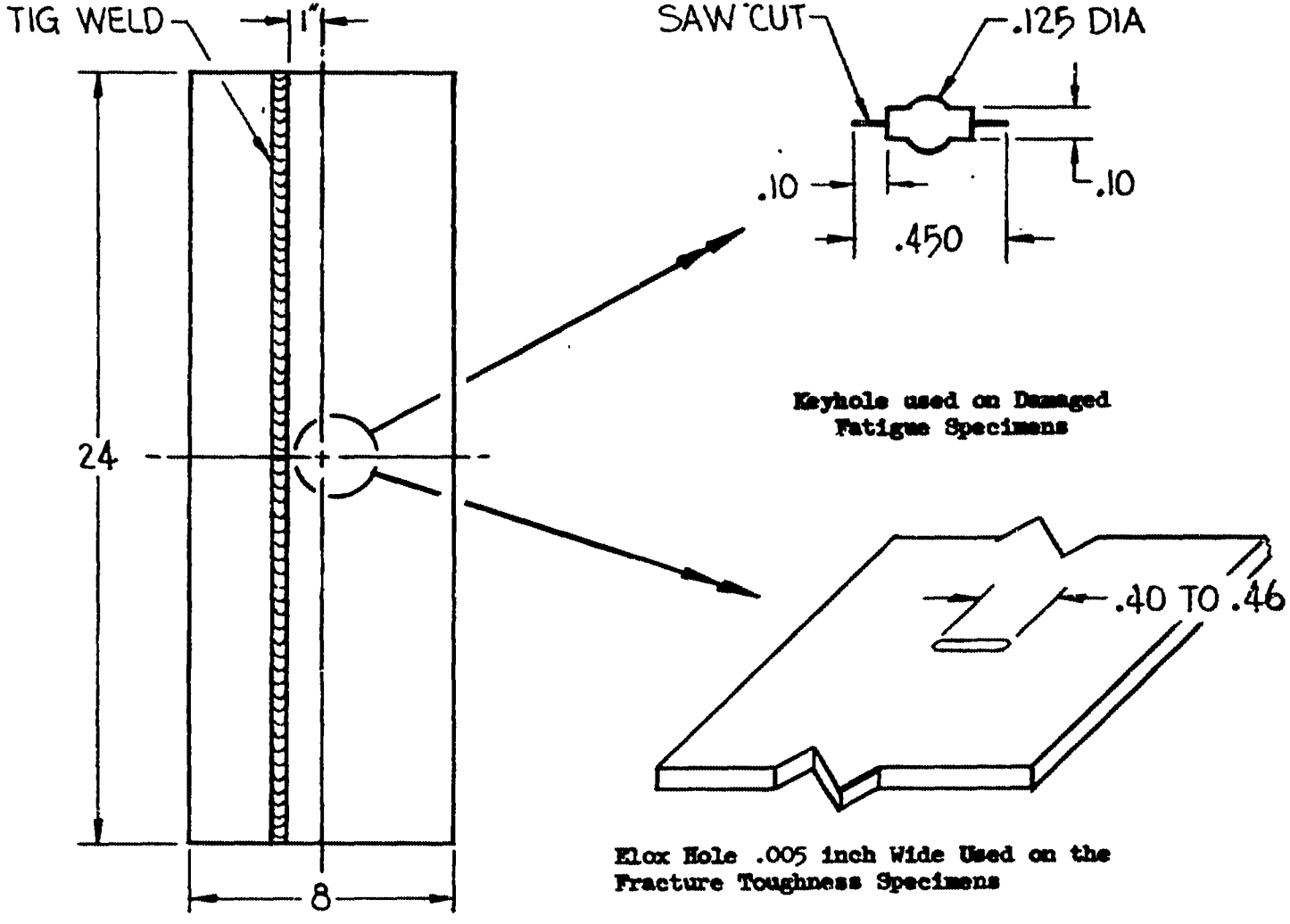

Figure 8. Configuration of Specimens Used in Fatigue Studies

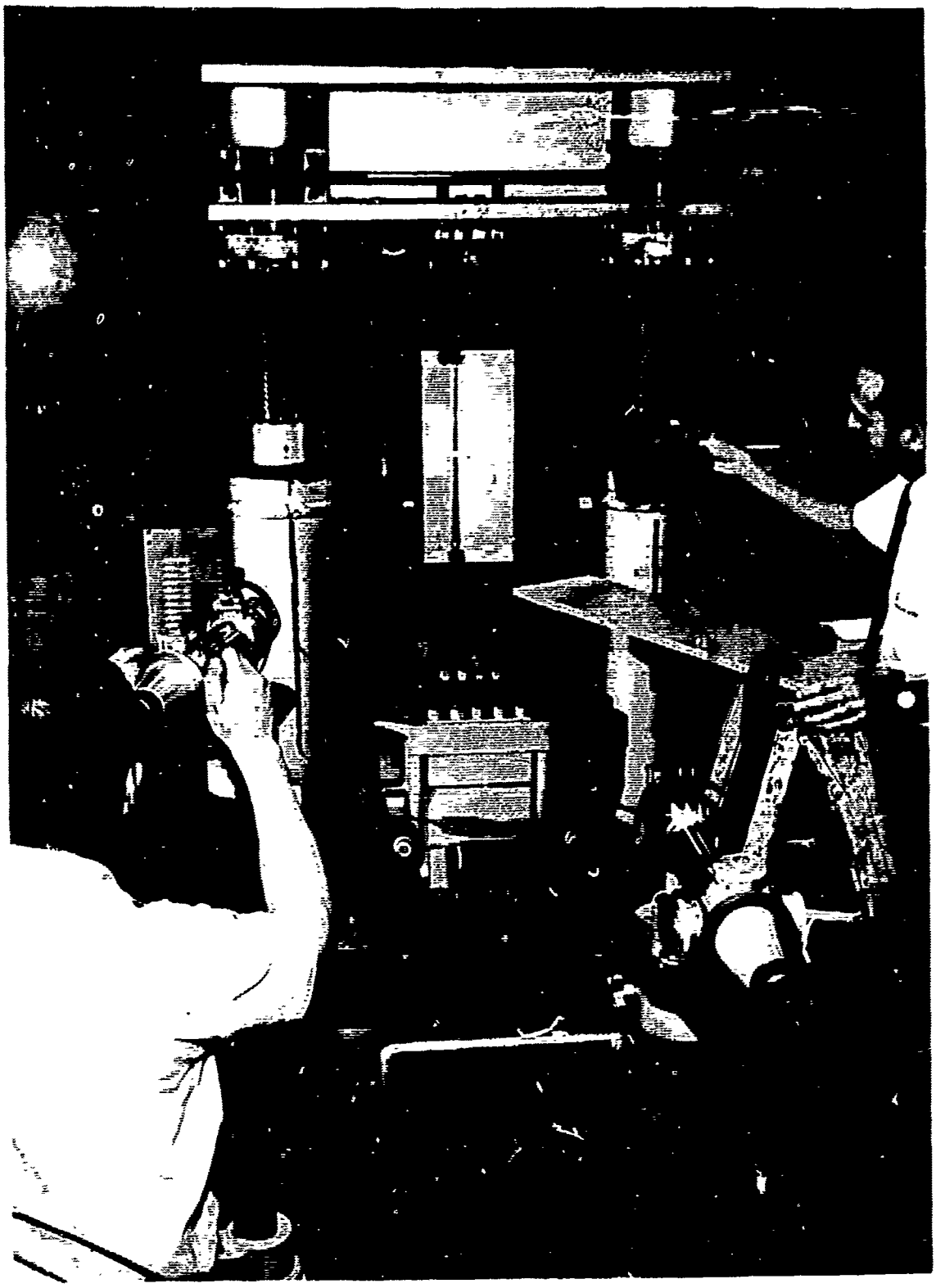

Figure 9. Crack Growth Measurement Technique

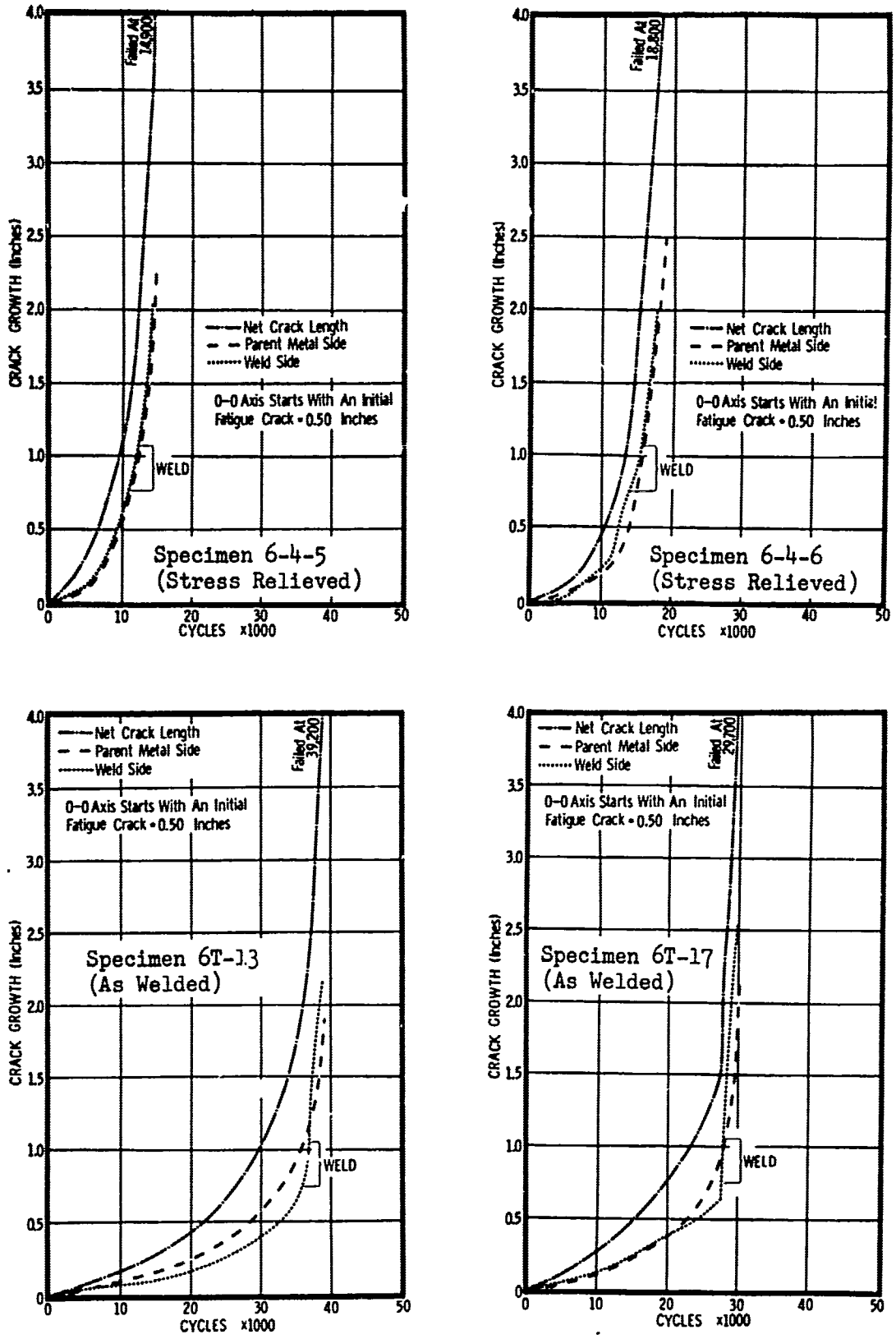

Figure 10. Fatigue Data for Center-Notched Ti-6Al-4V Specimens With Single Weld

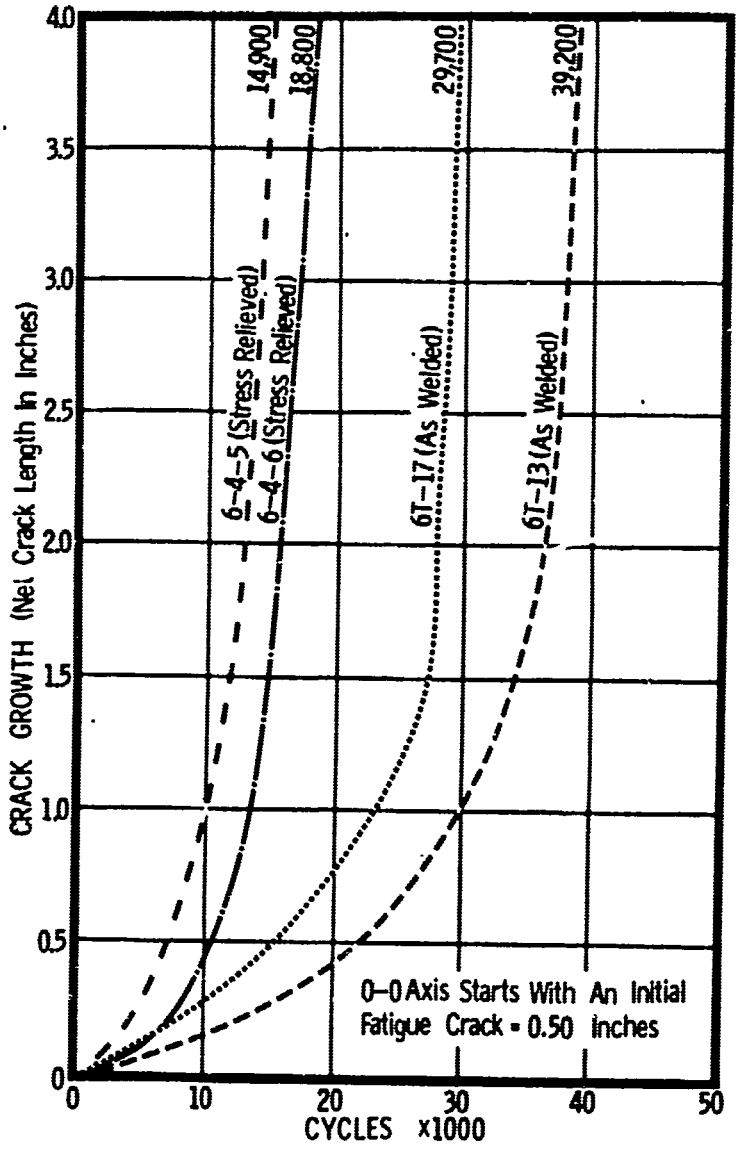

Figure 11. Composite Plot Showing Typical Crack Growth Versus Fatigue Cycles for As-Welded and Stress-Relieved Ti-6Al-4V Specimens With Single Weld

difference between the maximum applied tensile stress and the compressive residual stress at the crack tip, and the apparently lower stress thereby increases the cycles to failure. This was verified by comparing the crack growth on the weld side of the crack starter with the crack growth on the parent metal side of the crack starter for each set of conditions. The crack growth rate for the stress-relieved condition on both sides of the crack starter is identical for specimen 64-5 and almost identical on both sides for specimen 64-6.

The crack growth rate on both sides of the crack starter for specimen 6T-17 for the as-welded condition was almost identical up to 22,000 cycles, at which point the growth rate was less on the weld side of the crack starter, and finally, when the crack tip enters the area of the original residual stress tensile field, the growth rate increased rapidly and became greater than the growth rate on the parent metal side of the crack starter. In the case of specimen 6T-13, the initial crack growth rate was essentially the same on both sides of the crack starter, then the crack growth rate became slower on the weld side of the crack starter; as the crack tip approached the original residual stress tensile field, the crack growth rate increased rapidly and became greater than the crack growth rate on the parent metal side of the specimen. The final crack growth rate was essentially the same for all four specimens. The difference in fatigue life of the two as-welded specimens (38,100 versus 54,800 total cycles and 29,700 versus 39,200 cycles starting from a total fatigue crack length of 1/2 inch) is attributed to the difference in the length of the initial crack starter, since a smaller initial crack starter would have a smaller effect on the redistribution of stresses.

Photographs of the failed fatigue specimens are shown in figures 12 and 13. Since failure did not propagate completely across any of the specimens, tensile loading was required to completely fail the specimens. Fatigue failure propagated through the parent metal side of the specimens in the stress-relieved condition and through the weld side of the specimens in the as-welded condition. This difference was due to the sudden rapid rate of crack growth through the residual tensile stress field, which resulted in unbalanced loading of the as-welded specimens; the apparent unbalanced load in the stress-relieved specimens was due to the higher strength of the weld metal combined with the weld bead reinforcement. No notable differences were apparent in the appearance of the failure faces of the as-welded and stress-relieved specimens.

CENTER-NOTCHED Ti-6Al-4V FATIGUE SPECIMENS WITH TWO PARALLEL WELDS

The effect of residual stresses on fatigue behavior was studied further using welded Ti-6Al-4V specimens containing two parallel welds. The welds were equally spaced on opposite sides of the specimen centerline such that the inside edge-to-edge distance between the welds was 1/2 inch. (See figure 14.) An eloxed crack starter slot approximately 0.45 inch long was then machined into the specimen between the welds such that the ends of the slot were within 0.1 inch of the edges of the welds (weld heat-affected zone); consequently, the initial crack fronts were originated and grown within tensile residual stress fields. Fatigue tests were conducted in the same manner as the single-weld center-notched specimens. Results of the crack growth and fatigue life of the as-welded and stress-relieved specimens are indicated in figure 14. It is shown that the stress-relieved specimens have a slow rate of fatigue crack growth and fatigue life twice as long as the as-welded specimens. This result is just opposite to that found in single-weld specimens, where the as-welded specimens exhibited twice the fatigue life of the stress-relieved specimens.

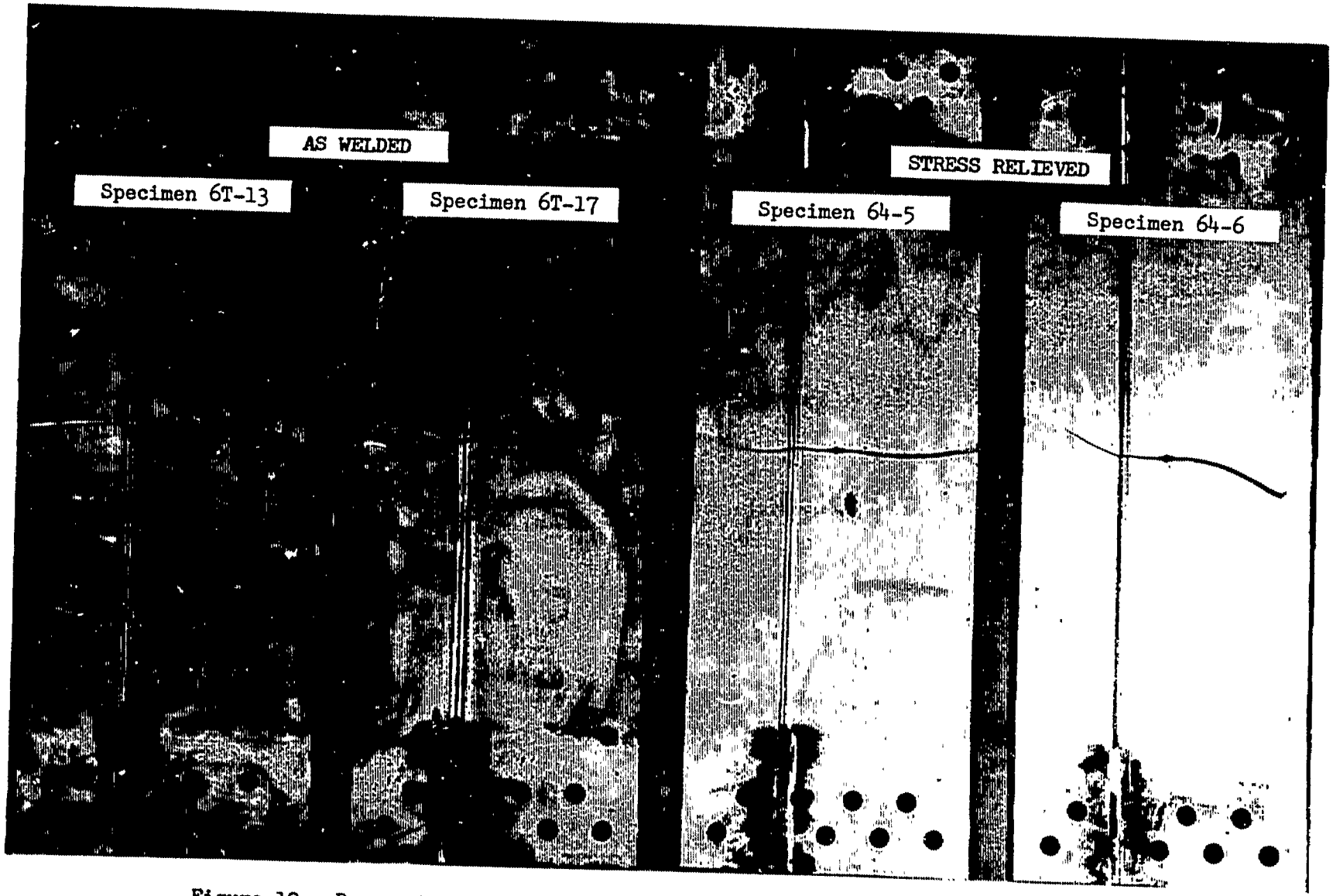

Figure 12. Precracked Fatigue Specimens From 0.200-Inch Ti-6Al-4V Weld Panels

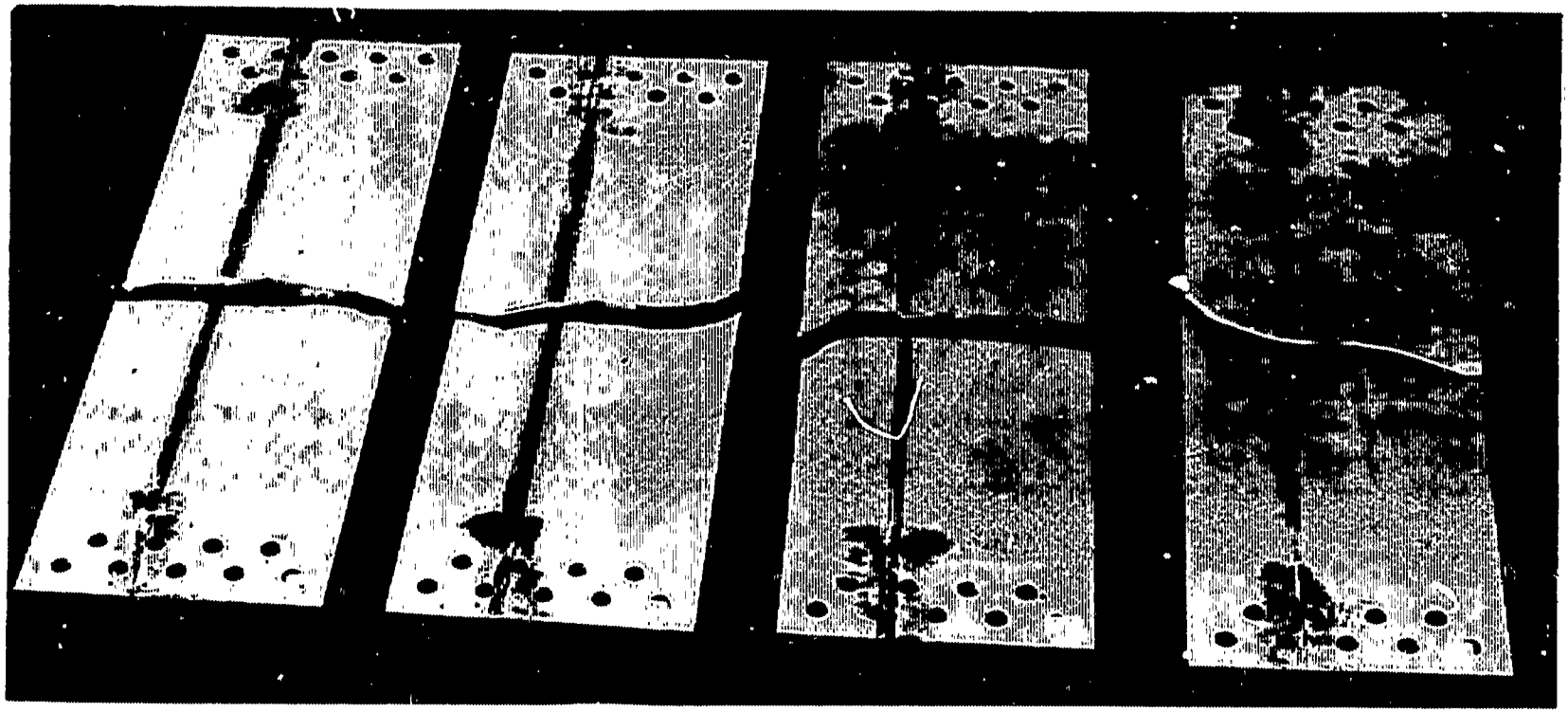

	AS WELDED		STRESS RELIEVED	
Specimen	6T-13	6T-17	64-5	64-6
Cycles to Failure	39,200	29,700	14,900	18,000

Figure 13. Failed Ti-6Al-4V Notched Fatigue Specimens

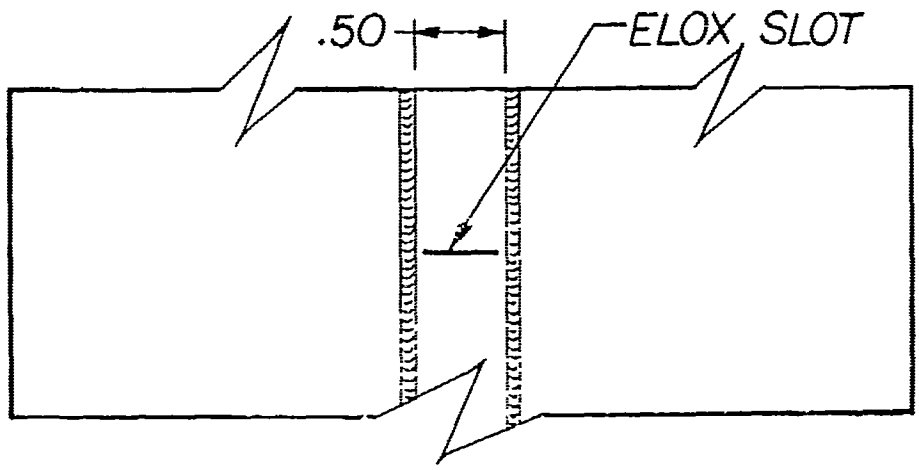

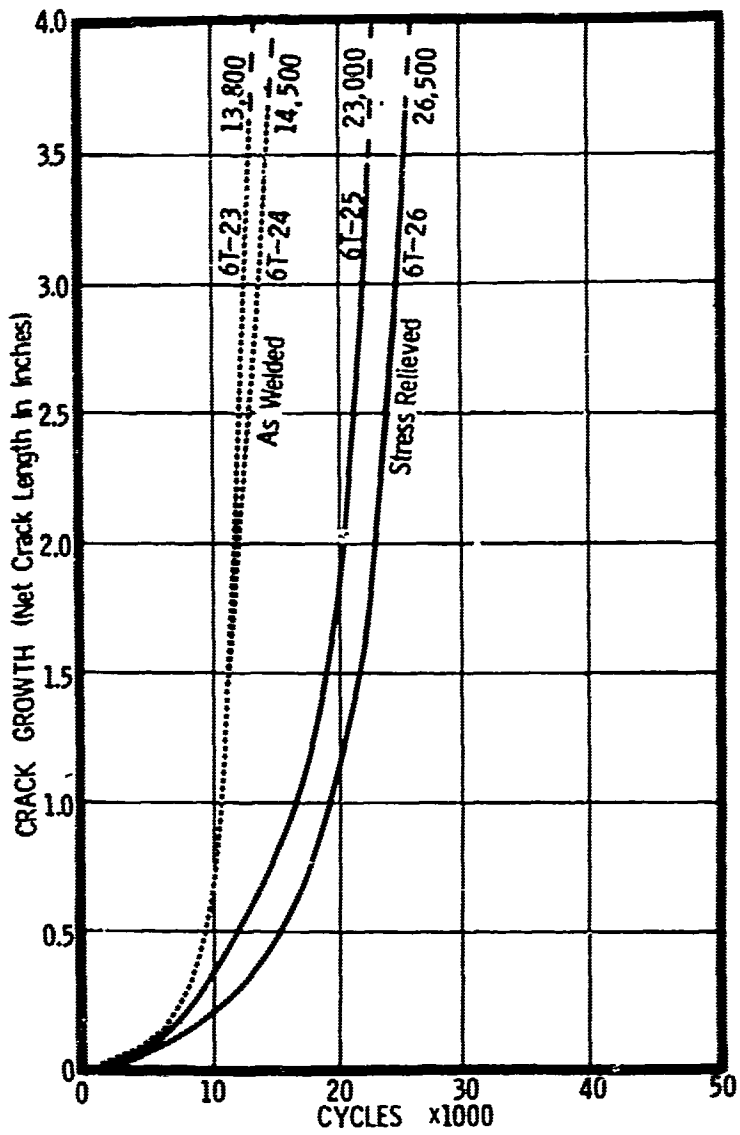

Figure 14. Fatigue Data for Center-Notched Ti-6Al-4V Specimens With Two Parallel Welds 1/2 Inch Apart

The explanation for this difference is that of a difference in the residual stress field where the crack initiates and propagates. In the case of the single-weld specimens, the crack front was in the region where compressive longitudinal stresses are counteracting the tensile fatigue load. In the case of the twin-weld specimens, the crack starter and crack front are in a residual tensile stress field and the additive tensile stress effect results in faster crack growth and lower fatigue life in the as-welded twin-weld specimens.

UNNOTCHED FATIGUE TESTS

Specimens of the configuration shown in figure 15 were used to establish the effects of residual stress on undamaged fatigue behavior. Originally it was planned to conduct these tests with the weld bead left on; however, on testing the first specimen, premature failure occurred in the vicinity of the load plates. This was caused by a notch which was left when the weld area was machined flush to accept the load plates. This factor combined with the difficulty encountered in obtaining failure in the reduced area led to a decision to grind the weld bead flush with the specimen surface.

Fatiguing was performed in a servocontrolled hydraulic machine. All fatigue testing was axial tension-tension using a maximum to minimum stress ratio (R factor) of 0.06 and a maximum load of 60 percent of ultimate tensile strength at a load rate of three cycles per second. Figure 16 shows the equipment with a specimen mounted in the load plates.

The results of the fatigue tests are listed in Table VIII. Photographs of the failed specimens are shown in figure 17. A closeup view of these specimens is shown in figures 18 and 19.

Table VIII indicates that the fatigue life of the as-welded specimens is about half of that of the stress-relieved specimens or the parent metal specimen. In other words, the fatigue resistance of the parent Ti-6Al-4V metal can be completely recovered by the stress-relieving heat treatment, whereas detrimental effects can result from no postweld stress relieving. All failures occurred through the reduced area of the specimens. Examination of the fracture faces revealed a small pore in each fracture face from which failure initiated in fatigue. Following a small amount of crack growth around the individual pores, pop-in type failure occurred after which fatigue growth again took place. The fatigue crack continued to grow to the point of instability (transition from fatigue to shear) where rapid fracture occurs by a plane stress mechanism or mixed mode. The shear lip fractured area extends from the edge of the fatigue zone to the end of the specimen. The transition from fatigue to shear is evident in specimens 64-3 and 6T-22 in figure 19.

The data obtained on the basis of examination of the failure surfaces are listed in Table IX. All the pores which initiated the failures are extremely small and would be considered as acceptable weld defects. A 2 percent definition in radiography would probably not even distinguish the pores of specimens 6T-20 and 64-3, considering weld bead reinforcement on 0.200-inch material. In order to obtain more insight on this subject, the failed Ti-6Al-4V specimens

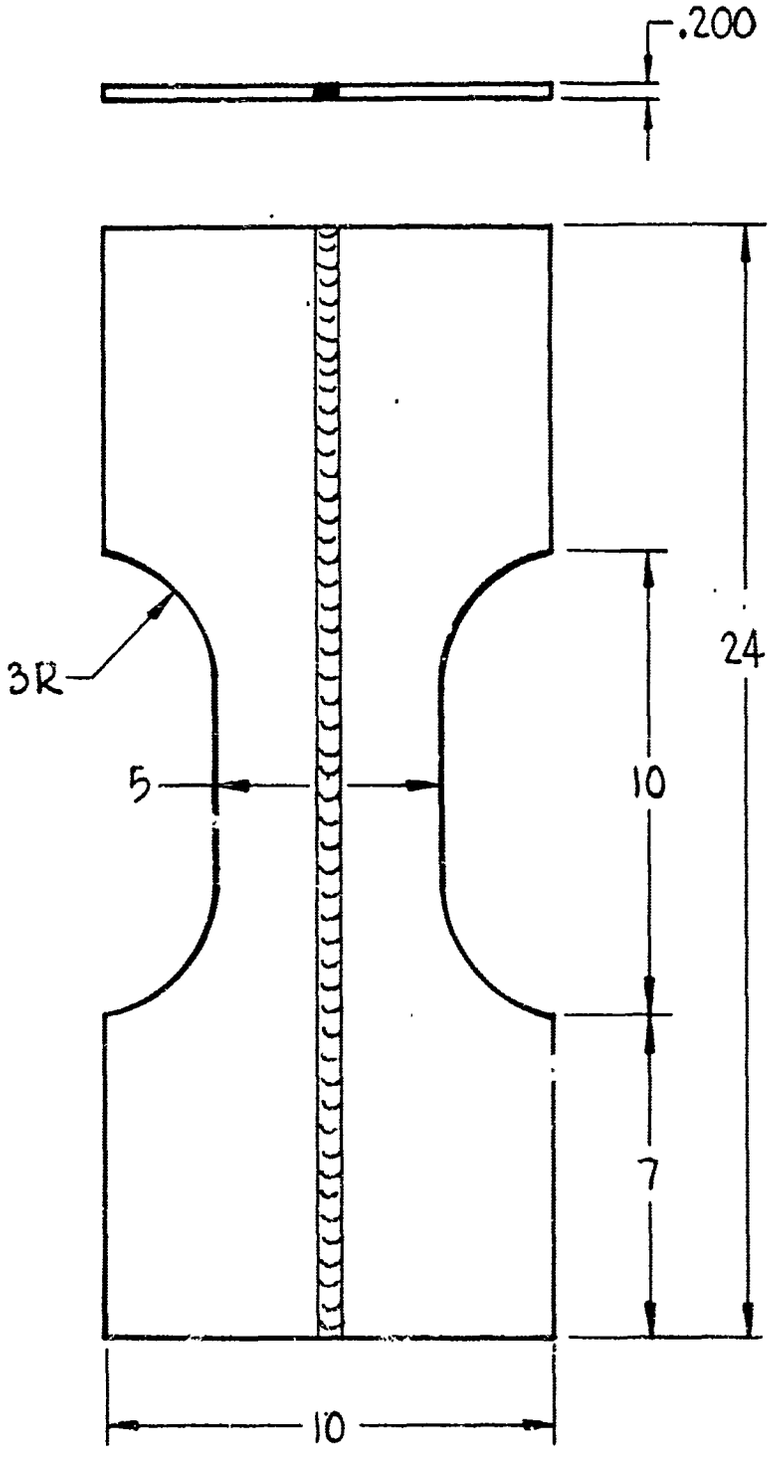

Figure 15. Unnotched 0.200-Inch Ti-6Al-4V Fatigue Specimen (Ground Flush)

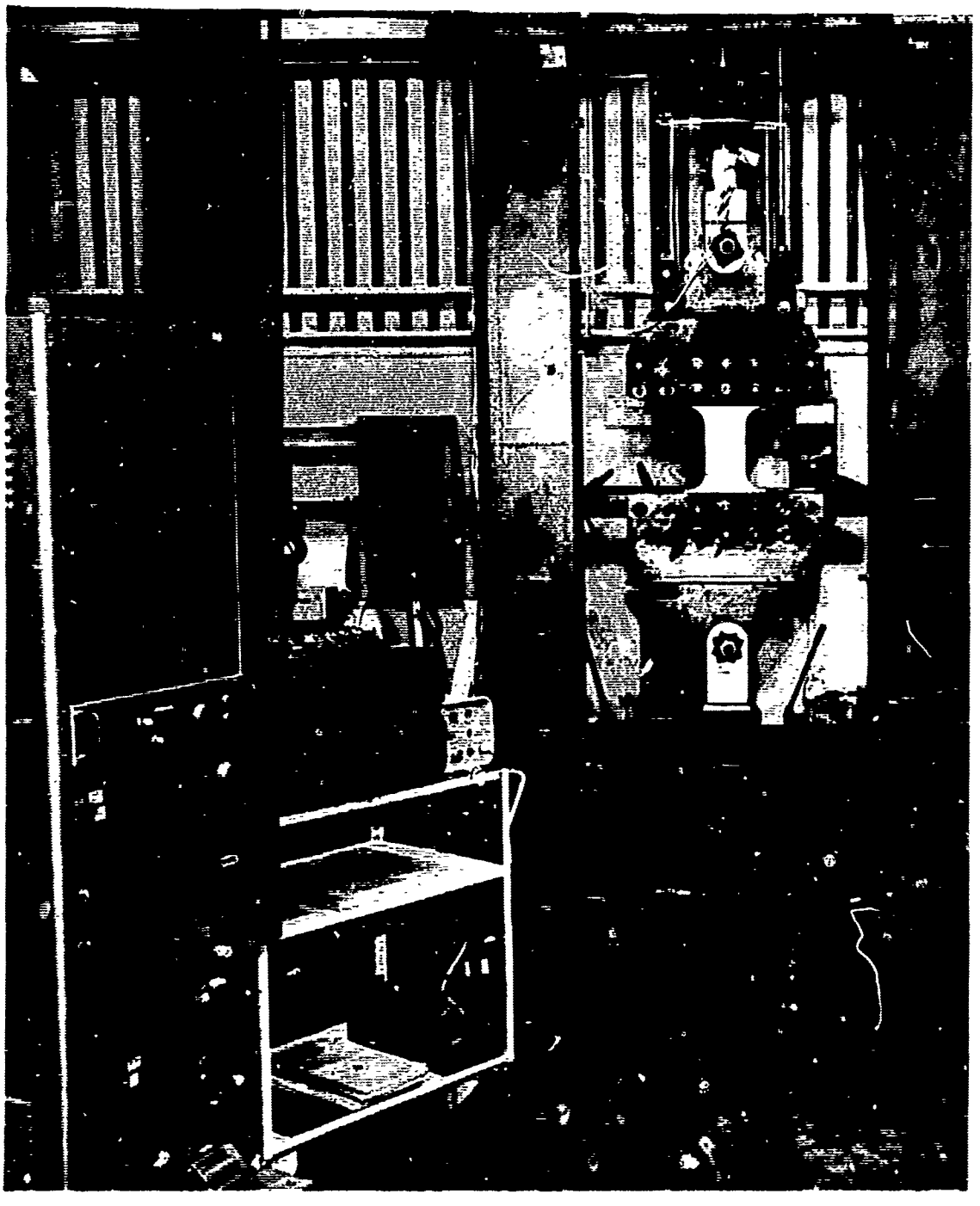

Figure 16. Fatigue Testing Setup

TABLE VIII

FATIGUE TEST DATA FOR 0.200-IN.
Ti-6Al-4V WELDED PANEL
(UNNOTCHED SPECIMEN)

Specimen Condition	Specimen Number	Cycles To Failure
Parent Metal (as received)	6T-34	42,854
As welded	6T-22	19,472
	6T-20	27,292
	6T-31	29,529
	6T-32	15,467
	Average	22,940
Stress relieved at 1450 F for 15 min., then air cooled	6-4-4	36,857*#
	6-4-9	30,972
	6-4-3	67,067
	6T-12	33,965
	6T-14	42,451#
	Average	42,262

* Weld reinforcement left on

\# Failed near load plates

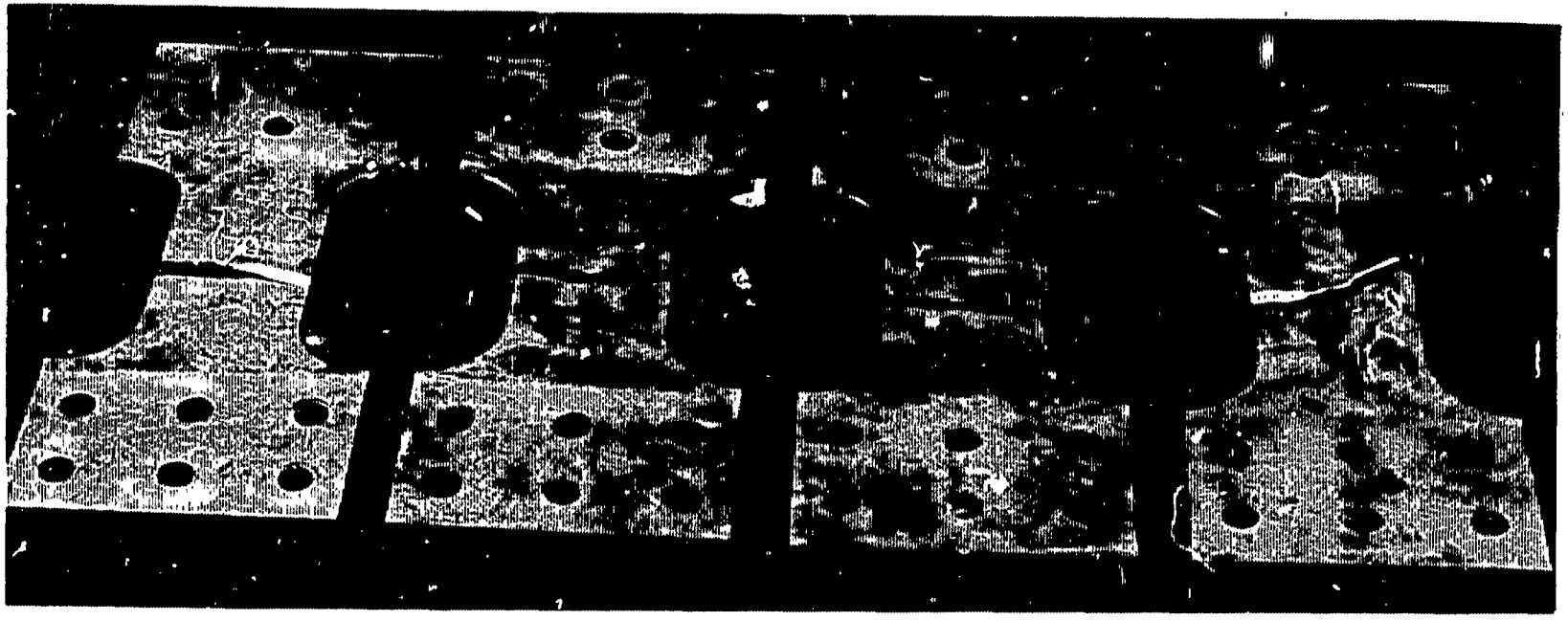

Specimen	6T-20	6T-22	64-3	64-9
Cycles to Failure	27,292	19,472	67,067	30,972

LOAD = Sixty percent of ultimate (135,000)
LOAD RATE = 3 cycles per second
R FACTOR = +0.06

Figure 17. Uncracked Fatigue Specimens of 0.200-Inch Ti-6Al-4V After Fatigue Test Conducted at Room Temperature

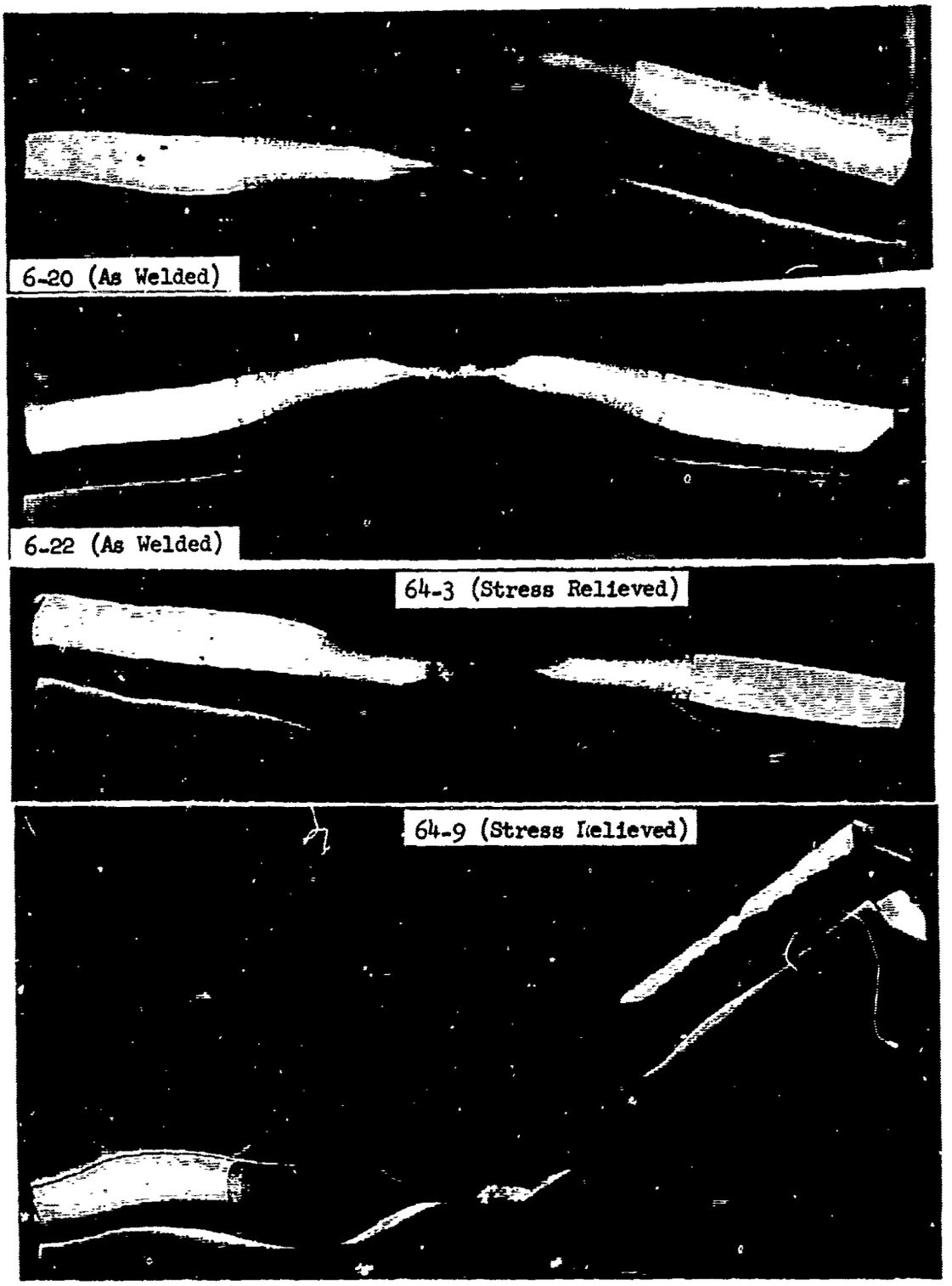

Figure 18. Enlarged View of Fracture Faces of 0.200-Inch Ti-6Al-4V Fracture Specimens

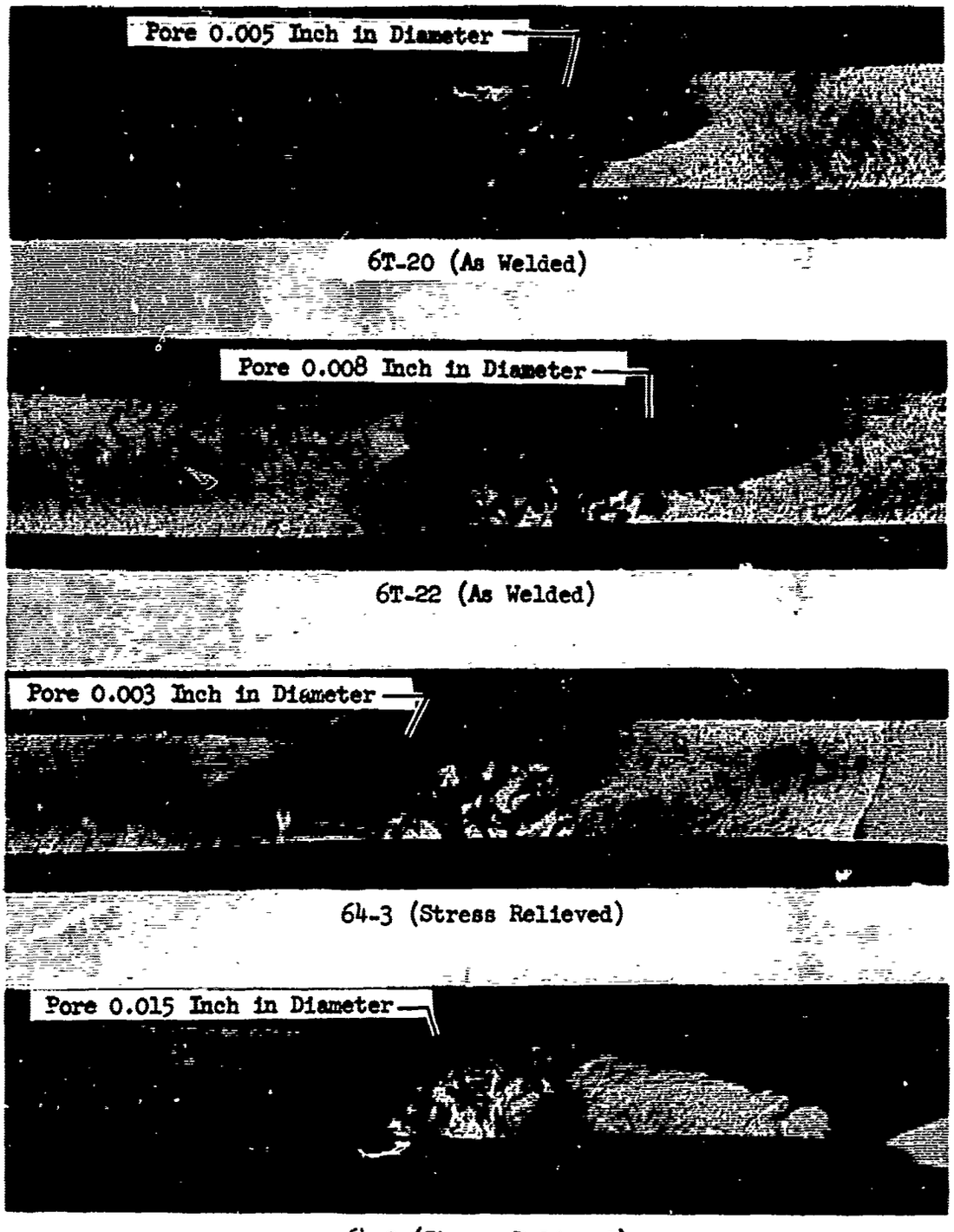

Figure 19. Fatigue Specimen Fractured Areas in 0.200-Inch Ti-6Al-4V Weld Panels, Mag. 3X

Table IX

FATIGUE TEST FRACTURE FACE DATA

Specimen Number	Pore Diameter (inches)	Depth of Pore From Surface (inches)	Distance From Edge of Weld (inches)	Initial Fatigue Crack Around Pore (inches)	Pop-In Length (inches)		
					Pore Side of Weld	Opp. Side of Weld	Total (Including Weld)
As Welded							
6T-22	0.008	0.030	0.050	0.035 dia	0.240	0.120	0.720
6T-20	0.005	0.015	0.020	0.030 dia	0.275	0.100	0.66
6T-31	0.006	0.005	0.030	0.035 dia	0.120	0.250	0.75
6T-32	0.0075 0.004	0.020 0.090	0.050 0.10	0.035 dia 0.020 dia	0.250 0.120	0.120 0.250	0.75 0.75
Stress Relieved							
6T-12	0.005	0.015	0.025	0.025 dia	0.250	0.060	0.70
6T-14	0.002	0.060	0.160	Not discernible	0.32	0.140	0.75
64-9	0.015	0.025	0.030	0.090 dia	0.360	0.060	0.65
64-3	0.003	0.008	0.035	0.075 surface width 0.040 depth elliptical			

were X-rayed to establish the quantity and location of any weld defects within the reduced area of the specimens. Examination of the radiographs revealed that specimen 64-3 contained seven pores. The maximum pore diameter was 0.015 inch and the minimum pore diameter was 0.005 inch. The pores were scattered along the length of the specimen with none of them being in the vicinity of the failure (minimum distance of a pore from failure was 1.3 inches).

Specimen 64-9 has 24 pores. These were scattered along the length of the weld with most of them being located within 0.75 inch of each side of the failure area. One pore was 0.040 inch in diameter with the remaining pores being 0.015 inch in diameter or less. These defects (size, quantity, and distribution) are acceptable under present specifications of North American Aviation. The 0.040-inch diameter pore is 0.55 inch from the failure and within the reduced section of the specimen.

Specimen 6T-20 had 15 pores which were scattered along the length of the weld in the test area. One pore 0.005 inch in diameter was found 0.07 inch from the fracture; a second pore approximately 0.007 inch in diameter was located 0.20 inch from the failure. Three pores (other than the one located in the fracture) were found in specimen 6T-22. One pore 0.005 inch in diameter was 1 inch from the failure; one pore 0.005 inch in diameter was 1.5 inches from the failure; and one pore 0.007 inch in diameter was 0.75 inch from the failure.

A second group of fatigue test specimens, including two as-welded, two stress-relieved and one parent metal, was evaluated to determine further the effect of weld porosity and residual stresses on the fatigue life. These specimens were fabricated and tested using the same procedure as described earlier. Results are presented in Tables VIII and IX. The fatigue life (number of cycles to failure) of the parent metal specimen and the average fatigue life of the stress-relieved specimens are about equal, whereas the as-welded specimens show an average fatigue life of about 50 percent of the stress-relieved and parent metal specimens. The number and size of pores visible through examination of the fractured surface agree well with data obtained from the first group. All specimens contained one pore in the fractured wall except specimen 6T-32, which has two defects. Based upon these results, it is believed that the size and frequency of pores in the failure have no major effect on the fatigue properties; however, the fatigue life of welded Ti-6Al-4V is affected by residual stresses. The fatigue life is improved when the residual stresses are completely removed (stress relieved). The lower fatigue life of the as-welded specimens may be attributed to the high tensile residual stresses existing in the weld.

FRACTOGRAPHIC ANALYSIS OF FATIGUE SPECIMENS

The fatigue fractured specimens were examined at low and high magnifications to determine the modes of failure and distinguishing features of the fractured face between as-welded and stress-relieved specimens. A photomicrograph of the fractured surface at and near the weld and electron fractographs of several locations in the fractured zones are shown in figures 20 and 21 for as-welded and stress-relieved specimens. In figure 20, fractographs A, B, and C exhibit the common feature of striations associated with fatigue fractures, and D shows the interior surface of a pore in the weld. The type of striations varies from very closely spaced and well defined lines in A to broad and widely

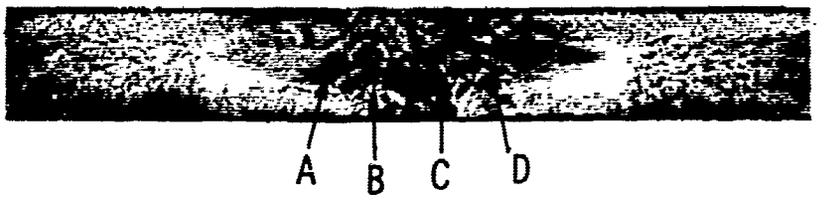

A - HEAT AFFECTED AREA (15,000X)

C - WELD AREA (15,000X)

B - EDGE OF WELD (15,000X)

D - SURFACE OF PORE (5000X)

Figure 20. Electron Fractographs of As-Welded Ti-6Al-4V Fatigue Specimen 6T-22

A - MIXED MODE FRACTURE (15,000X)

C1 - WELD ZONE (15,000X)

B - FATIGUE STRIATIONS (15,000X)

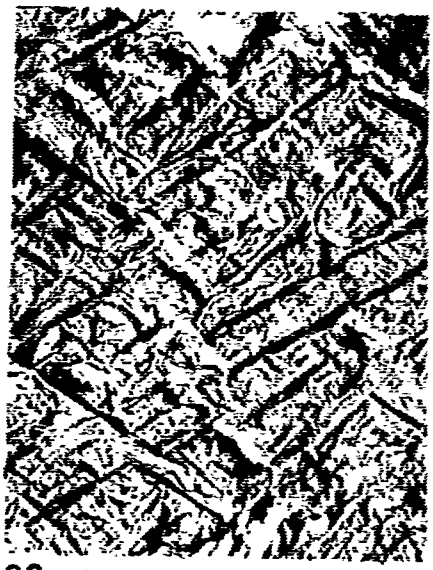

C2 - WELD ZONE (2500X)

Figure 21. Electron Fractographs of Stress-Relieved Ti-6Al-4V Fatigue Specimen 64-

spaced bands in C, with B somewhere in between. This indicates that area A has the features of high cycle fatigue, whereas area C has the features of low cycle fatigue. The mechanism by which the as-welded specimen fractured in fatigue can now be formulated. As stated earlier, initiation of crack most likely originated from pores in the weld. Electron microscope data substantiate these findings. Fatigue fracture initially propagates from a pore in the weld at a rapid rate accentuated by the high longitudinal tensile stress (location C). The cracking rate is reduced slightly at the edge of the weld (location B) and considerably at the heat-affected zone (location A).

Fractographs of the stress-relieved specimen that failed in fatigue are shown in figure 21. In this case, a cleavage type of fracture is evident at the weld edge (location C-1) where the high temperature induced Widmanstaetten structure (C-2) of alpha-beta titanium alloy shows brittle behavior. Fatigue striations are apparent in the rather flat area (location B), whereas mixed mode of fatigue striations and plane strain fracture seem to exist in location A. Rapid shear lip type of fracture occurred beyond this transition area.

Section VI

FRACTURE TOUGHNESS STUDIES

Fracture toughness studies were conducted using specimens taken from all three types of titanium alloy weld panels. The fracture toughness studies encompassed: (1) center-crack fracture toughness, (2) edge-cracked fracture toughness, and (3) slow bend fracture toughness. Weld specimens in the as-welded and stress-relieved condition were tested to obtain data for correlation with the residual stress and fatigue test data. Data obtained from the tests were tabulated and later plotted to provide a graphic display of test results. Test specimens were subjected to metallographic examination to determine the effects of the thermal cycles on the microstructure and to determine the types of failure as a result of the tests.

CENTER-CRACK FRACTURE TOUGHNESS TEST

All unstable fracture specimens were of the configuration shown in figure 8. Prior to fatigue cracking, all of the eloxed holes were washed with acetone. Fatiguing was performed in a Baldwin-Lima-Hamilton IV-12 fatigue machine with a load multiplier at a stress ratio (R factor) of 0.1 to a maximum stress of 25,000 psi at a rate of 1200 cycles per minute. Crack growth versus cycles was measured as described in Section V, Fatigue Studies. All cracks were grown to within a maximum distance of 0.1 and a minimum of 0.01 inch of the weld edge to ensure that the crack tip would be within the original residual tension field.

After cracking, the specimens were loaded into an electromechanical Tinius Olsen testing machine as shown in figure 22. The breakaway extensometers were placed over the center of the weld (1-inch gage length) in order to observe any deflection difference in the weld area behavior in the as-welded and the stress-relieved welded specimens. The synthetic sea water exposure test setup was similar except a tape dam was used to expose the crack to synthetic sea water during the test. Synthetic sea water conforming to ASTM D 141-52 was used. All specimens were loaded to failure at a head travel speed of 0.05 inch per minute. Load versus deflection was automatically plotted during testing.

Crack growth versus cycles is shown graphically in figure 23 for Ti-6Al-4V. These are typical of the curves obtained for the specimens tested. The cycles required to grow the crack to a length of about 2 inches was greater in all cases for the as-welded condition than for the stress-relieved condition. This is in agreement with the results obtained on precracked fatigue specimen testing (Section V). Also in agreement with the crack growth rate effect obtained on the precracked fatigue specimens, the cracks grew at a slower rate on the weld (left) side of the crack starter than on the parent metal (right) side of the crack starter due to the larger residual compressive stress on the weld side of the crack starter.

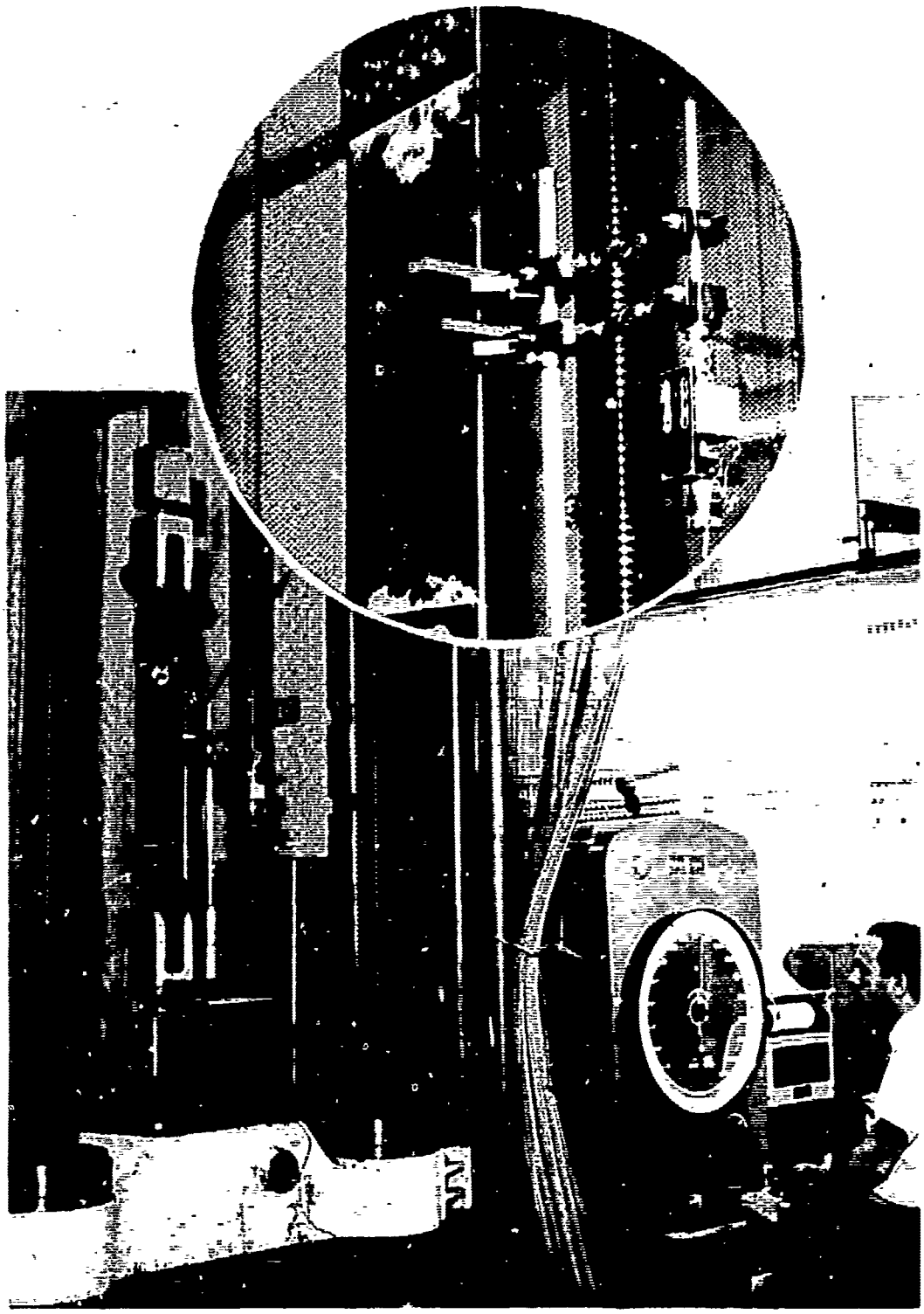

Figure 22. Tensile Testing of Fracture Toughness Specimens

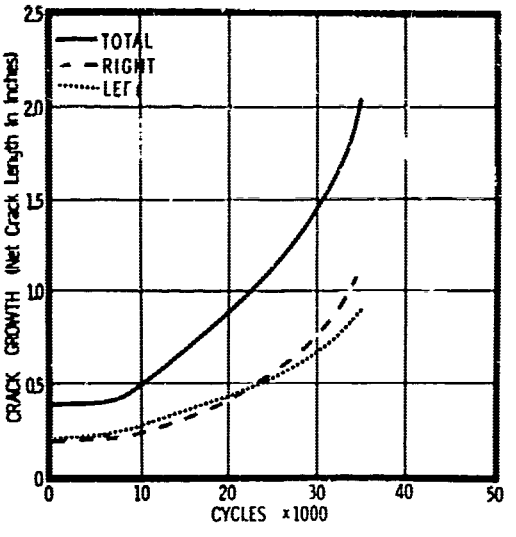

Specimen 6T-19 (As Welded)

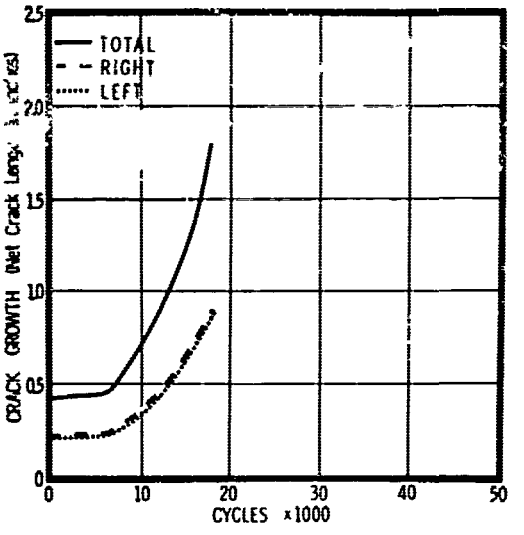

Specimen 6.4-2 (Stress Relieved)

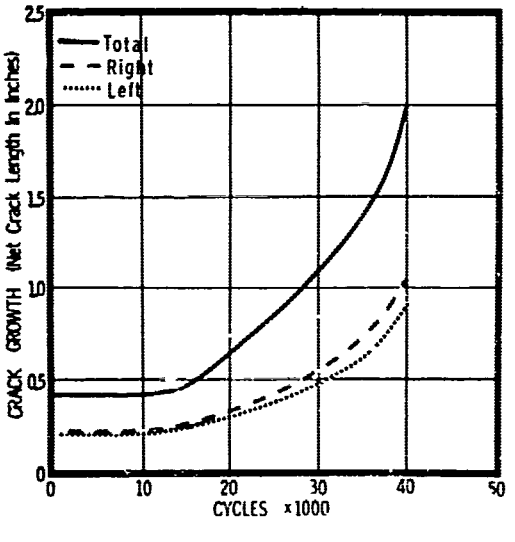

Specimen 6T-15 (As Welded)

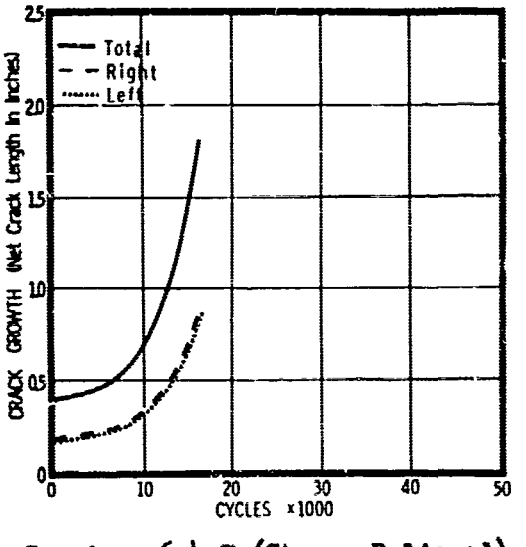

Specimen 6.4-7 (Stress Relieved)

Figure 23. Typical Crack Growth Data for Ti-6Al-4V Fracture Toughness Specimens

Ti-6Al-4V CENTER-CRACKED FRACTURE TOUGHNESS RESULTS

Center-cracked Ti-6Al-4V weld panel specimens were subjected to a series of fracture toughness tests in both air and sea water environments. The data obtained for the specimens are shown in Table X. Comparative load deflection curves are shown in figure 24. Photographs of the failed specimens are shown in figures 25 and 26.

A pop-in type noise was obtained at least once while testing each specimen. In some cases a secondary noise, much less audible, was also heard. The load at which primary pop-in occurred was slightly less for the stress-relieved specimens than for the as-welded specimens when testing was in air; however, further data obtained from the test specimens exposed to simulated sea water could not confirm the difference in pop-in load level.

The major difference observed in the test data was the level at which deflection increased with no increase in load (figure 24). For the two stress-relieved specimens, this occurred at loads of 99,000 and 88,000 pounds, while for the as-welded specimens this occurred at approximately 57,000 pounds. Further, the deflection rate was greater for the as-welded than for the stress-relieved specimens. This increase in deflection rate or crack propagation rate in the as-welded specimens is most likely due to the effect of stresses within the weld zone. There was little or no difference between the as-welded and stress-relieved specimens or between fracture toughness in air or sea water environments on the basis of the net area failure stress.

A study of the fracture faces of the specimens shown in figure 25 did not reveal any notable differences between the stress-relieved and as-welded specimens or with respect to those specimens which were failed in air. No evidence of corrosion due to exposure to synthetic sea water was observed immediately after testing.

FRACTOGRAPHIC ANALYSIS OF FRACTURE TOUGHNESS SPECIMENS

Ti-6Al-4V fracture toughness specimens were examined optically and with the electron microscope (using the replica technique) to determine modes of failure. Figures 27 and 28 are photographs of as-welded and stress-relieved specimens. The fracture surface consists principally of three distinct zones: (a) fatigue precrack area, (b) and (c) plane strain zone, and (d) shear lip area. Fractographs of location (a) on both figures show typical fatigue striations. Spacing of striations in the as-welded and stress-relieved specimen appears to be about equal. Similarity in features was also found in the plane strain areas for both types of specimens, though shear lip dimples were evident in some areas [location (c)]. Shear lip area dimples are indicative of rapid fracture beyond the plane strain area. Comparison of fractographs of as-welded and stress-relieved specimens gave no evidence of significant difference in fracture surface morphology. Little or no difference was also found in fracture toughness testing between the two specimen conditions.

TABLE X

CENTER-CRACKED FRACTURE TOUGHNESS TEST RESULTS FOR 0.200-INCH THICK Ti-6Al-4V WELD PANELS

Condition	Specimen No.	Total Crack Length (in.)	Pop-in Load (lb)	Net Area Failure	
				Load (lb)	Stress (psi)
Test Media: air at room temperature					
As Welded	6T-11	2.18	54,000	117,500	98,300
	6T-19	2.04	57,000	124,000	101,000
Stress Relieved	64-2	1.84	50,250	128,300	105,000
	64-8	1.85	53,000	125,300	99,000
Test Media: sea water					
As Welded	6T-15	1.96	55,250	117,750	92,800
	6T-16	2.25	50,250	107,750	89,200
Stress Relieved	64-1	2.05	57,750	102,750	85,000
	64-7	1.84	45,500	119,400	91,900

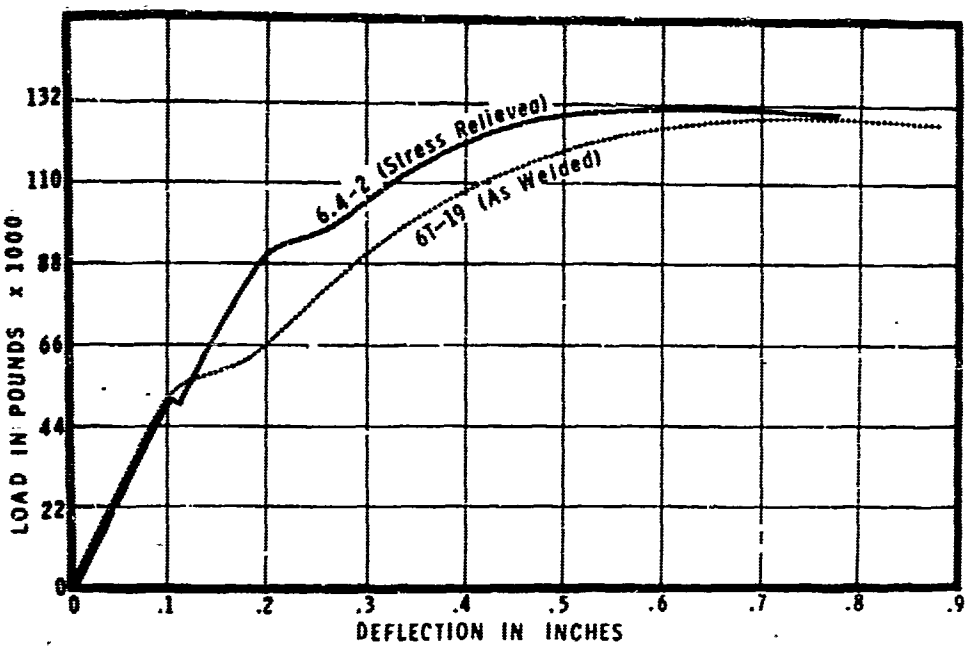

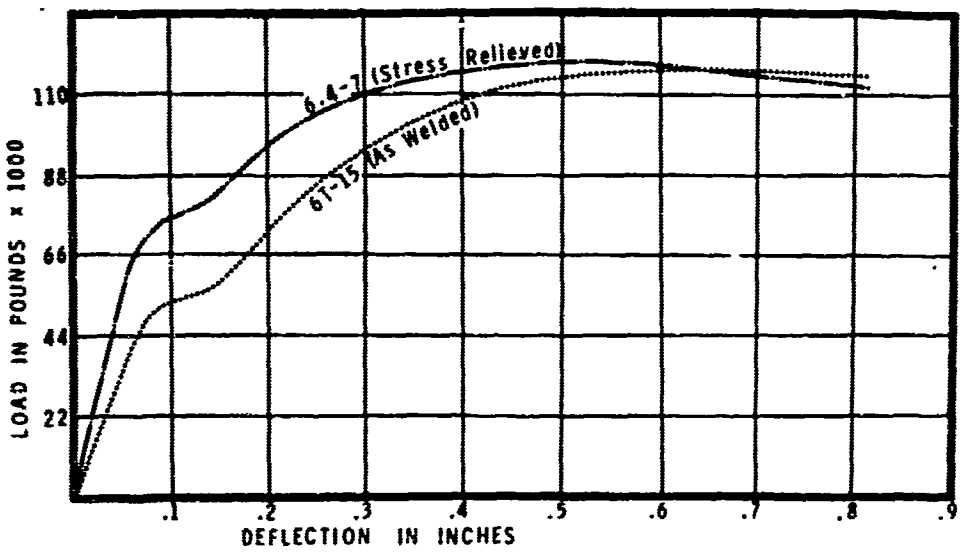

Figure 24. Load Versus Deflection, Fracture Toughness in Air (Top) and Synthetic Sea Water (Bottom) of 0.200-Inch Ti-6Al-4V Panel

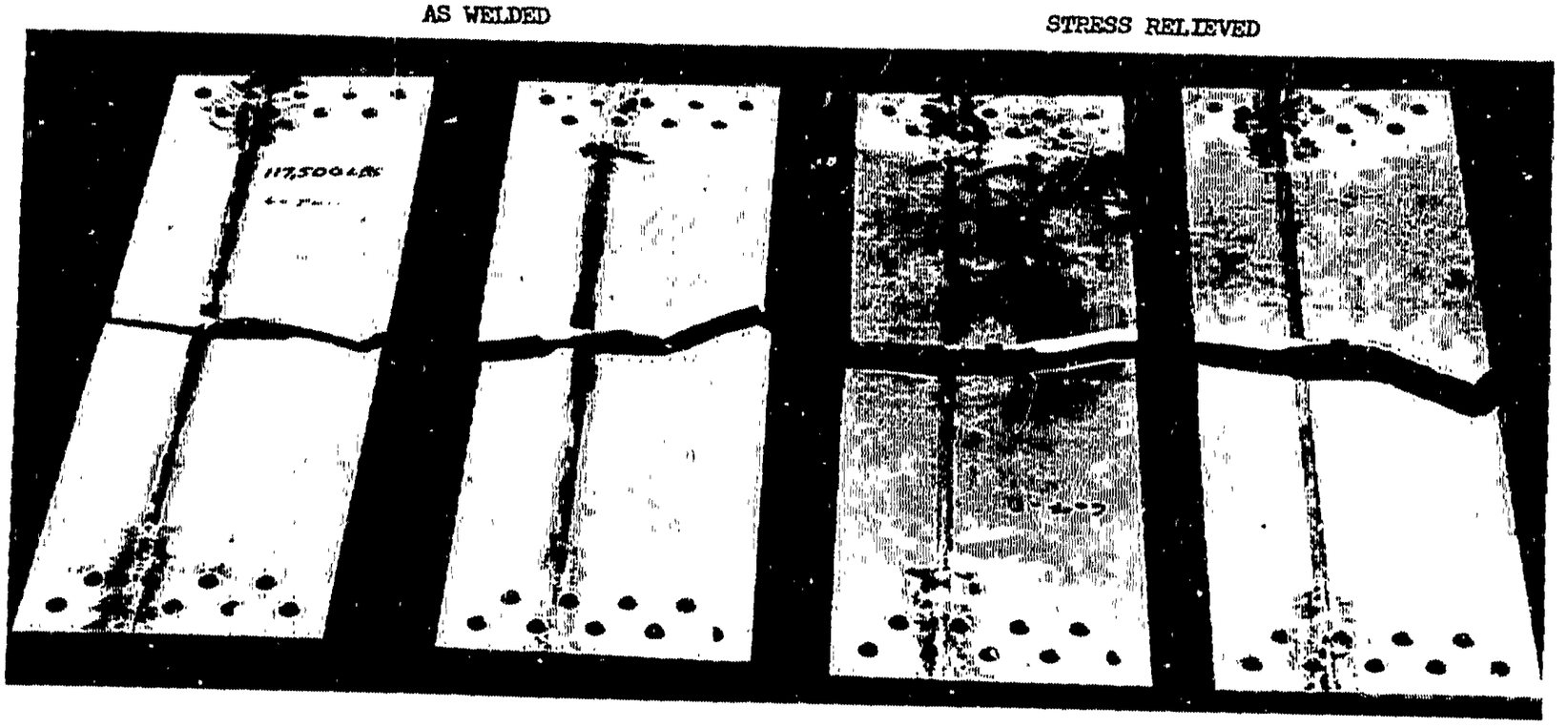

Figure 25. Unstable Fracture Toughness Specimens, 0.200-Inch Ti-6Al-4V Panels Tested in Air

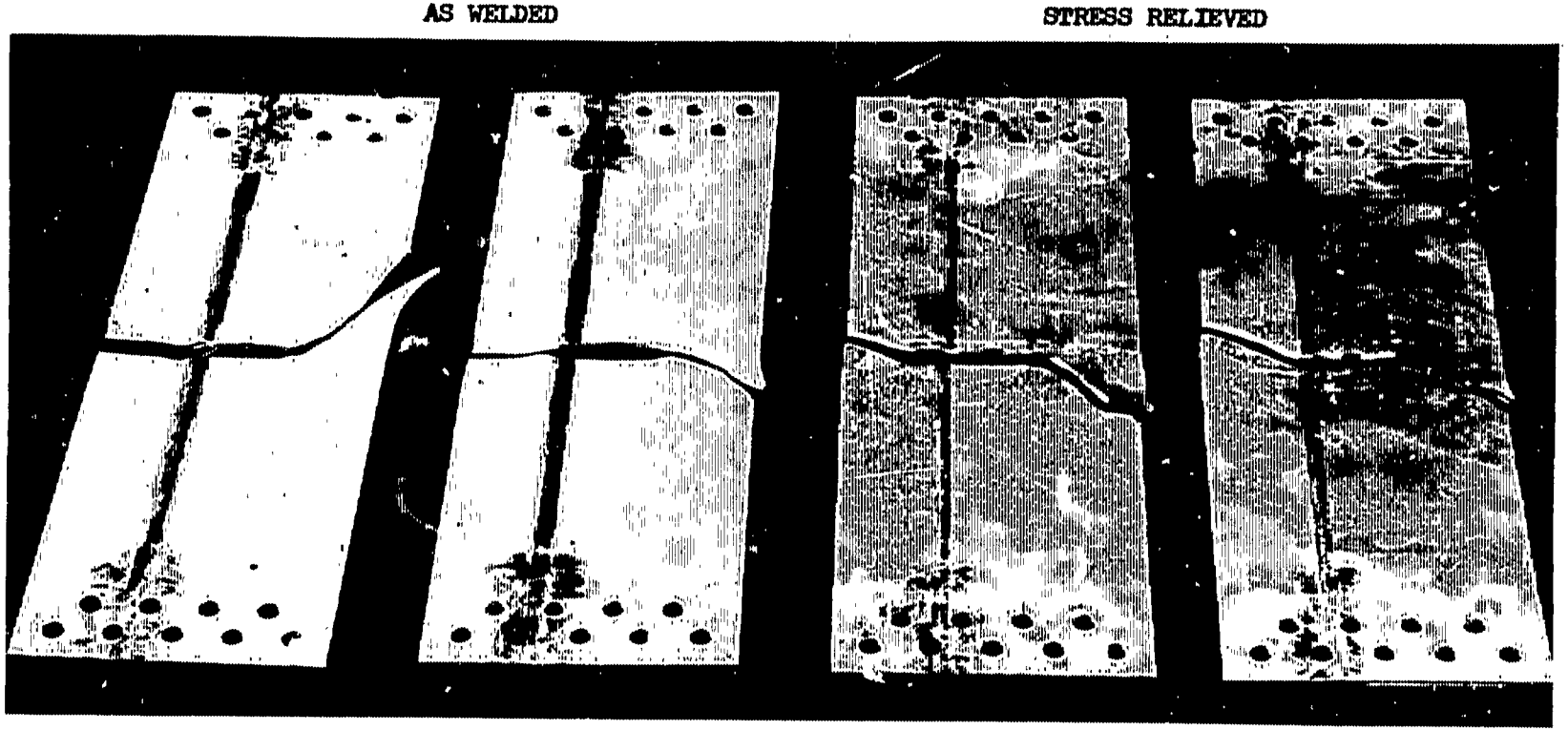

Specimen	6T-15	6T-16	64-1	64-7

Figure 26. Unstable Fracture Toughness Specimens, 0.200-Inch Ti-6Al-4V Panels Tested in Synthetic Sea Water

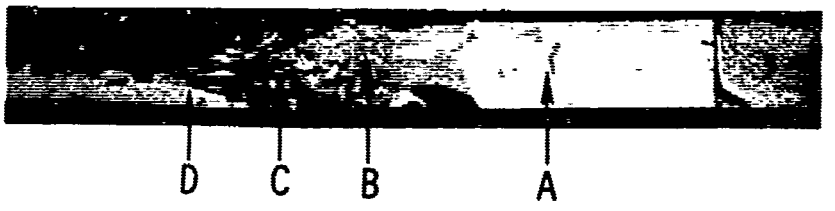

A - FATIGUE CRACK AREA

B - PLANE STRAIN ZONE

C - MIXED MODE FRACTURE IN WELD

D - SHEAR LIP AREA

Figure 27. Electron Fractographs of As-Welded Ti-6Al-4V Fracture Toughness Specimen (2500X)

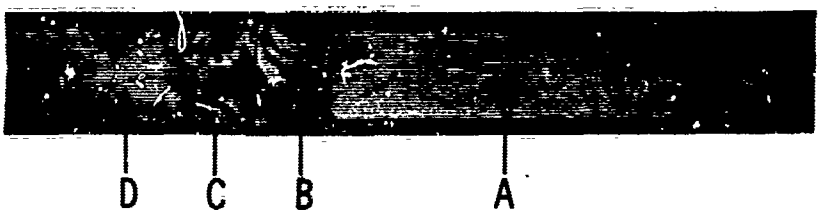

A - FATIGUE CRACK AREA

B - PLANE STRAIN ZONE

C - MIXED MODE FRACTURE IN WELD

D - SHEAR LIP AREA

Figure 28. Electron Fractographs of Stress Relieved Ti-6Al-4V Fracture Toughness Specimen (2500X)

CENTER-CRACKED FRACTURE TOUGHNESS TESTS ON SPECIMENS WITH TWO WELDS

Additional fracture toughness tests were performed on welded Ti-6Al-4V panels containing two parallel welds 2 inches apart. An eloxed slot of the same dimensions as shown in figure 8 was centered between the welds. The specimens were then fatigue precracked within 0.010 inch from the edge of the weld as was done with single-weld specimens. The rates of crack growth are plotted in figure 29. It was found that the as-welded specimens required twice as many cycles to initiate fatigue cracking and five times as many cycles to complete the same crack length as the stress-relieved specimens. The greater resistance shown by the as-welded specimens is attributable to the high compressive residual stresses existing between welds wherein the net tensile fatigue load was reduced appreciably. Results of residual stresses measurements have been discussed in the section under Residual Stresses.

After the specimens were precracked, tensile fracture toughness tests were conducted using the same procedure as in the single-weld specimens. Typical load-deflection curves are shown in figure 30 and results are tabulated in Table XI (results of the single welds are included in the table for comparison). In terms of net area fracture strength, there were no significant differences among the single-weld or twin-weld specimens in the as-welded or stress-relieved condition; however, the pop-in load of the as-welded twin-weld specimens is higher than that of the stress-relieved twin-weld specimen or the single-weld specimens in the as-welded or stress-relieved condition. It is not certain if this difference is significant and whether residual stresses or metallurgical factors are the causes. On the basis of the pop-in load and the total crack length estimated at this load, the plane strain fracture toughness factors K_{Ic} and G_{Ic} values shown in Table XI were computed by the relation

$$EG_{Ic} = K_{Ic}^2(1 - \mu^2) = \sigma^2 W \tan(\pi a/W)$$

where

- E = modulus of elasticity,
- G_{Ic} = critical strain energy for unstable plane strain fracture,
- K_{Ic} = critical stress intensity factor for unstable plane strain fracture,
- μ = Poisson's ratio,
- σ = gross stress at pop-in load,
- W = width of specimen, and
- a = one-half crack length at pop-in.

Ti-8Al-1Mo-1V AND Ti-5Al-2.5Sn CENTER-CRACKED TOUGHNESS RESULTS

In addition to testing these specimens in air at room temperature and in a sea water environment, a -100°F liquid nitrogen temperature test was employed to provide a more sensitive condition for determining the fracture toughness of Ti-8Al-1Mo-1V and Ti-5Al-2.5Sn welded panels. All specimens tested in air at room temperature and at -100°F were tension loaded, as before, continuously at a head travel speed of 0.05 inch per minute until fracture. Step loading at increasing increments of loads was used for the sea water test specimens according to the sequence shown in Table XII.

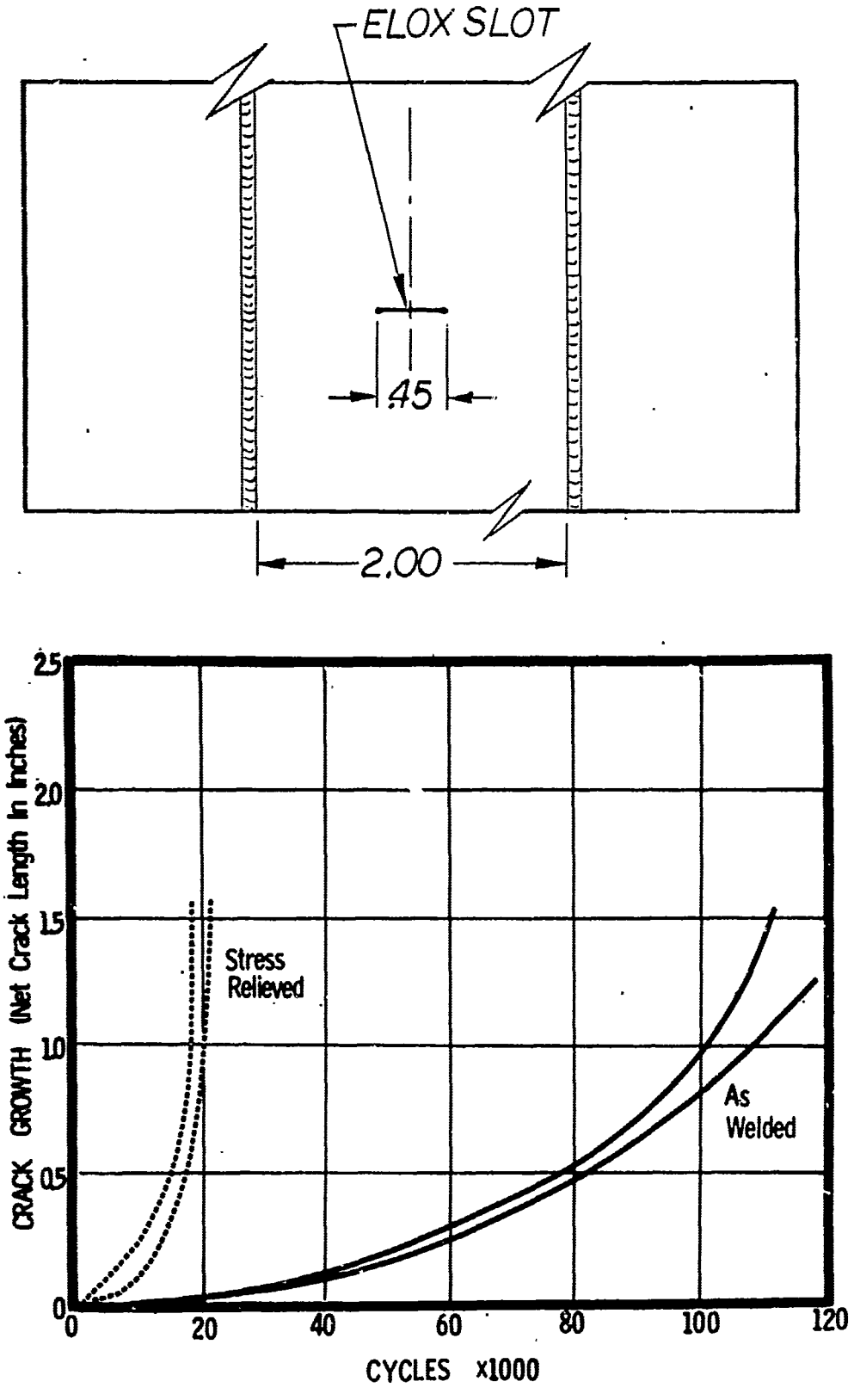

Figure 29. Fatigue Crack Growth Data for Ti-6Al-4V Specimens With Two Parallel Welds 2 Inches Apart

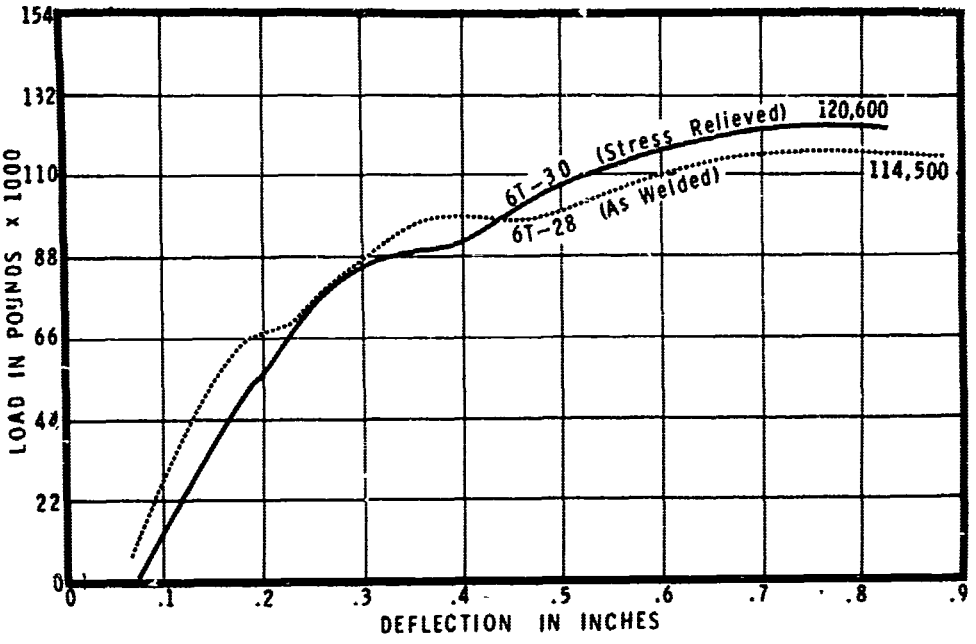

Figure 30. Load Versus Deflection Fracture Toughness of Ti-6Al-4V Specimen With Two Welds

TABLE XI

FRACTURE TOUGHNESS IN Ti-6Al-4V 0.200-INCH WELD PANELS

Weld Geometry	Spec. No.	Total Crack Length (inch)	Pop-in Load (lb)	Net Area Failure		K_{Ic}	G_{Ic}
				Load (lb)	Stress (psi)	(psi $\sqrt{in.}$)	(in.-lb/in.^{2})
As Welded							
Single weld	6T-11	2.18	54,000	117,500	98,300		
	6T-19	2.04	57,000	124,400	101,000		
Twin weld	6T-27	1.93	68,000	116,500	96,400	144,000	1,140
	6T-28	1.86	66,000	114,500	89,100	154,000	1,340
Stress Relieved							
Single weld	64-2	1.84	50,250	128,300	105,000		
	64-8	1.85	53,000	125,300	99,000		
Twin weld	6T-29	1.80	48,200	123,500	97,100	114,000	760
	6T-30	1.95	48,800	120,600	97,600	117,000	770

TABLE XII

TENSILE STEP-LOADING SEQUENCE IN
SEA WATER ENVIRONMENT

Alloy	Specimen	Condition(*)	Step Loading Sequence
Ti-8Al-1Mo-1V	8T-8	S.R.	30,000 lb 5 minutes; 42,000 lb 4 minutes failure
	8T-7	S.R.	23,000 lb 5 minutes; 35,000 lb 5 minutes; 47,000 lb 1 1/2 minute failure
	8T-4	A.W.	28,000 lb 5 minutes; 40,000 lb 5 minutes; 50,100 1 minute failure
	8T-3	A.W.	21,000 lb 5 minute; 33,000 lb 5 minutes; 45,000 lb 3 1/4 minutes failure
Ti-5Al-2.5Sn	5T-9	S.R.	52,000 lb 5 minutes; 64,000 lb 4 1/2 minutes failure
	5T-8	S.R.	65,000 lb 5 minutes; 77,000 lb 1 1/2 minutes failure
	5T-4	A.W.	54,000 lb 5 minutes; 62,500 lbs 2 1/2 minutes failure
	5T-5	A.W.	68,000 lb 5 minutes; 72,750 lbs failure

(*) S.R. = Stress relieved at 1450F for 15 minutes, air cooled

A.W. = As welded

The results on fatigue crack growth rate for Ti-6Al-4V, showing a wide difference between as-welded and stress-relieved welded specimens, are in agreement with the data obtained for Ti-8Al-1Mo-1V and Ti-5Al-2.5Sn. Typical results of crack growth versus number of cycles for the latter alloys are presented in figure 31. The number of cycles required to grow a 2-inch crack length in the 8-inch wide as-welded specimens was 40 and 200 percent greater than for the stress-relieved specimens of Ti-5Al-2.5Sn and Ti-8Al-1Mo-1V, respectively. The lower fatigue crack resistance of the Ti-5Al-2.5Sn alloy may be attributable to the lower compressive stress field in the notch origin for this alloy as compared to Ti-8Al-1Mo-1V and Ti-6Al-4V.

Typical load-deflection curves are shown in figure 32 for Ti-8Al-1Mo-1V and Ti-5Al-2.5Sn under various environments. The Ti-8Al-1Mo-1V specimens generally failed at considerably lower stresses and total deflections than the corresponding Ti-5Al-2.5Sn specimens. No distinct pop-in zone, such as was found in Ti-6Al-4V, was evident in either alloy.

A summary of fracture toughness data for all center-precracked Ti-8Al-1Mo-1V and Ti-5Al-2.5Sn weld specimens is tabulated in Table XIII. The net area failure stress σ is computed by dividing the maximum failure load by the uncracked cross-sectional area normal to the tensile load. These results may be summarized as follows:

1. There is no distinguishable difference in unstable fracture behavior between the as-welded and stress-relieved welded specimens for either Ti-8Al-1Mo-1V or Ti-5Al-2.5Sn regardless of test conditions. In other words, fracture toughness is insensitive to residual stress induced by TIG welding.

2. Test environments have varying effects on fracture toughness of a given alloy. There is a 13 percent decrease in fracture strength for Ti-8Al-1Mo-1V when testing in -100°F LN_2 as compared to testing in air at room temperature. The decrease was 35 percent in sea water as compared to the fracture strength in air at room temperature.

3. There is no significant difference in fracture toughness between room temperature test in air and -100°F LN_2 for the Ti-5Al-2.5Sn alloy; however, the sea water environment reduces the fracture strength by 58 percent.

4. The fracture toughness behavior varies with each titanium alloy. In terms of fracture strength, particularly in sea water, the cracking resistance of Ti-6Al-4V in general is superior to Ti-8Al-1Mo-1V and Ti-5Al-2.5Sn. Ti-8Al-1Mo-1V shows the least resistance to unstable fracture under any of the environments investigated. The net area fracture strength of Ti-8Al-1Mo-1V in air at room temperature averaged 58,000 psi as compared to 100,800 psi for Ti-6Al-4V and 108,500 psi for Ti-5Al-2.5Sn. In -100°F LN_2, the Ti-5Al-2.5Sn showed a fracture strength of 109,900 psi as compared to 51,600 psi for the Ti-8Al-1Mo-1V. In a sea water environment, Ti-6Al-4V retains 90 percent (89,700 psi) of its air room temperature fracture resistance compared to 62 percent (36,100 psi) for Ti-8Al-1Mo-1V and 52 percent (55,600 psi) for Ti-5Al-2.5Sn.

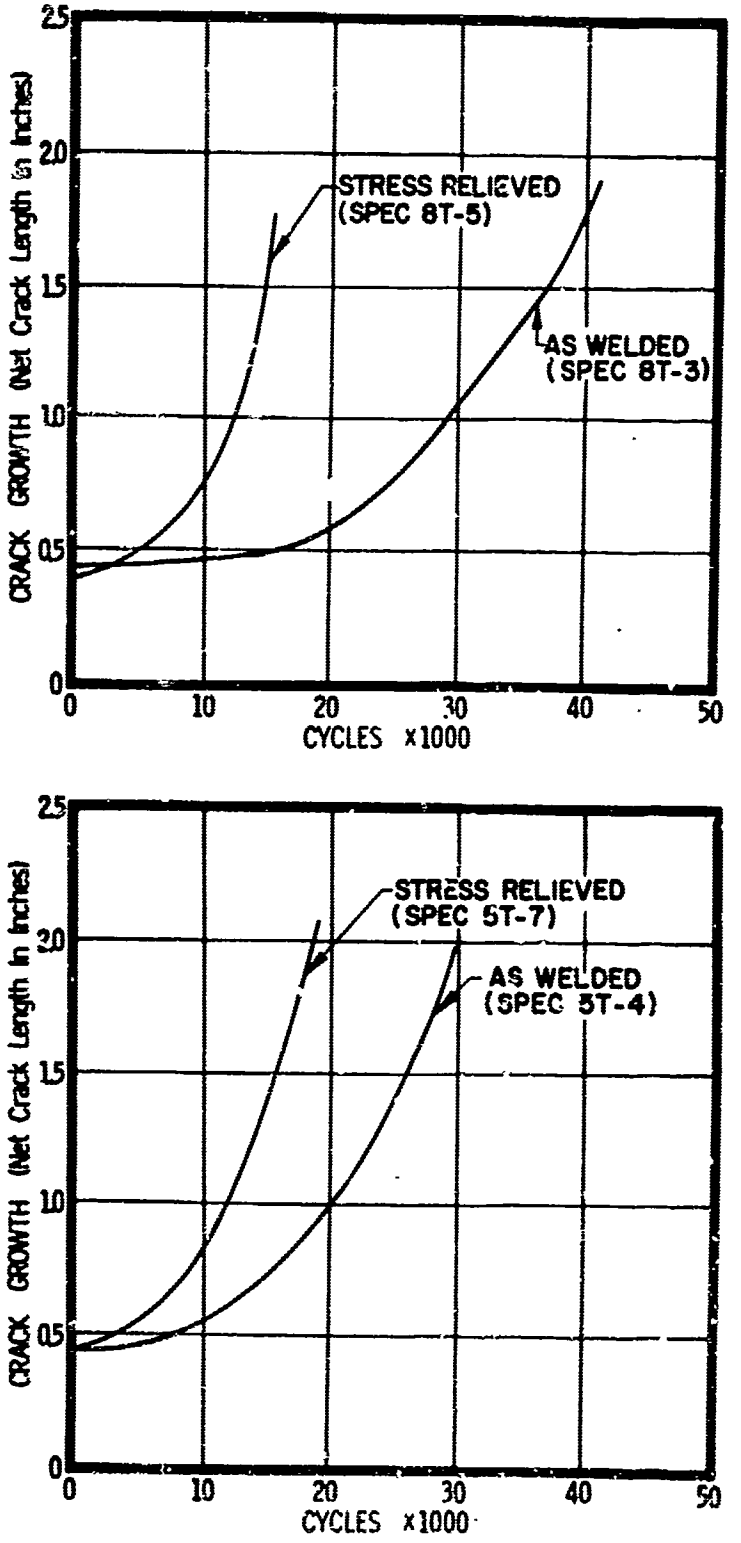

Figure 31. Typical Crack Growth Data for Ti-8Al-1Mo-1V (Top) and Ti-5Al-2.5Sn (Bottom) Fracture Toughness Specimens

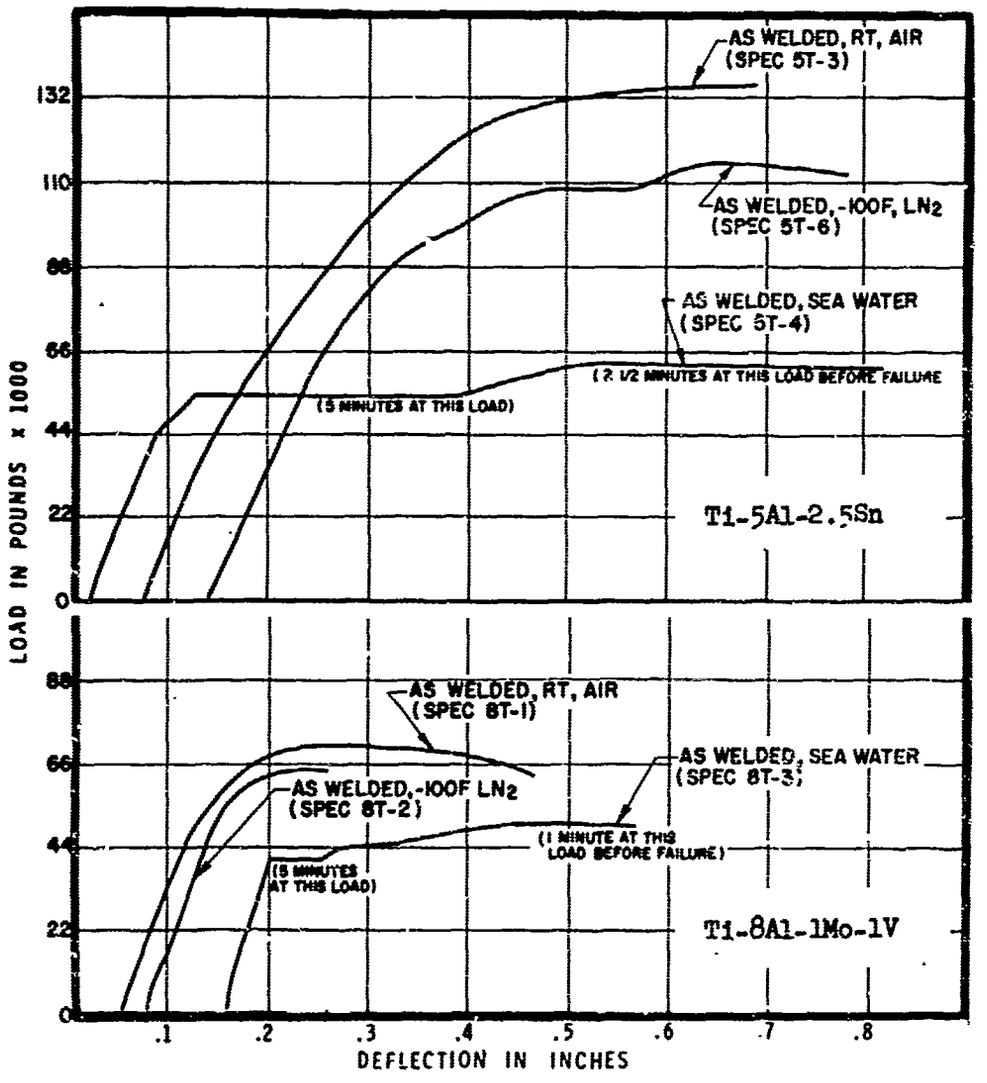

Figure 32. Typical Load Deflection Curves for 0.200-Inch Ti-8Al-1Mo-1V and Ti-5Al-2.5Sn Fracture Toughness Specimens Tested in Various Environments

TABLE XIII

FRACTURE TOUGHNESS DATA OF FATIGUE PRECRACKED Ti-8Al-1Mo-1V AND Ti-5Al-2.5Sn TITANIUM WELD SPECIMENS

Specimen	Specimen Condition	Total Precracked Length, (inches	Test Media	Net Area Failure Stress, (psi)	Fracture Mode and Appearance*
		Ti-8Al-1Mo-1V			
8T-1	As Welded	2.02	RT, Air	56,200	
8T-5	Stress Relieved	1.90	RT, Air	59,800	Normal, Mechanical Air Type
8T-2	As Welded	1.96	-100°F, LN_2	50,900	
8T-6	Stress Relieved	2.01	-100°F, LN_2	51,300	
8T-3	As Welded	1.94	Sea Water	35,500	Mixed Corrosion Embrittled Type (Fibrous) and Mechanical Air-Type
8T-4	As Welded	1.85	Sea Water	38,600	
8T-7	Stress Relieved	1.98	Sea Water	37,400	
8T-8	Stress Relieved	1.92	Sea Water	33,000	
		Ti-5Al-2.5Sn			
5T-3	As Welded	1.97	RT, Air	109,300	
5T-7	Stress Relieved	2.04	RT, Air	107,800	Normal, Mechanical Air Type
5T-6	As Welded	2.50	-100°F, LN_2	101,700	
5T-10	Stress Relieved	1.98	-100°F, LN_2	118,100	
5T-4	As Welded	1.97	Sea Water	50,700	Mixed Corrosion Embrittled Type (Fibrous) and Mechanical Air-Type
5T-5	As Welded	2.01	Sea Water	59,100	
5T-8	Stress Relieved	1.97	Sea Water	61,400	
5T-9	Stress Relieved	1.93	Sea Water	51,200	

* Each remark in this column applies to the four specimens listed opposite it.

Visual examination of the fracture surface of the test specimen was made; observations and remarks are noted in Table XIII. No pop-in cracks could be observed in either Ti-8Al-1Mo-1V or Ti-5Al-2.5Sn, in contrast to Ti-6Al-4V. This confirmed the patterns of the load-deflection curves obtained for these alloys. Generally speaking, all Ti-8Al-1Mo-1V and Ti-5Al-2.5Sn specimens tested in air at room temperature and at -100°F have shown plane-stress type fracture with a shear lip developing toward the end of the fracture. There seems to be a difference in fracture appearance on either side of the weld. Typical fracture faces are shown in the upper fractographs in figures 33 and 34. Also shown in these two figures are typical fracture surfaces of the specimens tested in sea water. The various well-defined zones are labeled on these photographs as well as being depicted schematically in figure 35. The existence of corrosion zones bordering both sides of the fatigue crack is significant and worth noting. The Ti-5Al-2.5Sn specimen has a 1-3/4 inch wide, and the Ti-8Al-1Mo-1V a 3/4-inch wide, corrosion zone. The difference in length of the zone is probably due partly to the difference in magnitude of the applied stress, which was held constant for 5 minutes. Corrosion induced cracking occurs at a slower rate in Ti-8Al-1Mo-1V than in Ti-5Al-2.5Sn. At the maximum failing load of the specimen, rapid crack propagation commences as soon as corrosion cracking reaches a point of instability in the specimen.

The corrosion induced fracture surface is characterized by its rough, fibrous, and lamellar appearance, occasionally showing lateral transverse cracks. These cracks have been examined metallographically in edge-cracked fracture toughness specimens described later in this report. Further analysis is necessary to relate fractography with stress corrosion and fracture resistance.

The experimental results obtained in this part of the study generally concur with other investigators (Ref. 6 and 7). The severity of embrittlement in titanium alloys has been attributed to the ordering reaction in the alpha phase and appears to be associated with the aluminum content or combination of aluminum and tin.

EDGE-CRACKED FRACTURE TOUGHNESS

Edge-cracked fracture toughness tests were performed to determine the effect of sea water environment on the crack resistance of the base alloys thermally treated to simulate postweld stress-relief cycles. Single edge-cracked specimens were fabricated from parent metal samples of each alloy according to the configuration shown in figure 36.

The following thermal conditions were included in the evaluation of each alloy:

Ti-5Al-2.5Sn	1.	As received (mill annealed)
	2.	As received, 1000°F for 3 hours, air cooled
	3.	As received, 1450°F for 15 minutes, air cooled
Ti-8Al-1Mo-1V	1.	As received (duplex annealed)
	2.	As received, 1000°F for 3 hours, air cooled
	3.	As received, 1450°F for 15 minutes, air cooled
	4.	2B2 treatment
	5.	2B2, 1450°F for 15 minutes, air cooled

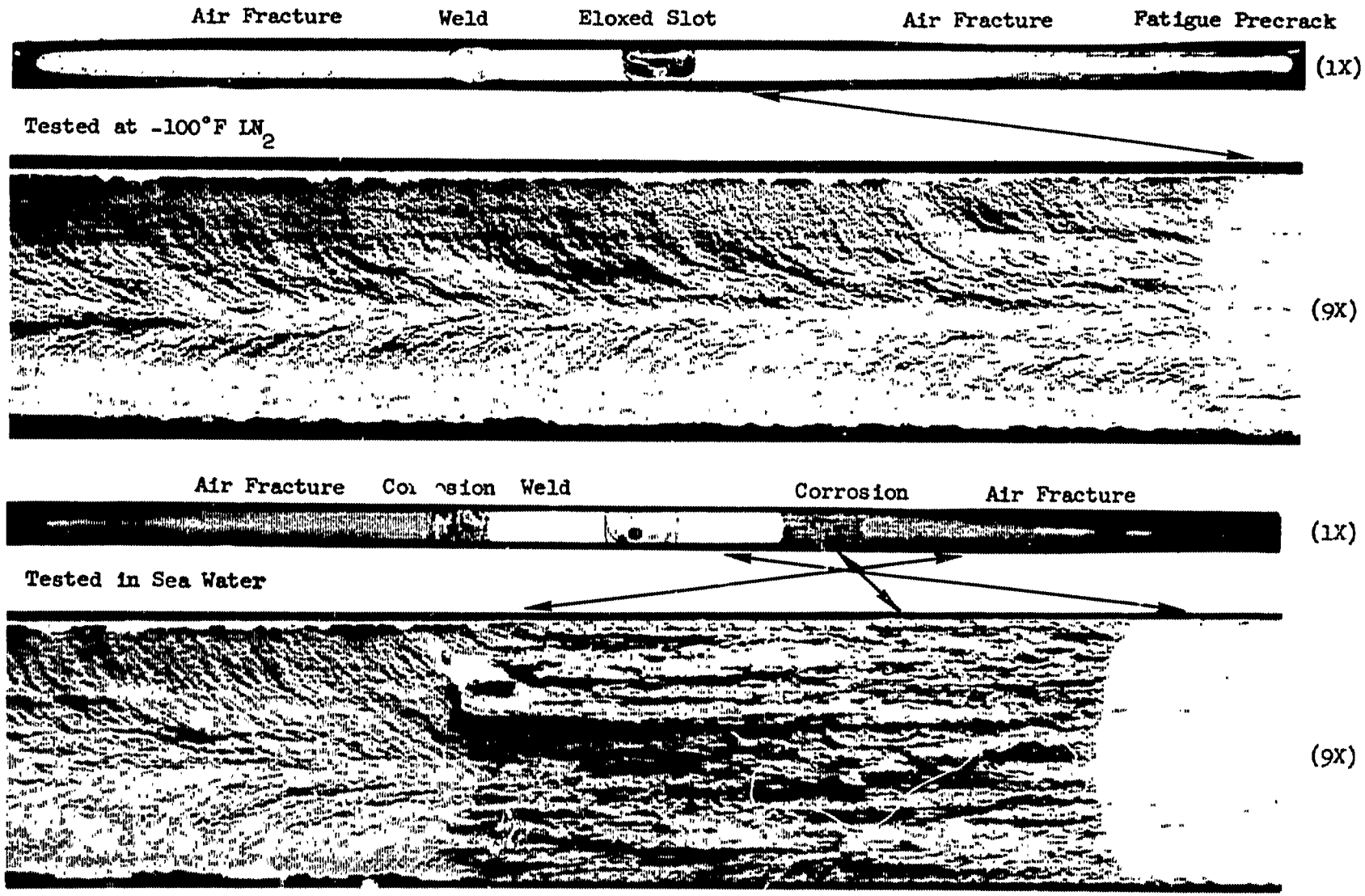

Figure 33. Appearance of Fractured Surface of Ti-8Al-1Mo-1V

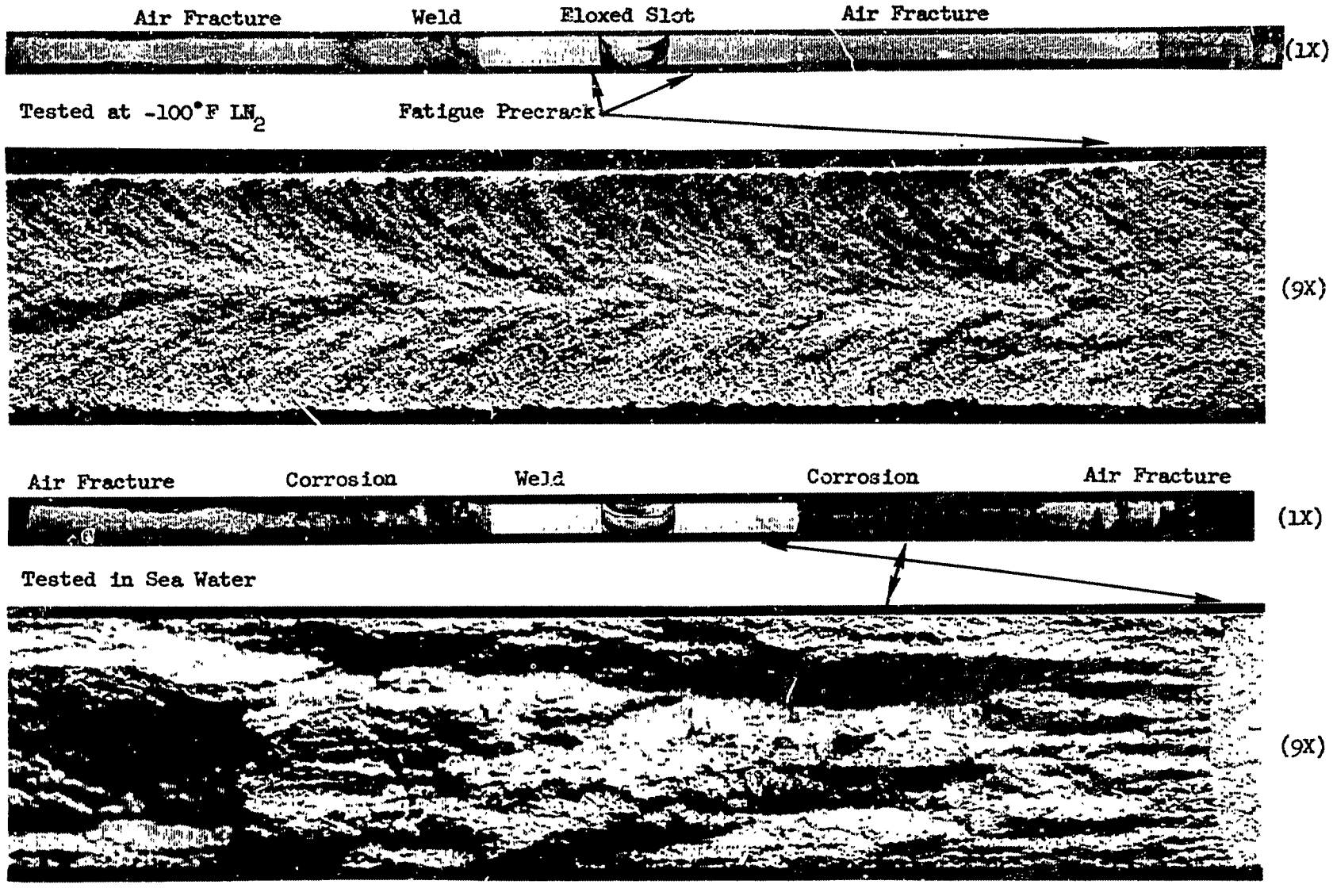

Figure 34. Appearance of Fractured Surface of Ti-5Al-2.5Sn

① WELD
② ELOXED SLOT
③ FATIGUE CRACK
④ AIR-TYPE MECHANICAL FRACTURE ZONE
⑤ CORROSION EMBRITTLED ZONE

Ti-6Al-4V, Ti-8Al-1Mo-1V, and Ti-5Al-2.5Sn
Tested in Air at Room Temperature; Ti-8Al-1Mo-1V
and Ti-5Al-2.5Sn at -100 F LN_2; and Ti-6Al-4V
in Sea Water

Ti-8Al-1Mo-1V Tested in Sea Water

Ti-5Al-2.5Sn Tested in Sea Water

Figure 35. Schematic Showing Zones Appearing on Fractured Surfaces

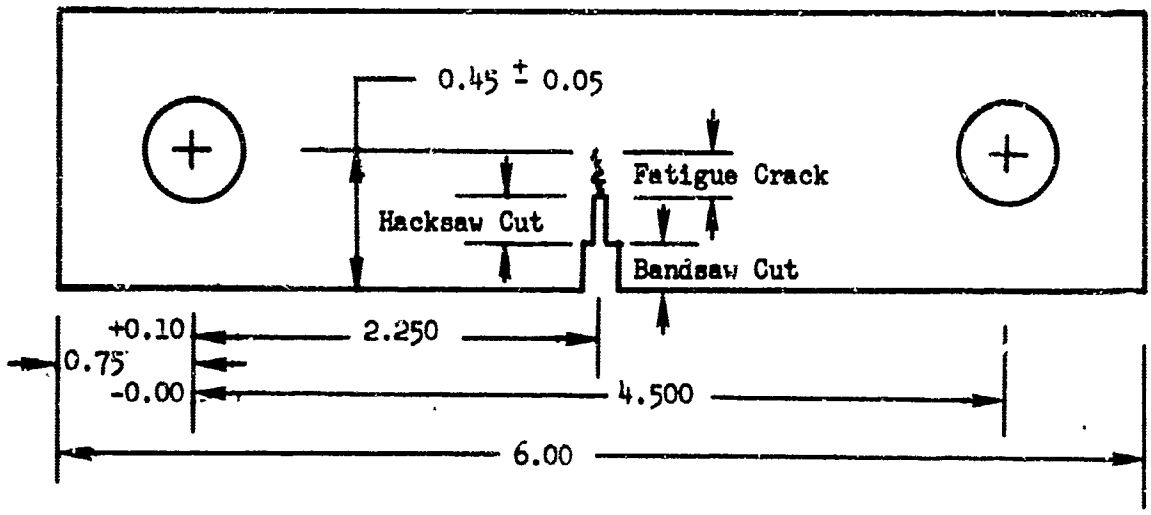

Figure 36. Edge Precracked Fracture Toughness Specimen Showing Crack Detail (Dimensions in Inches)

Ti-6Al-4V

1. As received, 1450°F for 15 minutes, air cooled
2. As received, 1000°F for 3 hours, air cooled
3. As received, 1450°F for 15 minutes, air cooled, 1450°F for 15 minutes, air cooled

Specimens in the as-received condition, representing conditions in which each material is welded, were tested to establish baseline properties and to indicate behavior of the mill material. A second set of specimens of each alloy was heated at 1000°F for 3 hours, a standard titanium stress relief treatment. This treatment is also known to result in reduced toughness in certain titanium alloys due to ordering in the alpha phase and is commonly prevalent in the high aluminum-content alloys, apparently associated with the formation of a Ti-Al compound. A third condition, consisting of treating as-received specimens at 1450°F for 15 minutes followed by air cooling, a treatment designed to disorder the structure and recover toughness, was produced in samples of each alloy. All the specimens discussed above were tested in full plate thickness (0.200 inch).

Two additional sets of specimens were prepared from Ti-8Al-1Mo-1V alloy sheet mill heat treated by the 2B2 process. This treatment is designed to alter the microstructure of the alloy to improve its performance under salt water cracking conditions. A set of the 2B2 specimens was heat treated at 1450°F for 15 minutes and air cooled to simulate the effect of stress relieving a welded structure. These specimens were fabricated to the previously described test configuration from 0.050-inch sheet material. Precracking was accomplished by axial fatigue loading at about 20,000 psi, using an R factor of 0.1 and a cyclic rate of 1200 cpm. Fatigue crack depth on all specimens ranged between 0.102 and 0.164 inch except for one specimen (0.058 inch).

Specimens were loaded in tension at a head travel speed of 0.05 inch per minute until failure. Synthetic sea water was admitted to both sides of the specimen, completely immersing the precracked region immediately before loading. The instantaneous load during tensile testing was autographically monitored up to failure.

The nominal stress σ at the crack for each specimen was calculated from failure stress according to the equation

$$\sigma = \frac{P}{B(W - a)} + \frac{3Pa}{B(W - a)^2}$$

where P is the fracture load, B is the specimen thickness, W is the specimen width, and a is the total crack depth.

A summary of the test results is shown in Table XIV. In general, regardless of alloy condition, it may be concluded that Ti-6Al-4V was the least affected, followed by Ti-5Al-2.5Sn and Ti-8Al-1Mo-1V, the latter being most severely affected on the basis of the fracture strength. These results correlated qualitatively with the findings for center-cracked specimens presented in the previous section; however, the 2B2 processed Ti-8Al-1Mo-1V was significantly better than the duplex annealed Ti-8Al-1Mo-1V in crack resistance. The effect of thermal treatment appears to be quite pronounced in some cases. Each

TABLE XIV

EFFECT OF HEAT TREAT CONDITION ON NOMINAL STRESS AT CRACK ROOT OF FATIGUE CRACKED SINGLE EDGE NOTCHED SPECIMENS IN SYNTHETIC SEA WATER

Alloy	Nom. Thick. (in.)	Nominal Fracture Stress (ksi)		
		Original Condition	1000 F for 3 Hrs., Air Cool	1450 F for 15 Minutes, Air Cool
Mill Annealed, 1450 F for 45 Minutes, Air Cooled				
Ti-6Al-4V	0.2	142.4 144.4	118.7 132.3	135.5 126.5
	Average	143.4	125.5	131.0
Mill Annealed				
Ti-5Al-2.5Sn	0.2	103.9 113.1	82.9 95.6	90.8 110.2
	Average	108.5	89.3	100.5
Duplex Annealed				
Ti-8Al-1Mo-1V	0.2	63.9 66.8	60.4 52.1	73.0 78.0
	Average	65.4	56.3	75.5
2B2 Treatment (1850 F for 5 Minutes, Air Cool)				
Ti-8Al-1Mo-1V	0.05	109.5 122.6		112.4 111.6
	Average	116.1		112.0

alloy with a prior heat treatment at 1000°F suffered varying degrees of degradation in this environment. The adverse effect caused by the 1000°F heat treatment agrees generally with the results obtained in slow bend tests described in the discussion which follows. Except for the duplex annealed Ti-8Al-1Mo-1V, all specimens after the 1450°F, air cool, treatment also exhibited degradation, though to a lesser extent. Differences in resistance among the alloys are more marked than those among the thermal treatments employed.

The relative susceptibility of alloys to sea water attack was readily discernible from the specimen fracture faces shown in figure 37. The results are quite similar to those obtained with the center-cracked specimens discussed previously. Regardless of thermal history of the specimens, fracturing of Ti-6Al-4V was mainly mechanical with no evidence of corrosive effect. Both Ti-8Al-1Mo-1V and Ti-5Al-2.5Sn show a corrosion induced zone immediately adjacent to the precrack, followed by a zone of rapid mechanical fracture. The appearance of the fractured surface of Ti-5Al-2.5Sn shows greater susceptibility to sea water attack than Ti-8Al-1Mo-1V, as shown in figure 38. The 2B2 treated Ti-8Al-1Mo-1V showed little or no evidence of corrosive attack; the appearance of the fractured surface is similar to that of Ti-6Al-4V.

Sections taken through the rough textured fracture surface, normal to the fracture face and through the specimen thickness, were examined metallographically and revealed the presence of considerable secondary cracking in the Ti-8Al-1Mo-1V and Ti-5Al-2.5Sn alloys. The branchlike nature of these cracks is similar in appearance to those produced in these alloys under stress corrosion cracking conditions. Examples are presented in figures 39 and 40. Ti-6Al-4V, while showing a roughened texture, was found to be free from secondary branch cracks.

SLOW BEND FRACTURE TOUGHNESS

Slow bend fracture toughness tests, using fatigue precracked Charpy specimens, were conducted to provide data for correlation with previous fracture toughness test results. The slow bend tests also provided a basis for investigation of the effect of a 1000°F stress relief treatment on the fracture toughness of the weld metal.

The specimens were machined so that the V-groove lay entirely in and parallel to the weld direction (figure 41). All specimens were precracked to a depth of 0.015 to 0.035 inch, the average being about 0.025 inch. Precracking was accomplished using Manlabs Fatigue Precrack Machine Model FDM-300B. Special attention was made during the precracking operation on all specimens to achieve a uniform precrack depth to the extent possible so as to avoid discrepancies in fracture toughness due to varying precrack depth (Ref. 8). Slow bend tests were conducted with Manlabs Slow Bend Machine Model SB-750. The energy W required to propagate fracture was automatically integrated and registered. The quantity W/A, a measure of the fracture toughness of a material, is computed by dividing the energy W by the cross-sectional fracture area A.

Slow bend test results are tabulated in Table XV for all three alloys in three processing conditions. In all cases the as-welded condition exhibits the highest toughness, followed by the 1450°F stress-relieving condition and the 1000°F stress-relieving condition. The gross loss in toughness resulting from

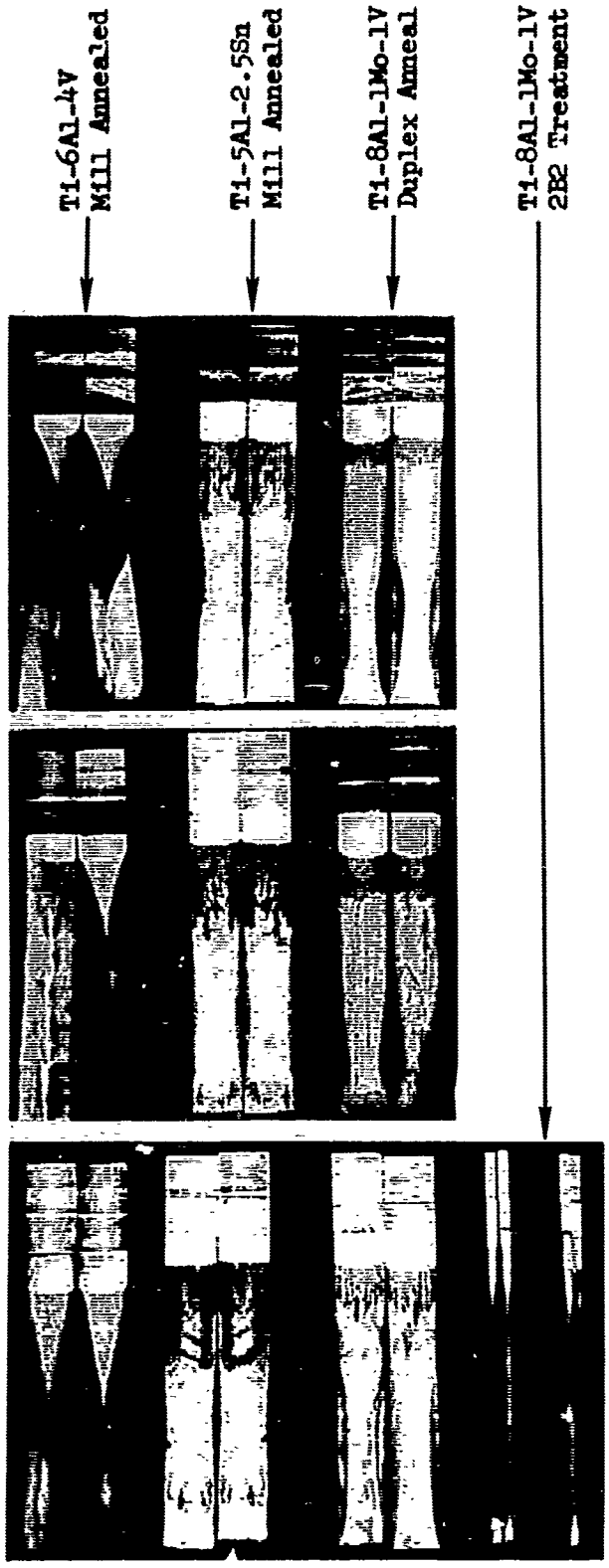

Figure 37. Appearance of Fractured Surfaces of Edge-Cracked Specimens in Sea Water

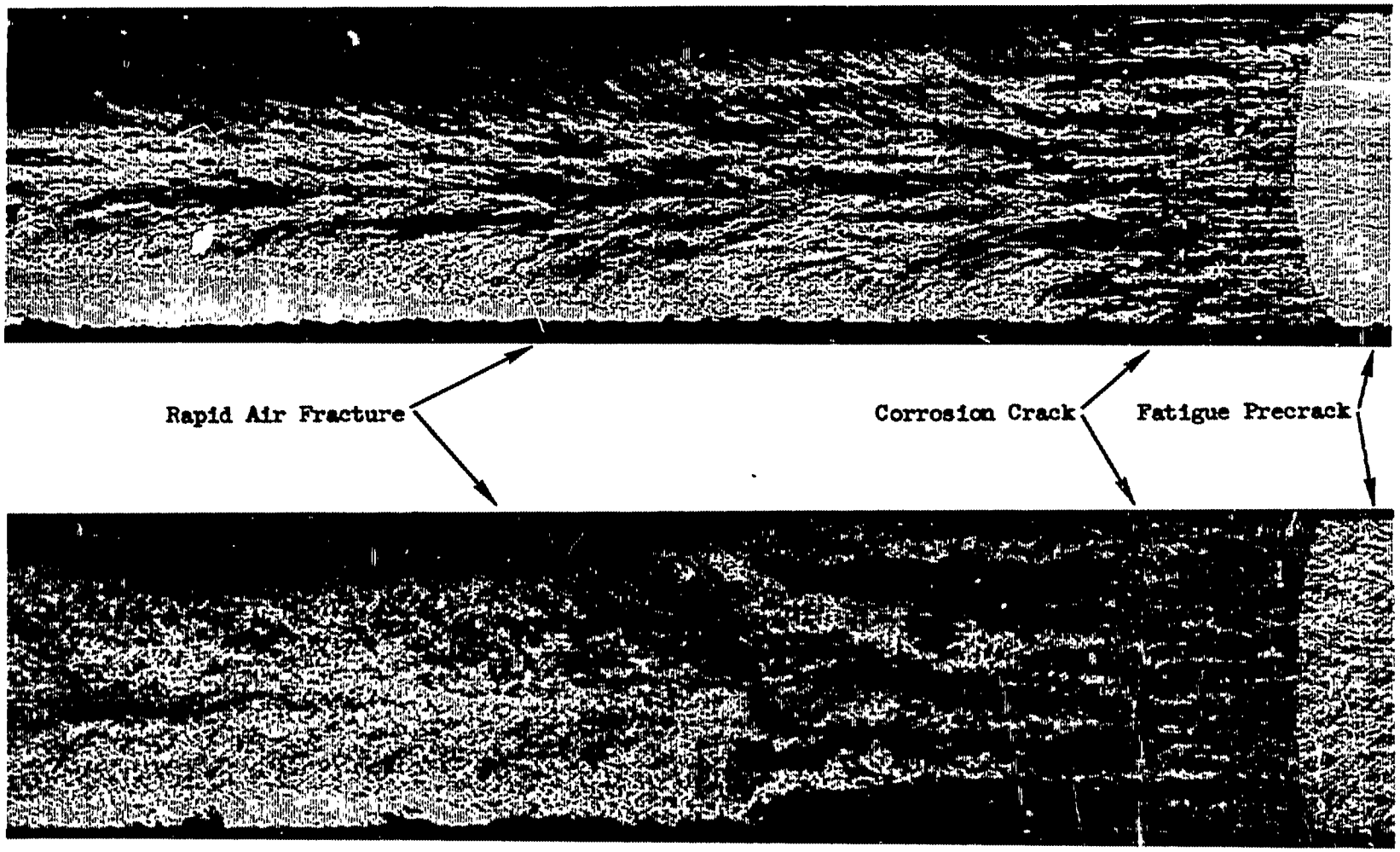

Figure 38. Fracture Appearance of Ti-8Al-1Mo-1V (Top) and Ti-5Al-2.5Sn (Bottom) Edge Precracked Specimens

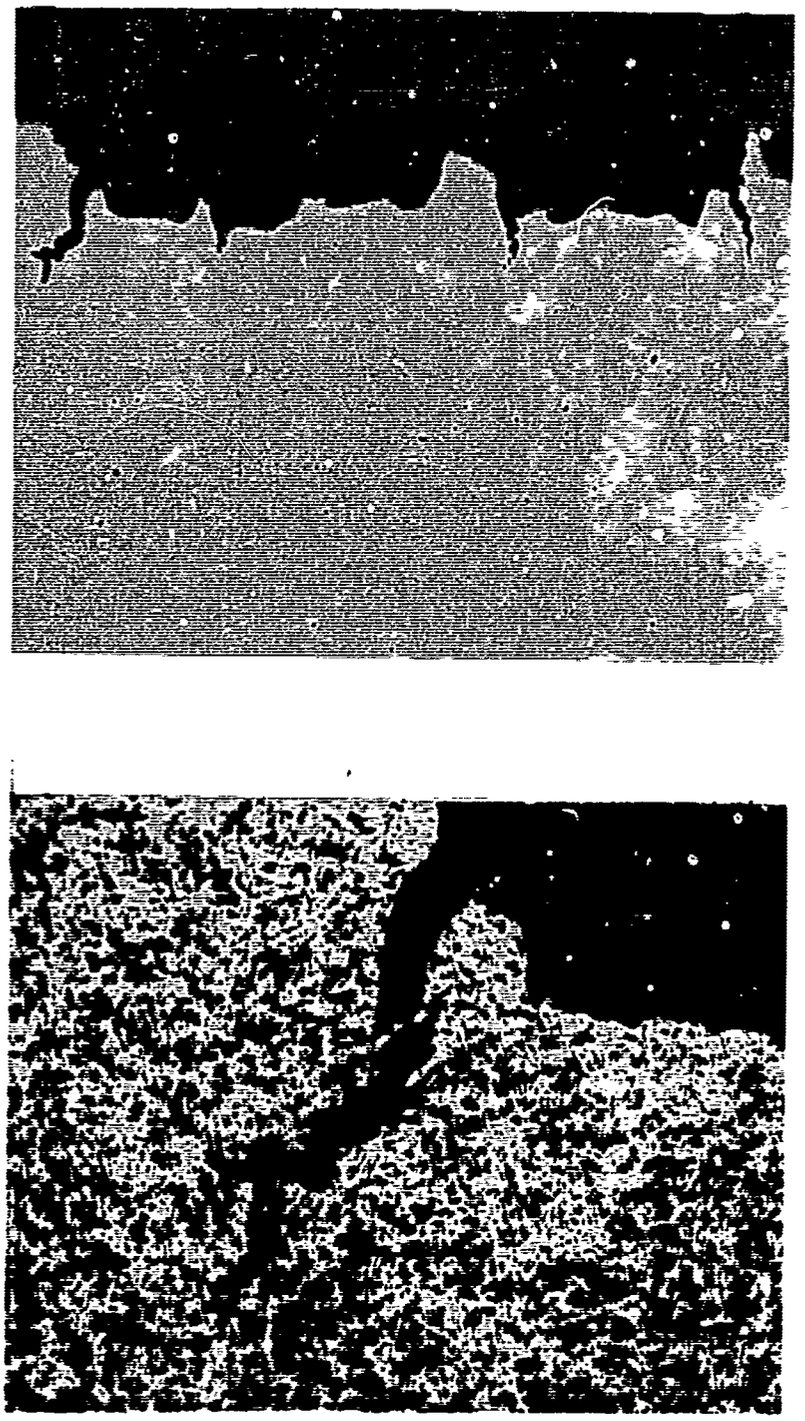

Figure 39. Cross Section Transverse to Fracture Surface of Ti-8Al-1Mo-1V, Unetched 50X (Top) and Etched 250X (Bottom)

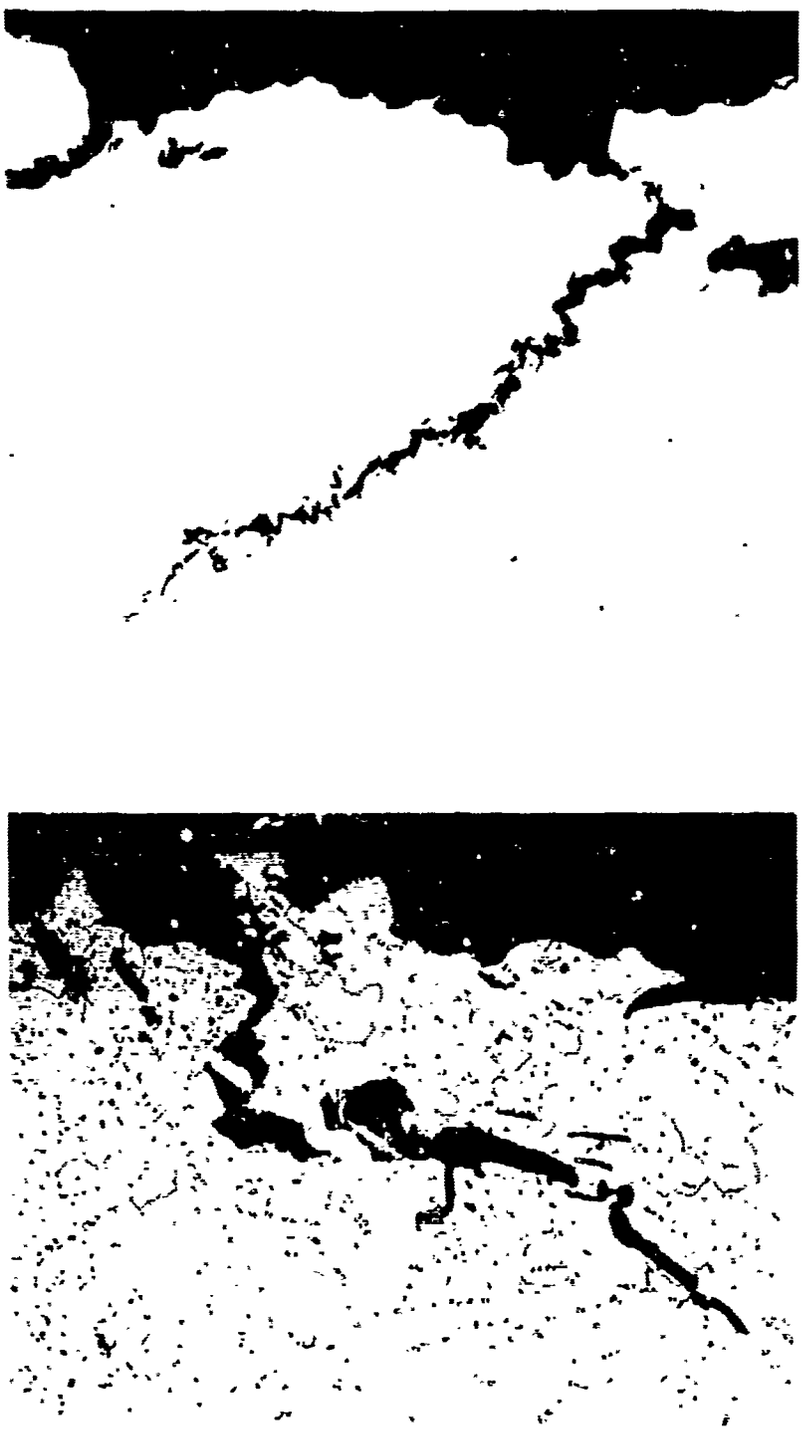

Figure 40. Cross Section Transverse to Fracture Surface of Ti-5Al-2.5Sn, Unetched 50X (Top) and Etched 250X (Bottom)

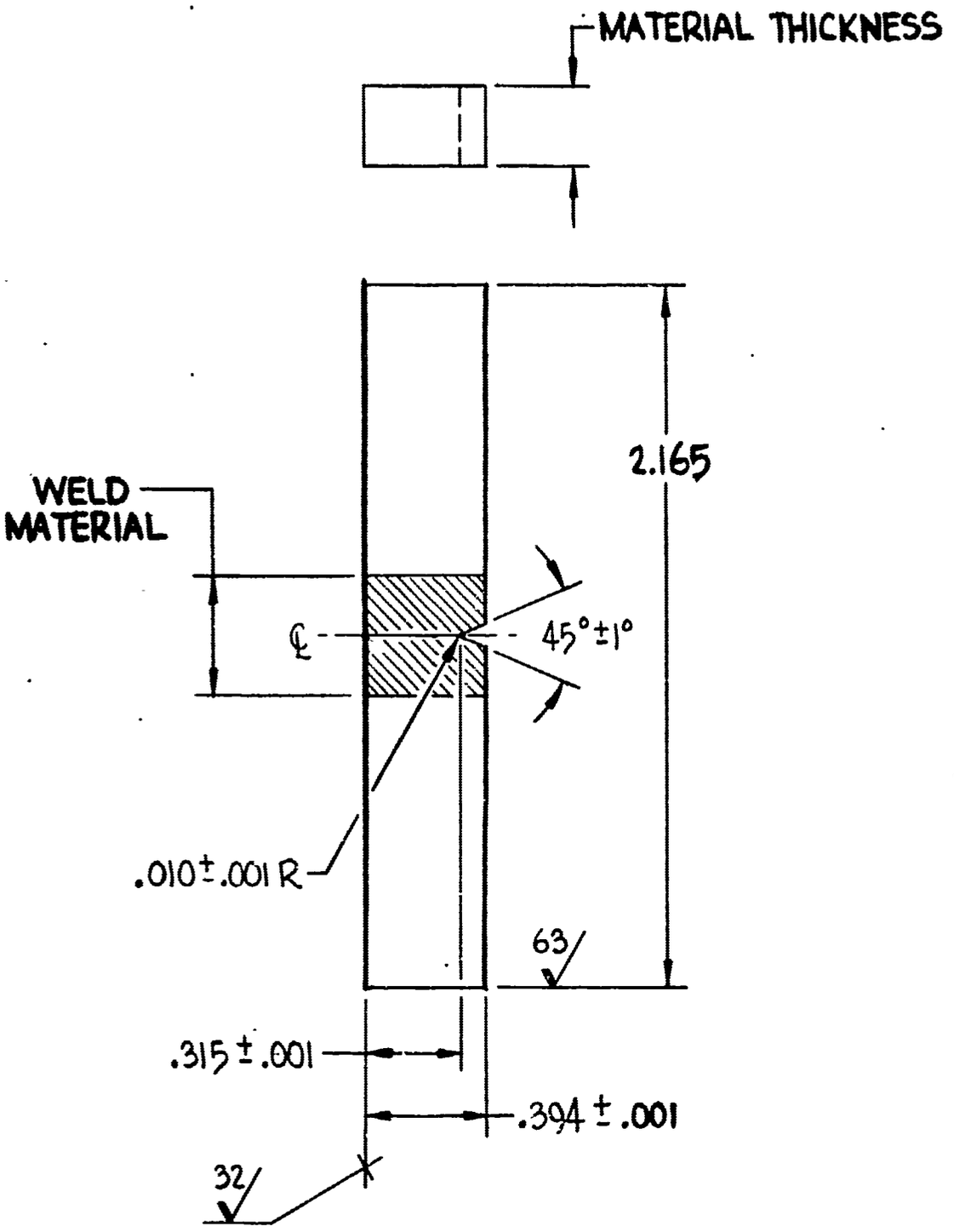

Figure 41. Slow Bend Specimen Configuration

TABLE XV

SLOW BEND PRECRACK CHARPY PROPERTIES
AT ROOM TEMPERATURE

Condition	W/A (in. lb /in.^{2})		
		Material	
	Ti-6Al-4V	Ti-8Al-1Mo-1V	Ti-5Al-2.5S
As-Welded	426	535	761
	348	416	913
	408	417	913
	414	395	
	348	572	
Average	389	478	862
Stress relieve at 1000 F for 3 hours followed by air cooling	290	268	481
	259	313	536
	251	273	404
	258	295	
	224	399	
Average	256	310	474
Stress relieve at 1450 F for 15 minutes followed by air cooling	299	306	1004
	333	294	699
	331	339	690
	394	307	
	352	324	
Average	342	314	798

NOTE: All specimens were precracked to a depth between 0.015 and 0.035 inch, with 0.025 inch the average depth.

the 1000°F postweld heat treatment was significant for all three alloys investigated. The 1450°F heat treatment for Ti-8Al-1Mo-1V also caused almost as much reduction in toughness as the 1000°F treatment. Comparison of the W/A results for the alloys showed that Ti-5Al-2.5Sn is significantly better in fracture toughness than Ti-8Al-1Mo-1V or Ti-6Al-4V.

Although considerable scatter was shown in the W/A data for each condition, there was no indication that this variation could be attributed to the variations in precracked depth. Photomicrographs of the cross section of the precracked area are shown in figures 42 through 44. Fatigue cracks traverse the acicular structure transgranularly across a prior beta grain. The direction of cracking does not appear to follow any pattern or orientation in the microstructure. Examination of the weld and the unaffected base metal failed to reveal any microstructural differences between the as-welded, 1000°F stress-relieve, and 1450°F stress-relieve conditions which could be a clue to explain the difference in fracture toughness behavior.

Visual examination was made on the fracture surface of the Charpy specimens shown in figures 45 through 47. It was found that Ti-5Al-2.5Sn generally exhibits shear type of fracture, whereas Ti-6Al-4V and Ti-8Al-1Mo-1V show evidence of cleavage. This observation seems to be in agreement with the magnitudes of W/A determined for each alloy. Also the degree of flat fracture appears to be more pronounced in the 1000°F stress-relieved and 1450°F stress-relieved specimens than in the as-welded specimens, indicating greater toughness in the latter as was shown by the slow bend fracture toughness data. The difference in fracture surface appearance among the Ti-5Al-2.5Sn specimens was not readily apparent.

As Welded

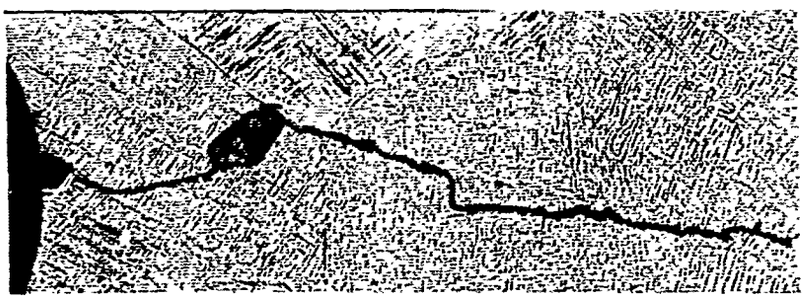

Stress Relieved at 1000°F for 3 Hours
Followed by Air Cooling

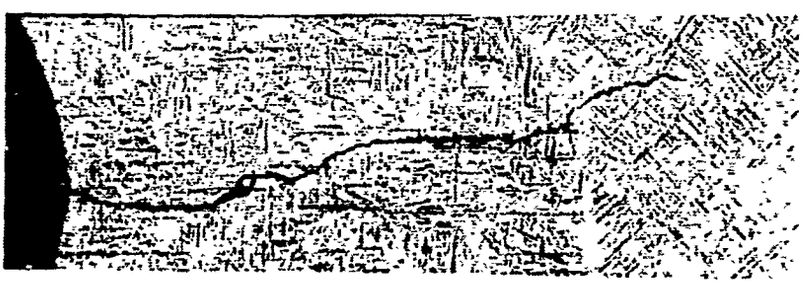

Stress Relieved at 1450°F for 15 Minutes
Followed by Air Cooling

Figure 42. Precracked Ti-6Al-4V Charpy Specimens, Mag. 150X

As Welded

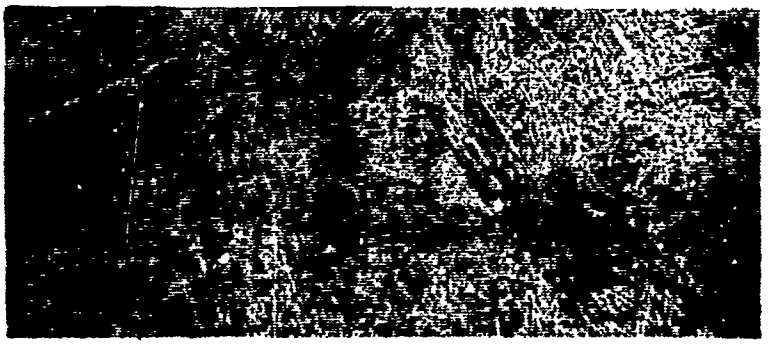

Stress Relieved at 1000°F for 3 Hours
Followed by Air Cooling

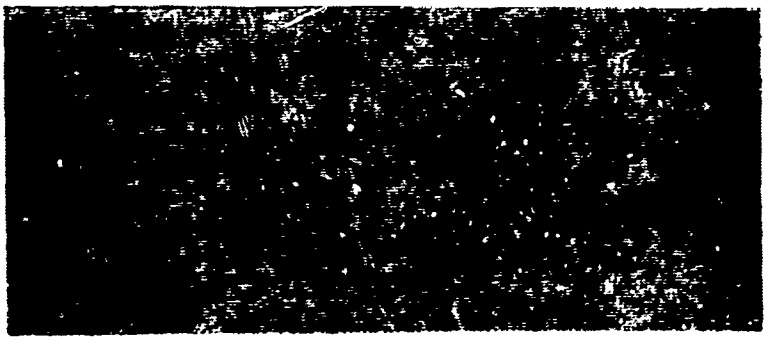

Stress Relieved at 1450°F for 15 Minutes
Followed by Air Cooling

Figure 43. Precracked Ti-8Al-1Mo-1V Charpy Specimens, Mag. 150X

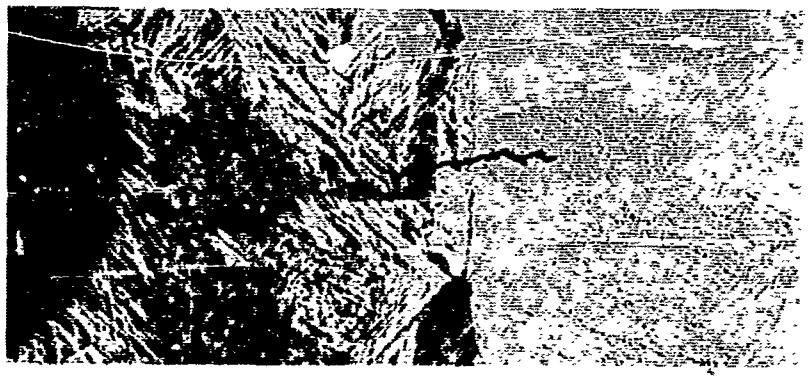

As Welded

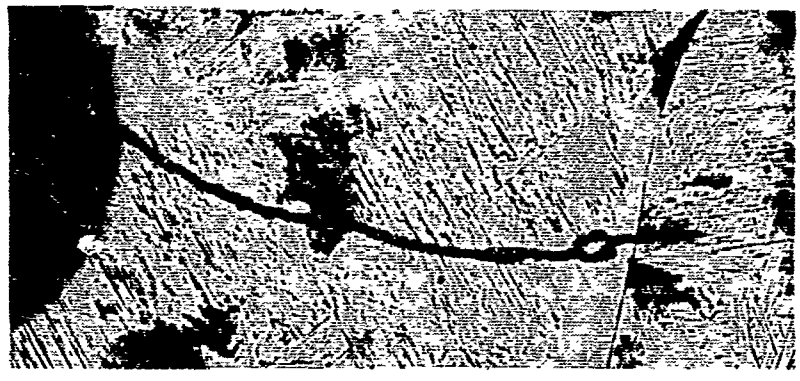

Stress Relieved at 1000°F for 3 Hours
Followed by Air Cooling

Stress Relieved at 1450°F for 15 Minutes
Followed by Air Cooling

Figure 44. Precracked Ti-5Al-2.5Sn Charpy Specimens, Mag. 150X

As Welded

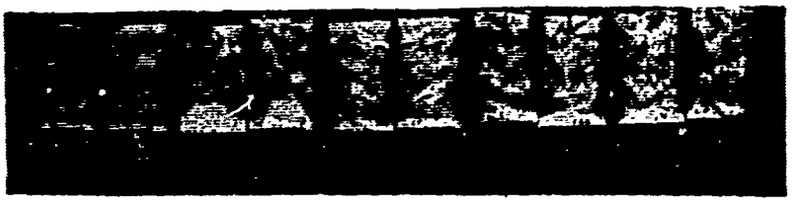

Stress Relieved at 1000°F for 3 Hours
Followed by Air Cooling

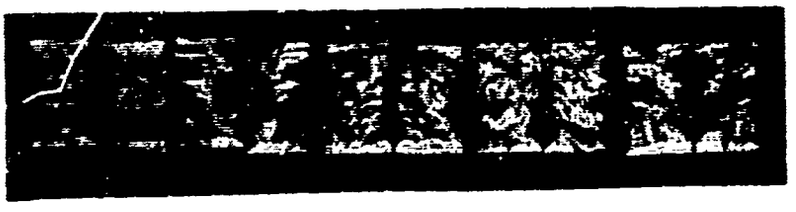

Stress Relieved at 1450°F for 15 Minutes
Followed by Air Cooling

Figure 45. Fractured Faces Precracked Ti-6Al-4V Charpy Specimens, Mag. 2X

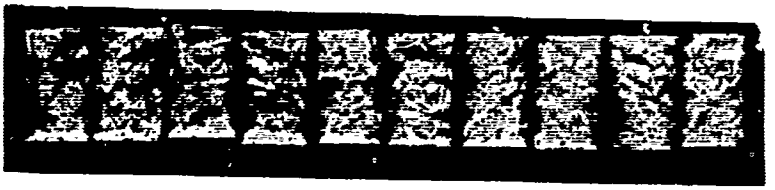

As Welded

Stress Relieved at 1000 F for 3 Hours
Followed by Air Cooling

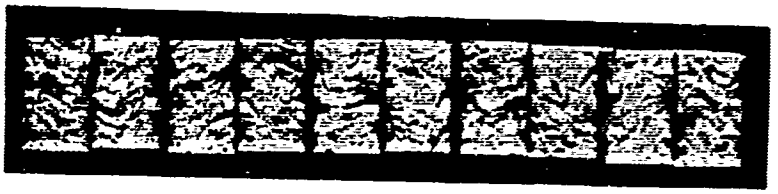

Stress Relieved at 1450 F for 15 Minutes
Followed by Air Cooling

Figure 46. Fractured Faces Precracked Ti-8Al-1Mo-1V Charpy Specimens, Mag. 2X

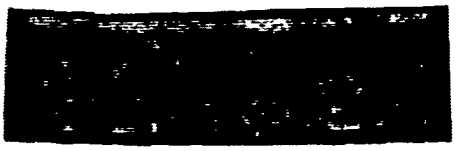

As Welded

Stress Relieved at 1000 F for 3 Hours
Followed by Air Cooling

Stress Relieved at 1450 F for 15 Minutes
Followed by Air Cooling

Figure 47. Fractured Faces Precracked Ti-5Al-2.5Sn Charpy Specimens, Mag. 2X

Section VII

CONCLUSIONS AND RECOMMENDATIONS

1. TIG welding of titanium alloys produced residual stresses of various magnitudes and directions. Longitudinal stresses in the weld are all tensile, whereas the transverse stresses are generally compressive. The longitudinal tensile stress in the weld drops sharply to compression within 1/2 inch from the weld centerline. The residual stresses can be completely removed by a stress relief heat treatment of 1450°F for 15 minutes.

2. Crack growth is retarded by residual compressive stresses and increased by residual tensile stresses. Fatigue crack growth rate is appreciably higher in the stress-relieved condition than in the as-welded condition if the crack propagation is in the compressive residual stress field and vice versa when crack propagation is in the tensile residual stress field.

3. The fatigue life of welded Ti-6Al-4V is increased by a factor of two when completely free of residual stresses based on results of smooth unnotched specimens. Tests on center-notched weld specimens, with the crack edge in the compressive residual stress field, indicate twice as much fatigue life in the as-welded condition as in the stress-relieved condition.

4. There is no difference between the as-welded and stress-relieved welded specimens on the basis of the net area fracture strength.

5. Test environments have varying effects on fracture toughness of a given alloy. Ti-6Al-4V is superior to Ti-8Al-1Mo-1V and Ti-5Al-2.5Sn in terms of their overall fracture toughness performance. Both Ti-8Al-1Mo-1V and Ti-5Al-2.5Sn suffered a gross loss in fracture resistance in a sea water environment, whereas the effect on Ti-6Al-4V was negligible.

6. The stress-relieving treatment of 1000°F caused a general degradation in all three titanium alloys based on results of slow bend fracture toughness tests at room temperature. The detrimental effect is attributed to a metallurgical factor such as ordering reaction rather than residual stresses.

7. Further studies are recommended to include: (1) effects of residual stresses on complex loading conditions, such as biaxial stress and impact tests; (2) fabrication and testing prototype structures having known residual patterns; and (3) further analysis of the mechanism associated with the effect of residual stresses and metallurgical conditions induced by welding on mechanical behavior.

REFERENCES

1. Specification ST0170GB0001, "Wire, Filler, Welding, Uncoated", North American Aviation, dated 6 February 1967

2. Specification HB0170-011, "Sheet and Plate Weldable Titanium Alloy (5Al-2.5Sn)", North American Aviation, Columbus Division, dated 1 March 1962

3. Specification HB0170-013, "Sheet and Plate; Titanium 80,000 PSI Tensile Strength (Annealed)", North American Aviation, Columbus Division, dated 20 November 1963

4. Specification LB0170-177, "Titanium Alloy Sheet, Strip, and Plate (8Al-1Mo-1V)", North American Aviation, Los Angeles Division, dated 16 July 1964

5. Specification LA0107-004, "Fusion Welding", North American Aviation, Los Angeles Division, dated 28 June 1965

6. I. R. Lane, et al., "Fracture Behavior of Titanium in the Marine Environment", MEL Report 231/65, U.S. Navy Marine Engineering Laboratory, July 1965

7. T. Murphy and N. G. Feige, "Preliminary Evaluation of Degradation of Titanium Crack Resistance in Sea Water Environment", TMCA Report, May 7, 1965

8. C. E. Hartbower and G. M. Orner, "Metallurgical Variables Affecting Fracture Toughness in High Strength Sheet Alloys", ASD-TDR-62-868, Part I, Manlabs, Inc., October 1962

BLANK

UNCLASSIFIED
Security Classification

DOCUMENT CONTROL DATA - R & D

(Security classification of title, body of abstract and indexing annotation must be entered when the overall report is classified)

1. ORIGINATING ACTIVITY (Corporate author) North American Aviation, Inc. Los Angeles Division International Airport ~~Los Angeles, California~~ 90015	2a. REPORT SECURITY CLASSIFICATION UNCLASSIFIED 2b. GROUP NA

3. REPORT TITLE

Investigation of Magnitude and Distribution of Stresses in Welded Structures

4. DESCRIPTIVE NOTES (Type of report and inclusive dates)
Summary Technical Report, 1 July 1966 to 31 August 1967

5. AUTHOR(S) (First name, middle initial, last name)
Rocco Robelotto
Albert Toy
John M. Lambase

6. REPORT DATE	7a. TOTAL NO. OF PAGES	7b. NO. OF REFS
September 1967	93 plus ii thru x	9

8a. CONTRACT OR GRANT NO.	9a. ORIGINATOR'S REPORT NUMBER(S)
AF 33(615)-5433	AFML-TR-67-293
b. PROJECT NO. 7351	
c. Task No. 735102	9b. OTHER REPORT NO(S) (Any other numbers that may be assigned this report)
d.	NA-67-716

10. DISTRIBUTION STATEMENT This document is subject to special export controls and each transmittal to foreign governments or foreign nationals may be made only with prior approval of the Air Force Materials Laboratory, Metals and Ceramics Division, Wright-Patterson Air Force Base, Ohio 45433.

11. SUPPLEMENTARY NOTES	12. SPONSORING MILITARY ACTIVITY
	AFML(MAMP) Wright-Patterson AFB, Ohio 45433

13. ABSTRACT An investigation on the magnitude and distribution of residual stresses in titanium sheets induced by TIG welding and their effects on mechanical properties was conducted. The study was made on three titanium alloys, Ti-6Al-4V, Ti-8Al-1Mo-1V, and Ti-5Al-2.5Sn. Residual stresses of similar patterns and magnitudes were obtained for all three alloys at two sheet thicknesses. The transition of residual stresses parallel to the weld occurs abruptly from a peak tension of about 60,000 psi in the weld to compression in the parent metal within 1/2 inch from the weld centerline. There was no apparent adverse effect attributable to residual stresses on the static tensile properties or fracture toughness behavior. Complete removal of residual stresses by thermal treatment significantly improves the fatigue life of unnotched welded specimens and of the center-notched specimens provided that the crack tip is not within a compressive residual stress field. Greater notched fatigue resistance was found to occur in as-welded specimens when the notch is in the compressive residual field because the effective net fatigue stress is lowered. Ti-6Al-4V was found to be superior to Ti-8Al-1Mo-1V and Ti-5Al-2.5Sn based on the overall fracture toughness performance, particularly in sea water environment. All three alloys suffer degradation in fracture toughness when heat treated at 1000°F. Fractographic analysis shows modes of failure of fatigue and fracture toughness tests, and results generally correlate with mechanical test data. (This abstract is subject to special export controls and each transmittal to foreign nationls may be made only with prior approval of the Air Force Materials Laboratory, MAMP, Wright-Patterson Air Force Base, Ohio 45433.)

DD FORM 1 NOV 65 1473

UNCLASSIFIED
Security Classification

14. KEY WORDS	LINK A		LINK B		LINK C	
	ROLE	WT	ROLE	WT	ROLE	WT
Welding Titanium Residual Stress Effects Fracture Toughness Fatigue Salt Water Stress Corrosion						